INFSO-ICT-248523 BeFEMTO

D5.3

Evaluation Report of Femtocells, Networking, Mobility and Management Solutions

Contractual Date of Delivery to the CEC:	M30
Actual Date of Delivery to the CEC:	M30
Author(s):	Tao Guo, Atta Quddus, Luis Cucala, Emilio Mino, Jaime Ferragut, José Nuñez-Martínez, Josep Mangues-Bafalluy, Miquel Soriano, Andrey Krendzel, Marc Portoles-Comeras, John Fitzpatrick, Nitin Maslekar, Marcus Schoeller, Frank Zdarsky, Mirosław Brzozowy, Zbigniew Kowalczyk, Konstantinos Samdanis
Participant(s):	NEC, TID, CTTC, UNIS, PTC
Workpackage:	WP5: Femtocells Access Control, Networking, Mobility and Management
Estimated person months:	18.62
Security:	PU
Nature:	R
Version:	1.0
Total number of pages:	84

Abstract:

This final WP5 deliverable presents the results of detailed simulation and analytical model based performance evaluation studies for the networking, mobility and management mechanisms and policies developed in this work package.

Keywords:

Traffic Offloading, Distributed Routing, Traffic Management, Resource Sharing, Location Management, Handover, Mobility Management, Access Control, Security, Networked Femtocells, Energy Efficiency, Distributed Fault Diagnosis

Executive Summary

This document describes the final evaluation report for the schemes developed by BeFEMTO on the traffic management, mobility management, network management, and security concepts in Work Package 5 (WP5). Some of them have already been proposed and described together with some initial evaluation results in previous deliverable D5.2. This deliverable will present the final evaluation results following the work in D5.2. In addition, as a final deliverable in WP5, this document also provides a summary for all the solutions that have been developed within WP5 contributing to the BeFEMTO system concept as presented in WP2.

Chapter 1 introduces the structure of this document and also provides a general overview of the technical activities and achievements updated from D5.2.

Chapter 2 describes the activities related to traffic forwarding and resource sharing.

Chapter 3 presents the solutions and evaluation results for mobility management issues.

Chapter 4 deals with network management problems, in particular the energy management.

Chapter 5 focuses on security problems, in particular local access control in networks of femtocells for multi-operator scenarios.

Chapter 6 summaries all the innovations and the achievements developed by BeFEMTO during the 2.5 year project phase.

List of Acronyms and Abbreviations

3GPP	3rd Generation Partnership Project
4G	4th Generation
AAA	Authentication, Authorization, Accounting
ACK	Acknowledgement
ACL	Access Control List
AKA	Authentication and Key Agreement
AP	Access Point
API	Application Programming Interface
BeFEMTO	Broadband evolved FEMTO networks
CA	Carrier Aggregation
CSG	Closed Subscriber Group
CSS	CSG Subscription Server
dB	Decibel
dBm	decibel (referenced to one milliwatt)
DL	Downlink
DSCP	Differentiated Services Code Point
EAP	Extensible Authentication Protocol
eNB	Evolved Node-B (LTE macro base station)
EPC	Evolved Packet Core
EUTRAN	Evolved Universal Terrestrial Radio Access Network
FAP	Femto Access Point
FTTH	Fibre To The Home
GHz	Gigahertz
GPRS	General Packet Radio Service
GTP	GPRS Tunneling Protocol
HeNB	Home evolved Node-B
HetNet	Heterogeneous Networks
HLR	Home Location Register
HNB	Home Node-B
HO	HandOver
HPLMN	Home Public Land Mobile Network
HCSG	HPLMN CSG Roaming
HSS	Home Subscriber Server
IMS	IP Multimedia Subsystem
IMSI	International Mobile Subscriber Identity
IMT-ADV	International Mobile Telephony – Advanced
IP	Internet Protocol
ISD	Inter Site Distance
ITU-R	International Telecommunication Union-Radiocommunication Sector
ITU-T	ITU-Telecommunication Standardization Sector
KPI	Key Performance Indicator
LAN	Local Area Network
LFGW	Local Femtocell GateWay
LGW	Local P-GW
LIPA	Local IP access
LLM	Local Location Management

LNO	Local Network Operator
LTE	3GPP Long Term Evolution
MAC	Media Access Control
MBMS	Multimedia Broadcast Multicast System
MHz	Mega Hertz
MME	Mobility Management Entity
MNO	Mobile Network Operator
MSISDN	Mobile Subscriber Integrated Services Digital Network Number
NAS	Non-Access Stratum
NASS	Network Access Support Subsystem
NoF	Network of Femtocells
ns	Nanosecond
OMA DM	Open Mobile Alliance Device Management
P-MME	Proxy Mobility Management Entity
QoS	Quality of Service
RACS	Remote Access Control Subsystem
RADIUS	Remote Authentication Dial in User Server
RSRP	Reference Signal Received Power
SCTP	Stream Control Transmission Protocol
S-GW	Serving GateWay
SINR	Signal to Interference plus Noise Ratio
SIPTO	Selected IP Traffic Offload
SIT	Service Interruption Time
SP	Strict Priority
S-TMSI	Serving Temporary Mobile Subscriber Identity
TA	Tracking Area
TAL	Tracking Area List
TAU	Tracking Area Update
TEID	Tunnel End-point IDentifier
TME	Traffic Management Entity
TTL	Time-to-Live
UE	User Equipment
UICC	Universal Integrated Circuit Card
UL	Uplink
UMTS	Universal Mobile Telecommunication System
UTRA	Universal Terrestrial Radio Access
UTRAN	Universal Terrestrial Radio Access Network
VBR	Variable Bit Rate
VLAN	Virtual LAN
VLTAG	VLAN Tag
VoIP	Voice over Internet Protocol
VPLMN	Visited Public Land Mobile Network
VCSG	VPLMN Autonomous CSG Roaming
WFQ	Weighted Fair Queuing
WID	Work Item Description
WP	Work Package

Authors

Partner	Name	Phone / Fax / e-mail
NEC		
	John Fitzpatrick	email: johnfitzpat@ieee.org
	Nitin Maslekar	Phone: +49 6221 4342 213 email: nitin.maslekar@neclab.eu
	Konstantinos Samdanis	Phone: +49 6221 4342 225 email: konstantinos.samdanis@neclab.eu
	Marcus Schoeller	Phone: +49 6221 4342 217 email: marcus.schoeller@neclab.eu
	Frank Zdarsky	Phone: +49 6221 4342 142 email: frank.zdarsky@neclab.eu
Telefonica I+D		
	Luis Cucala,	Phone: +34 91 3128799 e-mail: lcucala@tid.es
	Emilio Mino	Phone: +34 91 3128799 e-mail: emino@tid.es
PTC		
	Mirosław Brzozowy	Phone: +48 224135881 e-mail:Miroslaw.Brzozowy@t-mobile.pl
	Zbigniew Kowalczyk	Phone: +48 224136741 e-mail:Zbigniew.Kowalczyk@t-mobile.pl
CTTC		
	José Núñez	Phone: +34 93 645 29 00 e-mail: jose.nunez@cttc.cat
	Jaime Ferragut	Phone: +34 93 645 29 00, ext. 2113 e-mail: jaime.ferragut@cttc.cat
	Josep Mangues	Phone: +34 93 645 29 00 e-mail: josep.mangues@cttc.cat
	Andrey Krendzel	Phone: +34 93 645 29 16 e-mail: andrey.krendzel@cttc.cat
	Marc Portoles	Phone: +34 93 645 29 00 e-mail: marc.portoles@cttc.cat
	Miquel Soriano	e-mail: miquel.soriano@cttc.cat
University of Surrey		
	Tao Guo	Phone: +44 1483 689485 e-mail: t.guo@surrey.ac.uk
	Atta ul Quddus	Phone: +44 1483 683787 e-mail: a.quddus@surrey.ac.uk

Table of Contents

Table of Figures

1. Introduction

1.1 Scope

During year 1 and year 2 of the BeFEMTO project, Work Package (WP) 5 have developed a number of innovative concepts, mechanisms and evaluations in the area of traffic management, mobility management, security and network management of standalone, networked femtocells and mobile relay femtocells. These are described in the deliverable D5.1 [1] and D5.2 [2].

As a final deliverable, this deliverable will present the final evaluation results following the work in D5.2. In addition, this document also provides a summary for all the solutions that have been developed within WP5 contributing to the BeFEMTO system concept, as presented in WP2 D2.3 [3].

Finally, it is worth noting that WP5's scope is the research, development, and experimentation of novel femtocell technologies, but that detailed descriptions of the implementation of these technologies for the testbeds is outside WP5's scope, but is instead addressed by WP6 and documented in the its respective deliverables.

1.2 Organisation and Overview

The present deliverable is organised as follows:

Chapter 2 groups the work items related to the traffic forwarding of user and control plane traffic within a network of femtocells and to the sharing of that network's forwarding resources.

Chapter 3 presents the work items related to mobility management

Chapter 4 contains the work items related to the management of BeFEMTO femtocells in particular for energy saving.

Chapter **Error! Reference source not found.** is concerned with local access control in networks of femtocells for multi-operator scenarios.

Chapter 6 finally summarizes all the innovations made by BeFEMTO in WP5 during the whole project phase contributing towards the BeFEMTO system concepts

1.3 Contributions

During the last half year of the project, WP5 has made the following achievements and contributions:

The geographic+backpressure distributed routing protocol has been enhanced with a variable-*V* algorithm able to obtain an interesting trade-off between throughput, delay, and packet delivery ratio. Specifically, we propose a variable-*V* algorithm that dynamically adapts the weight of Lyapunov drift-plus-penalty routing decisions on a per-packet basis. The specific *V* parameter is function of the traffic load around the HeNB, and the number of hops traversed by data packets. On the other hand, the proposed routing protocol has been shown to be appropriate in the multi-LFGW scenario, and to overcome holes in sparse deployments, whilst still retaining its main features. We proposed a deployment strategy for multiple LFGW. The main advantage observed is the decrease of congestion in the Network of Femtocells (NoF) with respect to single LFGW NoF deployments, yielding to improvements in throughput, delay, and packet delivery ratio. Finally, we evaluated the distributed routing protocol under several sparse deployments. The study indicates the convenience of using the variable-V routing scheme to circumvent holes compared to fixed-V routing policies.

> *A paper presenting the distributed routing protocol for any-to any- traffic pattern with the use of the variable-V algorithm (i.e., uplink, downlink, and local routing) has been accepted for publication in IEEE HOTMESH WORKSHOP 2012.*

Analysis of the voice call capacity of long range WiFi as a femtocell backhaul solution has been studied.

> *A paper presenting this analysis has been submitted to the IEEE Journal on Selected Areas in Communications.*

Numerical evaluation of the local mobility management and traffic offload solutions described earlier in D5.1[1] has been carried out, illustrating their benefits in terms of reducing signalling and data traffic load on the backhaul links and mobile core networks. In addition, an analytical framework for traffic

modelling in mobile networks implementing offloading has been developed and performance bounds of the resource consumption in networks implementing offloading have been determined. These can be used for network dimensioning. Comparison of the required network resources before and after deploying offloading for providing a given quality of service has also been investigated.

A paper presenting this analysis has been submitted to the IEEE Journal on Selected Areas in Communications.

Design of a QoS based call admission control and resource allocation mechanism for LTE femtocell deployments and the evaluation of this mechanism.

A paper presenting this mechanism and its evaluation has been submitted to the IEEE Consumer Communications & Networking Conference (CCNC) 2012.

Design of a self-organized tracking area list (TAL) mechanism for large-scale networks of femtocells. The aim of this proposal is to improve the accuracy of standard 3GPP location management schemes, while reducing the signalling traffic over the network of femtocells. This mechanism allows MMEs/P-MMEs to provide UEs with adaptive TALs depending on their mobility state and, eventually, current network conditions.

A paper presenting this mechanism and its evaluation has been presented in IEEE International Conference on Communications (ICC) 2012.

A paper on Mobility management for large-scale all-wireless networks of femtocells in the Evolved Packet System has been submitted to a special issue on Femtocells in 4G Systems of the EURASIP Journal on Wireless Communications and Networking.

A chapter of a Wiley book on Heterogeneous Networks (HetNets) on Mobility management for large-scale all-wireless networks of femtocells has been accepted for publication.

A paper on Traffic and mobility management in Networks of Femtocells has been submitted to a special issue on Networked Femtocells of the ACM/Springer Journal on Mobile Networks and Applications (MONET).As of the time of writing this deliverable, we are reviewing it, based on the comments received.

Design of a distributed paging mechanism to reduce over-the-air (OTA) paging signalling traffic in large-scale, all-wireless NoFs. The proposed scheme leverages the standard 3GPP X2 interface between femtocells to propagate paging messages efficiently throughout the wireless multihop backbone.

A paper presenting this mechanism and its evaluation is going to be submitted in brief.

Design of a novel seamless handover procedure for user mobility from a macrocell to a femtocell and vice versa. In this scheme, downlink data received at S-GW is bicasted to both the source cell and the target cell after the handover procedure is actually imitated by the source cell. The proposed scheme has significantly reduced the downlink service interruption time while still avoiding the packet loss during handover

A paper presenting the proposed seamless handover procedure based on reactive data bicasting and the performance evaluation has been submitted to IEEE Communications Letters.

Study on the implementation of networked femtonodes in an enterprise LAN including the LAN configuration changes that are needed to support the networked femtocell group as well as the logical connectivity of the networked femtonodes group to their corresponding femtonode subsystem. Additionally, networked femtonode radio planning, and analysis of effective radio coverage has also been carried out.

Study on procedures to reduce the interference level and the aggregated power consumption in a heterogeneous network deployment that combines a macro layer and a small cell layer served by indoor femtonodes. These procedures involve the power reduction of the macro layer thanks to the indoor service provisioning from the femtonodes, and the switching off of those femtonodes that are not providing any traffic when the users are not at their premises.

2. Traffic Forwarding and Resource Sharing

This chapter reports on results of BeFEMTO's work on traffic forwarding and resource sharing from the last half year of the project.

Sections 2.1 and 2.2 present extended results of prior work on traffic handling in networks of femtocells, i.e. how to efficiently forward traffic between femtocells and femtocell gateway or between femtocells, given that the transport network is a shared resource. Section 2.1 reports on results from the centralized traffic management case, in which forwarding is controlled by a Local Femtocell Gateway (LFGW) that has a complete view of the network. Focus is on the question how femtocell and non-femtocell traffic can share the common local networking resources efficiently. Section 2.2 then reports on extensions of the distributed backpressure routing algorithm that has been designed for the more challenging case of all-wireless networks of femtocells. Extensions are presented for auto-tuning this algorithm and for making it capable of working with multiple LFGWs and routing holes.

Section 2.3 then presents results from a complete study on traffic offloading, which was initially introduced in D5.2. In particular, it studies the effect that opportunistic offloading has on the load and characteristics of the remaining traffic that is still routed via the core network and the consequences this has on network dimensioning.

2.1 Centralized Traffic Management for Cooperative Femtocell Networks

In co-operative femto networks, management of femtocells, including cell provisioning and traffic prioritization, must be handled carefully. In addition to managing the femto traffic, it is also necessary to guarantee that femto traffic is not affected by the presence of non-femto traffic and vice versa. To provision this, either a separate IP network can be provided for femtocells or the femto traffic can be overlaid onto the existing internal network and provide strategies to manage the traffic.

In this context, a potential solution in co-operative femto networks is to provision packets on centralized flow based mechanisms. In flow-based strategies, packets are forwarded based on explicit forwarding state installed in the forwarding elements, allowing the network to be "traffic engineered" for higher resource utilizations. They also allow for a finer control on how network resources are shared between flows. Depending on the classifier used for forwarding, flows-based mechanisms can handle anything from micro flows to aggregate flows, even concurrently.

The current work focuses on networked femtocells case in general and an enterprise network in particular. The target is to design mechanisms necessary to allow resource-efficient traffic forwarding within the co-operative femto networks.

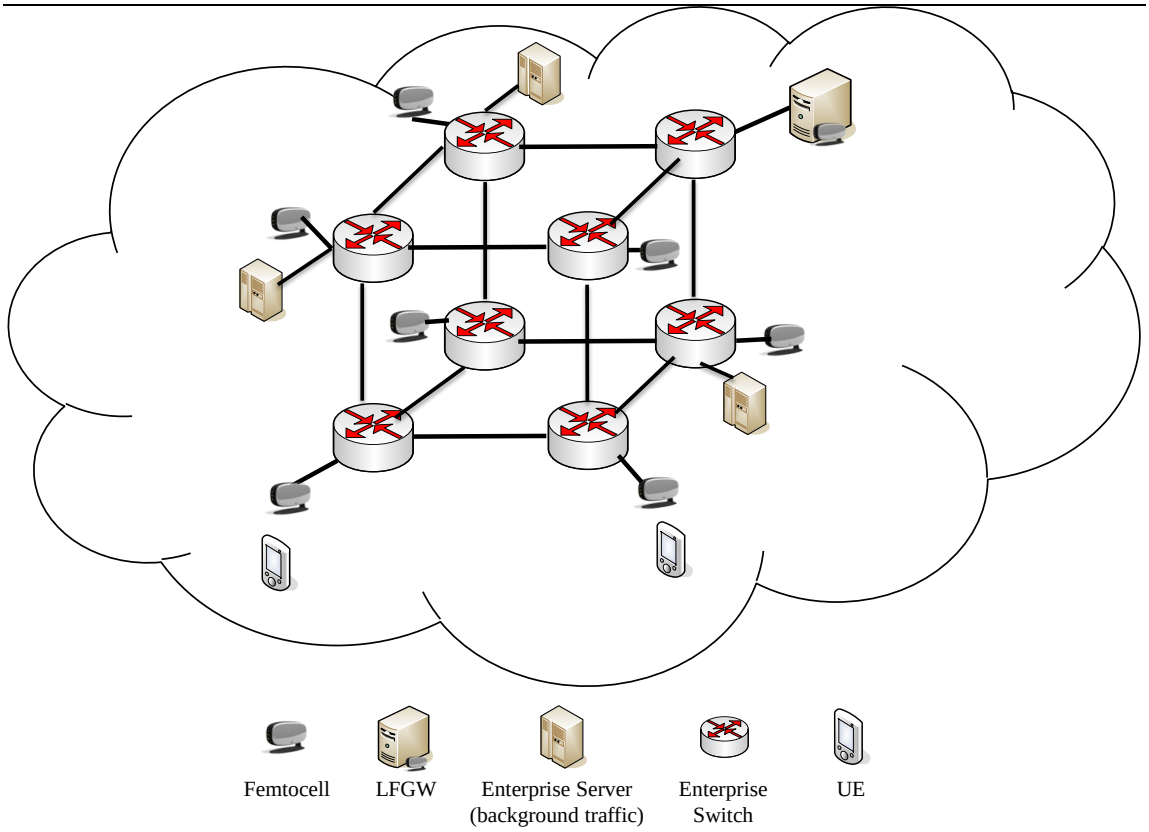

Figure 2-1 Enterprise femto network

The enterprise network under study is depicted in Figure 2-1. It consists of enterprise switches meshed into cubical manner. Further each switch is connected to femtocells and enterprise servers which generate real-time and non-real-time traffic. One of the switches is connected to a femto gateway where all the femto traffic within the enterprise network terminates. The objective of this work is to study the various parameters that affect the real-time traffic and to provide basis for resource sharing and QoS mechanisms for multi-class femto and non-femto traffic within an enterprise network.

This section is organized as follows. The evaluations scenarios for centralized routing solution are explained in section 2.1.1. In subsection 2.1.2, we summarize the simulation setup and the modules that are to be implemented for centralised traffic management. Finally, subsection 2.1.3 concludes this work.

2.1.1 Evaluation scenarios

The initial step is to understand the effects of co-existing traffic in a cooperative femto network. To accomplish this, a scenario for an enterprise network (Figure 2-1) is created where real-time and best-effort traffic, regardless of whether they originate from femto or non-femto, is mixed. The flow tables installed on the switches are based on the MAC addresses of source and destination and forwarding is based on a spanning tree protocol. In other words, the forwarding decisions entries are based on the shortest path between the source and the destination. This scenario will help in understanding the effects of co-existing traffic and will act as a baseline to further design the traffic management entity (TME). The results of the baseline evaluation should lead to answering following questions:

- The issues which arise due to sharing of network between the two traffic stakeholders and how it can be resolved?
- How can resources be guaranteed for the real-time femto and non-femto traffic without starving the best effort traffic?
- How can the operator validate that such resources or SLA are being met?

2.1.1.1 Scenario1

Building on the baseline analysis, the next logical direction is to segregate the femto and non-femto traffic through Virtual Local Area Networks (VLANs) and within each VLANs either provide strict priority or

weighted fair queuing (WFQ) mechanism. The forwarding paths are still based on shortest path algorithms. This can be achieved in two ways which are described below.

Case1: Strict Priority between real-time / non-real-time traffic and WFQ between femto and Non-femto traffic.

This case is shown in Figure 2-2, where a strict priority mechanism is implemented within each VLAN. This approach will ensure that the real time traffic within femto and non-femto network is treated with high priority so as to minimize the latency.

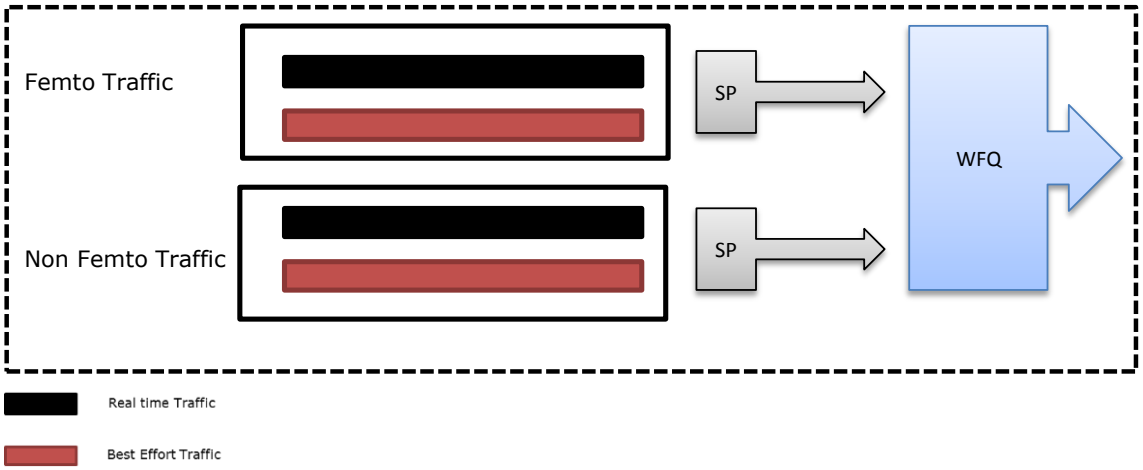

Figure 2-2 SP within VLAN and WFQ between VLANs

This implementation can help to treat the real-time traffic within femto and non-femto domain efficiently. However, WFQ between femto and non-femto traffic might lead to an overall degradation in the performance. Such degradation can be frequent if most of the non-femto traffic is best effort. Under this context, the real-time femto traffic might have to wait for a longer duration in the queue which results into an increased latency.

Case2: WFQ between real-time / non-real-time traffic and Strict Priority between femto and Non-femto traffic.

To overcome the drawback in previous method, as shown in Figure 2-3, we reverse the queuing principle and apply WFQ within the VLAN and then adopt a strict priority.

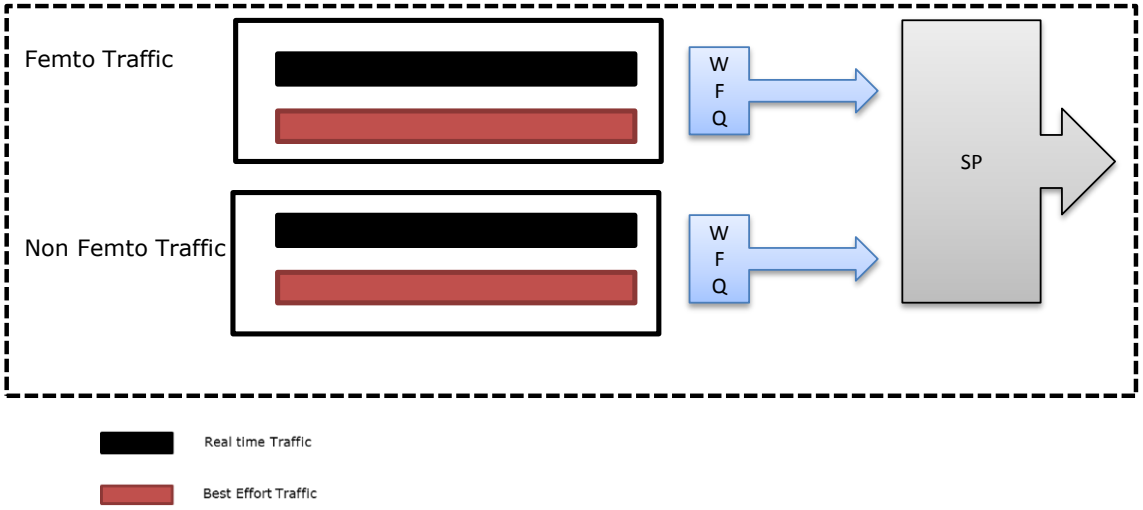

Figure 2-3 WFQ within VLAN and SP between VALNs

This method will work well if the problem mentioned is case 1 is persistent. However, there might be issue which arises when both femto and non-femto are dominant in real-time traffic. This issue can be addressed if we adopt an arbitrary routing mechanism within the enterprise network which will find suitable paths for real-time femto and non-femto traffic.

2.1.1.2 Scenario 2

In this scenario the traffic management will be based on fixed resource allocation method. This allocation can be based on flow tuples which can constitute a) (src_ip, dst_ip) tuple or b) (src_ip, dst_ip, dscp). The queuing mechanism utilised will be the same as scenario 1. However, fixed resource allocation may lead to following disadvantages:

- chronic underutilization of resources,
- highly restricted bandwidth for both enterprise and femto traffic,
- insufficient flexibility under conditions of increasing load.

The magnitude of these will be analysed and based on this analysis we propose a load balancing mechanism.

2.1.1.3 Scenario 3

The function or entity performing the routing for flows needs to be aware of a) the capacity on each link of the topology and b) the traffic within the network which includes the femto and non-femto traffic. Under these requirements a distributed approach for traffic engineering and routing would require a large signalling overhead to disseminate this information to all routing functions and would be more complex and thus more error-prone to implement. It therefore seems logical to take a centralized approach, in which traffic engineering and routing is performed within a single "routing controller" function that then installs paths with the forwarding entities in the network.

Based on the analysis of scenario 2, the logical direction for centralized routing in cooperative femto networks would be to introduce dynamic resource allocation mechanisms. Under this scope, in this work, we propose to implement and evaluate a centralized routing based on load-balancing architecture using OpenFlow switches which are connected to a common controller.

OpenFlow was created in 2008 by a team from Stanford University. OpenFlow switches are like a standard hardware switch with a flow table performing packet lookup and forwarding. However, the difference lies in how flow rules are inserted and updated inside the switch's flow table. A standard switch can have static rules inserted into the switch or can be a learning switch where the switch inserts rules into its flow table as it learns on which interface (switch port) a machine is. The OpenFlow switch on the other hand uses an external controller to add rules into its flow table. These rules can be based on more fine-granular identifier like QoS requirements, which will help in selecting the next forwarding hop and to route the femto and non-femto traffic efficiently within cooperative femto networks (Figure 2-4).

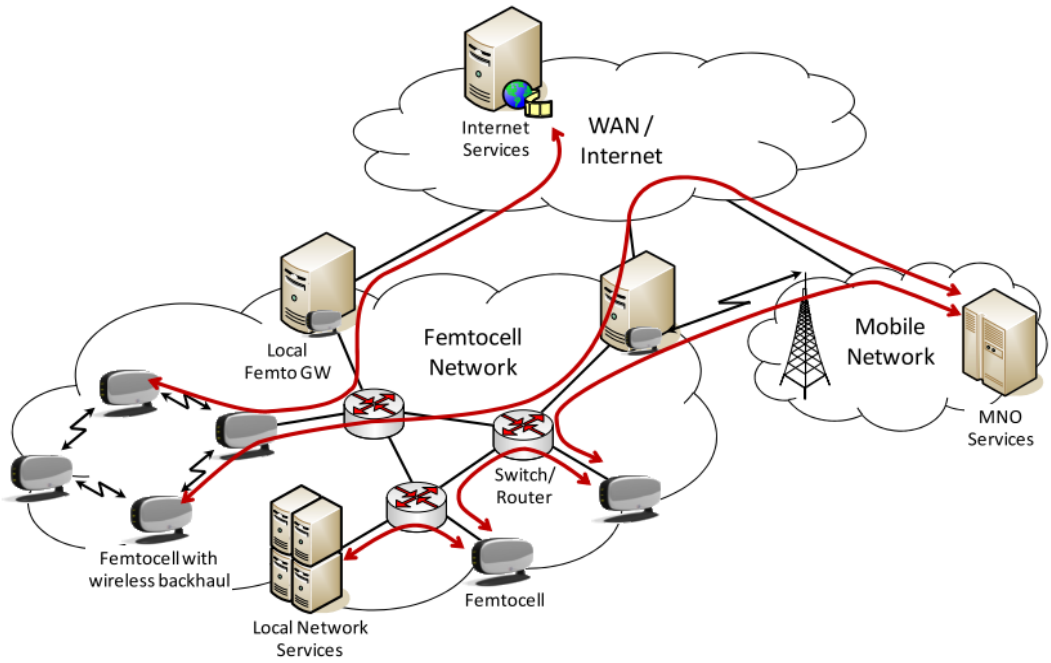

Figure 2-4 Centralized Routing Based on OpenFlow

As evident, the load balancing strategies in an OpenFlow based environment has to be designed at the controller to which the switches are connected. This design is governed by the following criterions:

- What kind of information does the controller require and where does it get it from?

  In an OpenFlow based solution the controller is responsible to install flow tables in the switches. To make an efficient decision the controller requires a constant influx of flow requirements. This information can be related to topology, capacity, utilization/load etc. In such a scenario it is necessary to decide if an external Traffic Management Entity (TME) is required in the network or it can be a part of the controller itself. Moreover, in a cooperative femto network, femto and non femto traffic may have different QoS requirements. Hence, the flow tables installed on the switches should be able to address these individual requirements.

- How long are flows valid?

  In cooperative femto networks the traffic flow can be very dynamic and hence the flow table should be update frequently. This can be done either pro-actively or reactively, whichever is suitable to optimize the traffic flow. However, frequent changes in the flow tables will result in a lot of traffic between the switches and the controller which will be an overhead in the network. Hence the flow tables should be able to adapt to these situations without inducing delay in decision making process.

With these two basic design requirements we analyse the cooperative femto network with basic configuration and based on the analysis we design a load balancing method in the controller.

The evaluation scenarios are summarized in Table 2-1

	Scenario 1	**Scenario 2**	**Scenario 3**	**Scenario 4**
Routing	Spanning Tree	Spanning Tree	Arbitrary Routing	Arbitrary Routing/ Load Balancing
Flow	Single flow	Flow based on (DSCP, VLTAG) tuple	Flow based on (Femto IP, Gateway IP)	Open switch Scenario, with flow based on TEID
No. of Queue	1	4	4	4
Queuing Principle	FIFO	SP and WFQ	SP and WFQ	Priority

Table 2-1 Evaluation Scenarios

2.1.2 Simulation Analysis

The analysis and implementation of the scenarios mentioned in 2.1.1 are carried out in the simulation environment of ns-3. Within the simulation environment, the switches presented in an enterprise hypercube structure (Figure 2-1) are modelled as OpenFlow switches connected to a controller. This controller can install flows on the switches according to the respective forwarding strategies (spanning tree, arbitrary routing or arbitrary routing with load balancing) of scenarios 1-4. Within ns-3 simulations OpenFlow switches are configurable via the OpenFlow API, which can provide extension for quality-of-service and service-level-agreement support. The OpenFlow modules and the configuration messages in ns-3 are kept the same format as a real OpenFlow-compatible switch, so the implementation of the

Controllers via ns-3 can presumably work on real OpenFlow-compatible switches. The network designed in ns-3 has the following characteristics:

- Data Rate: 1Gbps
- OpenFlow switches with either learning(Spanning Tree) or basic load balancing controller
- Queue Length at individual switches – 100 packets
- Queuing Discipline: Drop tail and Priority Queuing

In a traditional enterprise network, the traffic can be classified into three basic categories voice, video and background traffic. To study the performance of the network and to determine the point where the network degrades in the performance parallel flows of these three traffic types are initiated. The general characteristics of the traffic are:

- VoIP – For the simulations purpose the VoIP codecs mentioned in [4] are used. The codec has eight source encoding rates which range from 4.75kbps to12.2kbps for voice payloads, a sampling rate of 8 khz and a static frame size of 20ms is used for all rates. It should be noted that the 12.2kbps mode of AMR achieves almost the same voice quality as the commonly used G.711 (64kbps) codec but with significantly lower bit rates at the application layer.
- Video – Video streaming using UDP trace client application in ns-3 (MPEG4 video trace)
    a. Data Rate: 5-6 Mbps
    b. Variable Bit Rate (VBR)
- Background (Best Effort) – Generated in ns-3 using the tool based on the Poisson Pareto Burst Process (PPBP)
    a. Data Rate : 1Mbps
    b. Arrival Rate : 20 secs
    c. Burst Duration : 200ms

With these network and traffic characteristics the simulations are carried out and the evaluations are discussed further sections.

2.1.2.1 Evaluation of Scenarios

The first scenario under study is a network where the controller acts like a traditional switch and learns the network over a period of time. The simulation results show that presence of background traffic along with real time video and voice traffic severely affects the quality of the video (Figure 2-5).

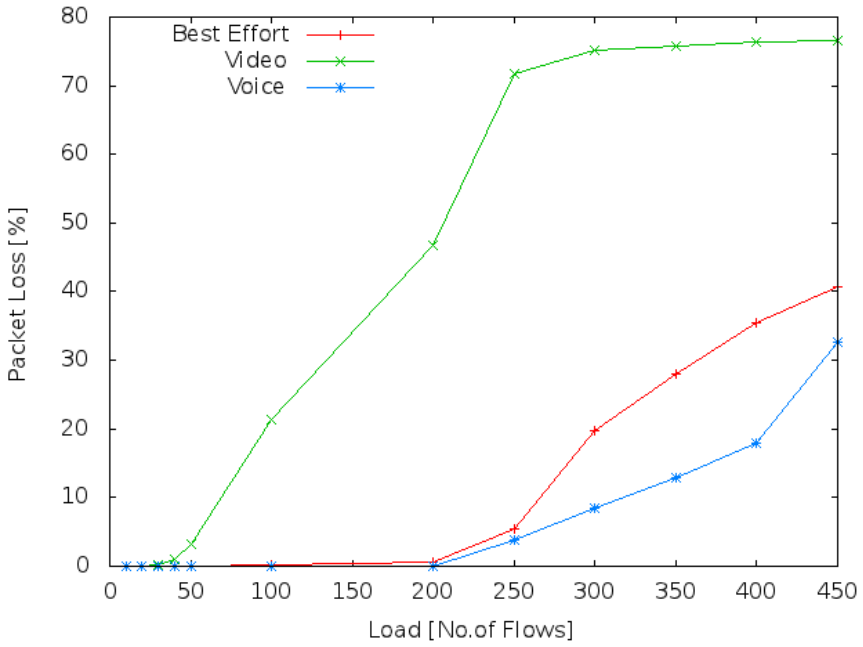

Figure 2-5 Packet Loss in baseline scenario

The base line scenario can at the maximum support 30 flows of video, voice and background traffic. During the simulations more flows are added onto the network; however the network does not support beyond 30 flows of videos. From 50 to 100 flows the packet loss experienced by video stream varies between 3% - 21%. Thus, indicating the zone where the video breaks down. In case of VoIP traffic, the flows break down between 200-250 parallel flows where the packet loss lies between 0.08% - 5%. In terms, of end-end delay experienced by the packets in the network (Figure 2-6) video streams experience a delay of 4- 5 ms for 50 – 100 parallel flows where are the voice traffic undergo a delay of 8- 11 ms while supporting 200-250 flows. This performance is certainly way below the desired QoS which is summarized as [5]:

- Voice
    a. Loss should be no more than 1 %
    b. One-way Latency (mouth-to-ear) should be no more than 150 ms
    c. Average one-way Jitter should be targeted under 30 ms.
    d. 21-320 kbps of guaranteed priority bandwidth is required per call (depending on the sampling rate, VoIP codec and Layer 2 media overhead).
- Video Streaming
    a. Loss should be no more than 5 %.
    b. Latency should be no more than 4-5 seconds (depending on video application buffering capabilities).
    c. There are no significant jitter requirements.

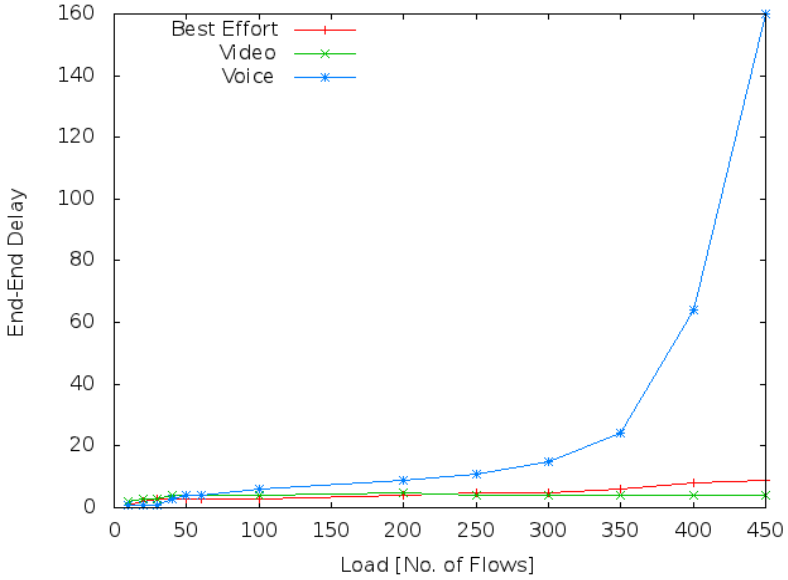

Figure 2-6 End-End Delay in baseline scenario

These results lead way for implementation of the priority queues within OpenFlow switches, the forwarding within this scenario is still based on OSPF with priority. The decisions taken by the controller are based on the DiffServ Code Point (DSCP) with VoIP being the highest priority and background traffic being the least. In this scenario the OpenFlow control messages are treated as highly important are prioritized over VoIP. Figure 2-7 and Figure 2-8 depict the packet loss and delay experienced by the flows in this scenario.

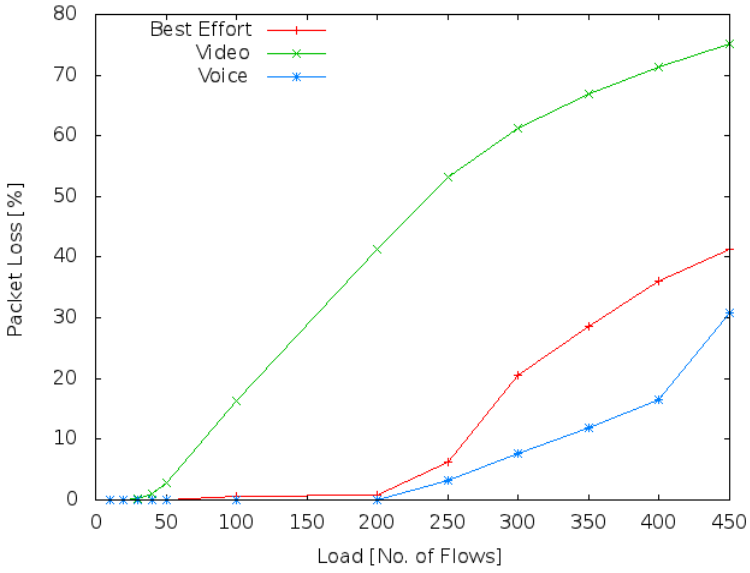

Figure 2-7 Packet Loss with priority

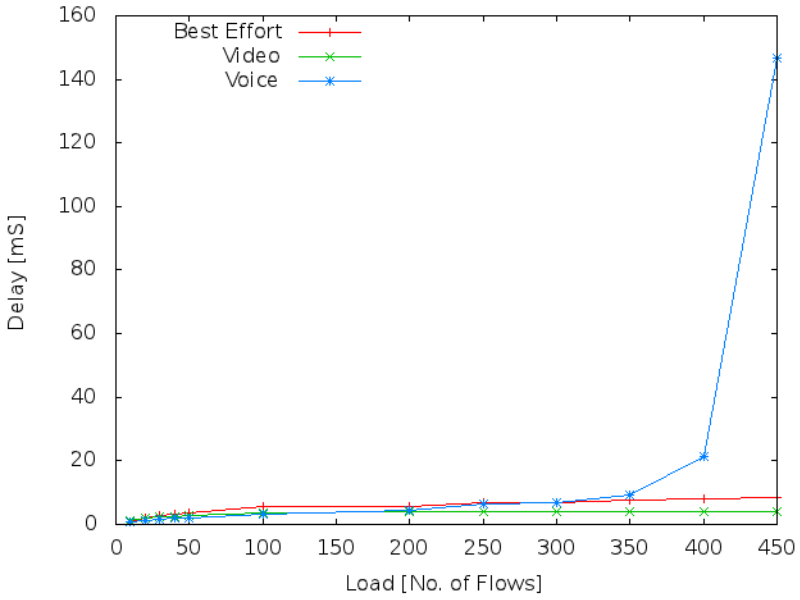

Figure 2-8 End-End Delay with priority

The results show that the performance of the network is improved in this scenario. This was quite expected because of the priority associated with the packet streams. The video stream experiences a packet loss of 2%-16% (50-100 Flows) and for voice it varies from 0.05%- 3% (200-250 Flows). In terms of delay the video streams range in between 2- 4 ms (50-100 Flows) and voice is placed between 3 – 4 ms (200-250 Flows). Though the priority treatment improves the performance in terms of packet loss and delays, these values are still below the expected QoS requirements. Moreover, they do not improve on the number of flows which can be supported in parallel. This situation calls for implementation of more advanced load balancing controllers which will not only assist in improving on the QoS within an enterprise network but also result into more parallel flows in the network. This criterion is especially important for the different stake holders in the enterprise femto network.

In the next section we introduce the well-studied valiant load balancing (VLB) technique [6] and analyse its performance in an enterprise femto-network.

2.1.2.2 Evaluation of Load Balancing Network

VLB can be useful in an enterprise femto network because of the following desirable properties when links fail or overload:

- In order to protect against k failures the fraction of extra capacity required is only k/N, where N is the diameter of the network. This is extremely efficient compared to other fault tolerance schemes.
- All of the working paths between a pair of nodes are used all the time, and flows are load-balanced across all working paths. Most other schemes require protection paths that are idle during normal operation.
- VLB naturally protects against multiple failures. One can decide during design what failure scenarios the network should tolerate, such as k arbitrary link or node failures or a particular set of failure patterns.
- All paths operate all the time, so rerouting is instantaneous

With these advantages, we implement the VLB controller in ns-3 environment with priority queues discussed in the previous section.

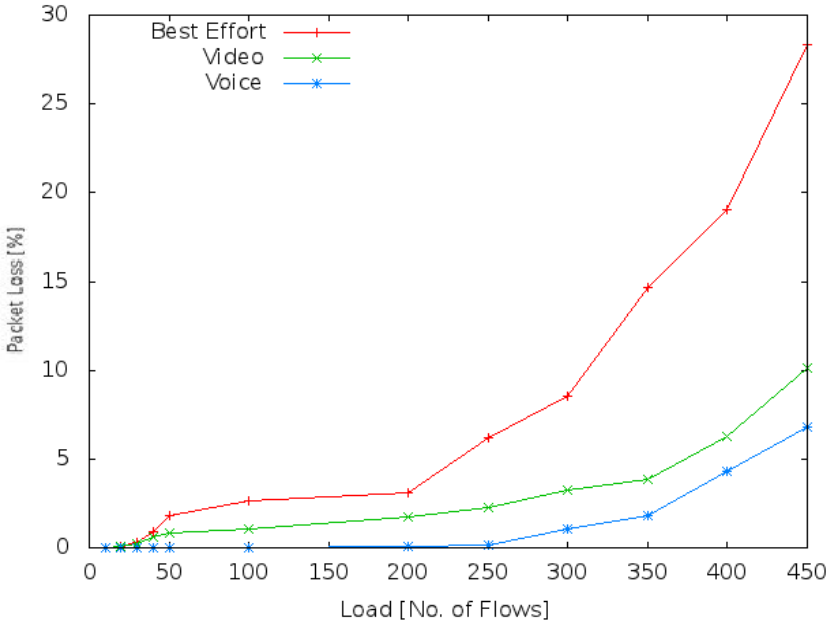

Figure 2-9 Packet Loss in VLB based scenario

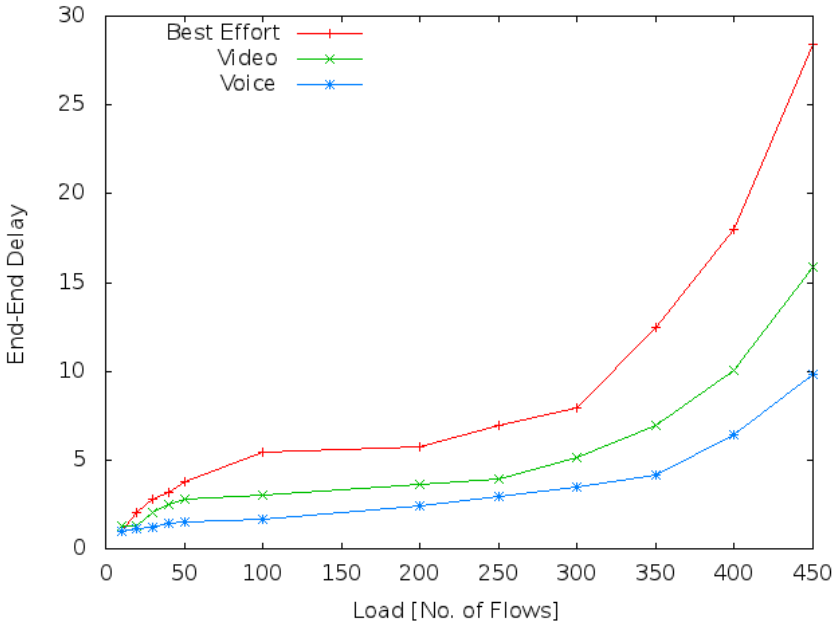

Figure 2-10 End-End Delay in VLB based scenario

Figure 2-9 and Figure 2-10 depict the performance of the enterprise femto network with a load balancing controller. It can be observed that load balancing helps in improving the video flows drastically; this is because availability of multiple paths reduces the overall load on the network since the packets can be alternately forwarded through multiple paths. In addition to this, more number of parallel flows can be supported within the network, which is encouraging for both the stake holders.

However, this implementation is a more proactive method, where the paths alternate. In an enterprise femto scenario there can be potential to balance the load based on reactive techniques, thereby further improving the QoS and the number of flows which can be supported.

Nevertheless, the results obtained from VLB are encouraging enough to promote the co-existence of traffic from different stakeholders, namely, the enterprise traffic (non- femto) and the femto traffic. The results also push deployment of networked femtocells without affecting the existing setup in an enterprise network.

2.1.3 Conclusion and Future work

The baseline scenario assisted in understanding the effects on the co-existing traffic. Here we found that the video and voice traffic experience a significant degradation in QoS and very few parallel flows can be supported. The analysis of second scenario, laid the foundation for understanding the overheads involved in such cases and if traffic management can be achieved through a simple approach. The results show that through priority queues the voice quality is significantly improved, however the video stream still observed a degraded performance. This meant that there is a need for a better load balancing technique in a cooperative femto network. The final scenario, facilitated to study the performance enhancement which can be achieved for different stakeholders in a networked femto cell scenario using VLB method. VLB when combined with OpenFlow switches can significantly improve the QoS for voice and video and also support more parallel flows of traffic from different stakeholders. The performance enhancements obtained from the load balancing scenario (OpenFlow with VLB controller) and further scope for improvement results into key inference that, different stakeholders in a networked femto scenario need to be supported by load balancing techniques to ensure the QoS. This can be ensured through the use of OpenFlow switches which are connected to a centralized load balancing controller.

2.2 Distributed Routing

One important concern of any MNO is to minimize the cost of deploying infrastructure for the backhaul. All-wireless network of femtocells (NoF) try to cover the necessity of giving cellular coverage in scenarios where there is the need for a fast deployment and/or the deployment of fiber/copper would be economically unfeasible (e.g., airports, shopping malls, temporary deployment in conference halls, or a fixed deployment in a rural zone). As a result, MNOs have an increasing interest in the use of other wireless technologies as backup technology, or even as primary backhaul due to the high cost and unfeasibility of deploying wired infrastructure.

In this context, we conceived and developed a distributed routing protocol suited to such challenging scenarios. If optimally tuned, this can entail several benefits for the MNO in terms of Operational Expenditure (OPEX). Though the scheme designed can be used over any underlying wireless technology, in this section we focus on studying the performance of Wi-Fi as a potential backhaul solution as a way of evaluating the concept. Our target is to evaluate its feasibility and to give hints on under what conditions (number of nodes, traffic load, number of gateways, etc.) these requirements may be fulfilled. Notice that in this context, backhaul is understood as the wireless multi-hop network interconnecting the femtocells that form the NoF, that is the local backhaul of the network of femtocells.

This section is organized as follows. In subsection 2.2.1, we summarize the work done during project year 2 on the extensive evaluation results of the distributed routing solution. After that, the final solution and evaluation of the distributed routing solution enhanced with the variable-V algorithm is presented in subsection 2.2.2. Subsection 2.2.3 presents the strategy taken for the deployment of multiple LFGW and how the routing protocol benefits from this strategy without changes. Subsection 2.2.4 evaluates how the proposed solution is able to circumvent holes in the NoF. Finally, subsection 2.2.5 draws conclusions.

2.2.1 Work during Year 2

The second project year consolidated the main ideas behind the distributed routing protocol proposed during the first year (see D.5.2 [2] for a detailed explanation). Specifically, we studied the routing problem from a Stochastic Network Optimization perspective exploiting Neely's theoretical work [7]. Remarkably, to our knowledge this is the first practical study based on Neely's Lyapunov optimization framework for an all-wireless NoF. Moreover, we perform extensive simulation through ns-3 simulator [8] of the resulting distributed backpressure routing protocol.

A summary of the main characteristics of the routing protocol shown in D5.2 follows. The resulting distributed backpressure routing protocol is practical in the sense that, unlike previous theoretical centralized algorithms [9], we presented a distributed implementation of the algorithm with low queue complexity (i.e., one finite data queue at each node) to deal with any-to-any communications (i.e., uplink, downlink and even local routing). In fact, we proposed a scalable and distributed routing policy that takes control actions based on Lyapunov's drift-plus-penalty minimization combining local queue backlog and 1-hop geographic information. Such framework offers a non-negative fixed parameter (V) for weighting between both mentioned components.

A summary of the main evaluation work carried out with the routing protocol in D5.2 follows. We first characterized its strengths and weaknesses against all-wireless NoF performance metrics such as throughput, delay, and fairness injecting several flows. By means of ns-3 simulations under different configuration setups, we studied the impact of the weight of the penalty function (i.e., the V parameter) on the network performance metrics. In addition, we showed the influence of the location of the source-destination pairs in these configuration setups. Finally, we evaluated the objective function-backlog trade-off that characterizes Lyapunov optimization frameworks.

One of the most remarkable findings noted during the evaluation carried out in D5.2 is the existent trade-off presented between 1) routing decisions for maintaining queue backlogs under control (and hence, the all-wireless NoF stable) and 2) routing decisions trying to get close to the optimal value of an objective performance metric. As a matter of fact, to achieve an appropriate trade-off the weight of the penalty function denoted by the fixed parameter V is of primal importance.

The second finding is that fixed-V policies configured in every Home eNodeB (HeNB) cannot efficiently handle NoF traffic dynamics in practical setups, since they will lead to queue overflows and/or degradation of the objective metrics. We proposed the use of a practical distributed variable-V algorithm that takes routing decisions aiming at achieving ideal objective metric values, yet not incurring into queue overflows. An initial set of ideas to build this variable-V algorithm came out at the end of the second year of the project.

Finally, we initiated the work towards the extension of the proposed distributed routing protocol to handle multiple LFGWs, and the management of sparse deployments which are also subject of further study during last half-year of the project.

In summary, along the next subsections, we provide a description of the work carried during the last half-year of the project to continue the work towards the study of the previously mentioned open research issues. Mainly:

- In section 2.2.2 we show current progress, enhancements, and evaluation on the variable-V (or adaptive weight) algorithm. Precisely, we come up with an additional variable-V algorithm which provides several enhancements with respect to the previous variable-V algorithm defined in D5.2.
- Design, implementation, and evaluation of the distributed routing protocol to handle multiple LFGWs leading to dynamic anycast backpressure routing in subsection 2.2.3.
- Study of how the routing protocol behaves under sparse deployments with dead-ends in an all-wireless NoF without changing its principles (i.e., stateless, distributed, self-organized, zero-configuration in HeNBs, agnostic of the wireless backhaul technology) in subsection 2.2.4.

2.2.2 Variable-V algorithm: Final Solution and Evaluation

Results previously shown in D5.2 suggested the importance of a variable-*V* algorithm to avoid queue drops at the NoF. Specifically, we showed that the traffic served could highly vary (in terms of throughput, delay, jitter and fairness) depending on the *V* parameter. In an all-wireless NoF, it is expected that the input rate matrix, and even the network topology could be variable in time. For instance, mobility of UEs could also lead to changes in the input rate matrix in the NoF(i.e., the HeNB injecting traffic coming from a given UE can change). On the other hand, HeNB in the network may fail tuning into an inoperable state, hence changing the network topology. The distributed routing protocol enhanced with a variable-V algorithm is able to react due to the adaptation to dynamic conditions the variable-V algorithm poses. Furthermore, the fact that the variable-V algorithm is also distributed, and self-organized satisfies the initial conditions posed by the all-wireless NoF (i.e., distributed, low-state…).

As explained in D5.2, the goal of the variable-V algorithm is to avoid queue drops while still minimizing the penalty function (see D5.2 for a more detailed explanation of the routing algorithm). In D5.2 the variable-V algorithm recomputed the V parameter for every HELLO message received from 1-hop HeNB neighbours (i.e., on a per HELLO message basis). In next subsections, we provide more insights behind this approach. Additionally, we propose two major changes in the calculation of the variable-V algorithm. On the one hand, there is an additional algorithm that corrects the algorithm periodically calculated on a per HELLO message basis per each data packet. On the other hand, there are some changes in the computation of the variable-V algorithm on a per HELLO message basis.

2.2.2.1 Updates on the Variable-V algorithm calculation on a per HELLO messages basis

A description of the final variable-V algorithm updated from the algorithm described in D5.2 to autoconfigure the *V* parameter in every HeNB follows. As depicted by Figure 2-11, a HeNB *i* builds a virtual queue describing network conditions in terms of network load exploiting 0-hop (i.e, the info in the current node), and 1-hop information of the data queues at every timeslot *t*. In other words, the variable-V algorithm aggregates the information gathered from 1-hop HeNBs in terms of congestion to estimate current, and future local network congestion conditions. To adjust V_i (t), the variable-V algorithm estimates an upper bound of the expected maximum queue backlog in the 1-hop neighbourhood at time slot *t+1*.

Specifically, the queue backlog has two components. First, a queue backlog quantifying congestion around the 1-hop HeNB neighbourhood during current timeslot *t*. Second, a queue backlog estimating future congestion at next timeslot *t+1*.

The goal of the variable-V algorithm is to increase the importance of the penalty function, while not leading to queue drops in the data queues of the HeNBs. On the other hand, we showed in D5.2 that there is a relation between the appropriate value of $V_i(t)$ and the number of packet transmissions of node *i*. The underlying idea behind our scheme lies in the fact that we consider $V_i(t)$ as the maximum number of packets that could potentially be greedily transmitted from node *i* to one of its neighbours *j* without exceeding Q_{MAX}. In this case, greedily means that Lyapunov drift minimization is not taken into account when sending traffic. This estimation is based on 1-hop queue backlog information at time slots *t* and *t-1*, being *t*>0. More specifically, we propose the following distributed algorithm:

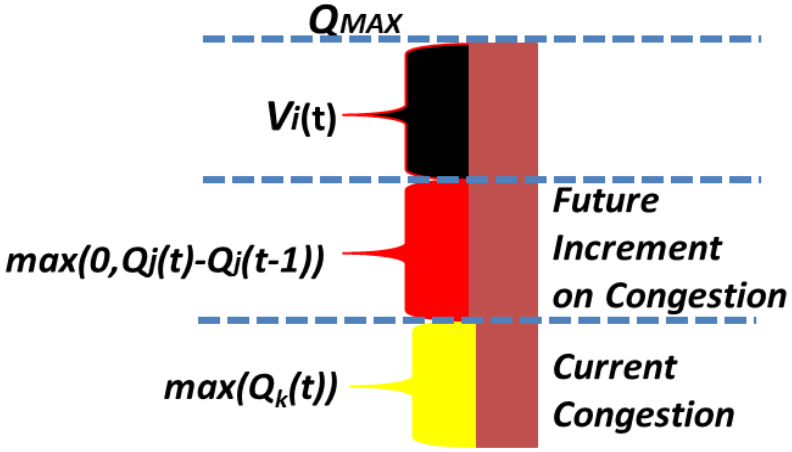

Figure 2-11 Illustration of the calculation of the variable value of V

Distributed Variable-V algorithm on a per HELLO message basis:

If t=0, $V_i(t)=Q_{MAX}$, at time t=1,2,3 … let

$$V_i(t) = \max(0, \max(Q_{MAX}, Q_{MAX} - \max \Delta Q_j(t) - \max Q_k(t))); k, j \in J$$

where max(Q_k (t)) is the maximum of all backlogs of nodes $\in$ J (i.e., the set of 1-hop neighbours of node *i*), and max(ΔQj *(t)*) is the maximum differential $Q_j(t)$-$Q_j(t-1)$ experienced by 1-hop neighbour queues of *J* between time slots *t* and *t-1*. The sum of $max(Q_k(t))$ and $max(0,Q_j(t)-Q_j(t-1))$ provides an upper bound (i.e., worst case) of the maximum queue backlog a neighbour of *i* may experience in time slot *t+1*, assuming there is no sudden change neither in the offered load in the network nor in the topology. The difference between Q_{MAX} and the estimated congestion at time slot *t+1* in terms queue backlog determines the value of $V_i(t)$ for time slot *t*. Figure 2-11 is a representation of the worst case queue backlog of the neighbor set of *i* expected at time slot *t+1*. Since the value of $V_i(t)$ represents the maximum number of allowed greedy transmissions from node *i* during a given time slot, $V_i(t)$ is also a key component in the estimation of the future more congested queue backlog in Figure 2-11.

1) Practical Considerations: The specific duration of the time slot determines the efficiency of the proposed distributed routing algorithm. More specifically, the algorithm is assuming the knowledge of past queue backlog differential information (i.e., $Q_j(t)$-$Q_j(t-1)$) to estimate future queue backlog differentials. In other words, it is implicitly assuming that there are no abrupt changes in the differential

of queue backlogs with neighbouring nodes, and so, in the offered load in the NoF during time slot (*t, t+1*). Thus, the smaller the duration of the time slot (*t, t+1*), the faster *V* would adapt to varying conditions.

In order to build this aggregated queue and so get the new value of the *V* parameter at a given node (see Figure 2-11, there are three basic components locally accessible to take into account:

Q_{MAX}: This is a constant value of the system corresponding to all the nodes in the NoF that denotes the data queue length limit allowed at a HeNB to do no experience queue drops. There is a significant disparity in the buffer size limit used in various research platforms. In this study, we opt for the most common buffer size of the MadWiFi legacy drivers (i.e., buffer size of 200 packets), which is the default value used in the ns-3 network simulator.

max(0,$Q_j(t)$*-*$Q_j(t-1)$*):* This component summarizes the previous event experienced in the neighbourhood of a given node including the local HeNB (i.e., the HeNB at 0-hops) that leads to the most increasing queuing backlog with respect to previous timeslot. The fact of including the local HeNB in this component increases the capacity of the variable-V algorithm is useful to react under sparse all-wireless NoF deployments. This is usually caused by the injection of a new flow or set of flows in the network, the increase in the offered load of an existing flow, or even the failure of a given HeNB which may cause other HeNBs to increase their load. It is calculated as the maximum increase experienced in the data queue length of a neighbour between two timeslots. The estimator uses this component to estimate the future next event that will cause an increment of data queue lengths. Basically, we are assuming that the bigger increase in data queue lengths during time interval (*t , t+1)* is the same as the one experienced during time interval (*t-1, t)*. This component can be calculated in a distributed manner by means of storing the queue lengths of every HeNB neighbour experienced in two consecutive timeslots.

max($Q_k(t)$*):* This component describes the HeNB with maximum data queue length from the set of HeNB nodes describing the current network congestion conditions. The fact of including the local HeNB in this component increases the capacity of the variable-V algorithm for reacting under sparse all-wireless NoF deployments. Note that the HeNB experiencing the maximum data queue length in the 1-hop neighbourhood could be different from the HeNB, which experiences the bigger increase during the previous timeslot. For instance, this could happen if a HeNB do not have enough transmission opportunities due to the CSMA/CA medium. Thus, in this case the HeNB keeps its data queue highly loaded.

$V_i(t)$: This corresponds to the maximum number of packets that potentially can be transmitted in the aggregated virtual queue without causing a queue overflow.

As a result, the sum of the previous three components corresponds to the queue limit of the HeNB in the NoF:

$$Q_{MAX} = max(0, Q_j(t)-Q_j(t-1)) + max(Q_k(t))+V_i(t)$$

2.2.2.2 Practical Variable-V algorithm: Calculation on a per-packet Basis

Recall that, so far, the recalculation of the *V* value at time slot *t* in each HeNB was carried out periodically, at every timeslot. In practice, the duration of a timeslot corresponds to the time required to receive HELLO messages from all the neighbours of a HeNB.

Precisely, every time a HeNB receives a set of HELLO messages from all its neighbours with their associated queue backlog information, the HeNB exploiting the variable-*V* mechanism presented in previous section, self-regulates the *V* parameter. Actually, the new V value at a HeNB remains valid until it receives a new set of HELLO messages from all its neighbours. Therefore, all the weights calculated for taking routing decisions within (*t, t+1*) use the same *V* value. This means that a considerable bunch of packets intended to be sent by every HeNB during interval (*t, t+1*) are routed using the same trade-off between the Lyapunov drift and the penalty function, even though they could have a different "necessity" to reach the destination. Note that a HeNB can keep in its queue data packets corresponding to different flows. And these packets may have different needs in terms of end-to-end delay.

The main intuition behind the recalculation of the *V* parameter on a per-packet basis can be illustrated with an example. For instance, consider two packets *a* and *b* accumulated in a data queue in a HeNB *i*.

Assume that the delay traversing the NoF of packet *a* and *b* is quite different. While packet *a* traversed *n>0* hops till $HeNB_i$ receives it, $HeNB_i$ generates packet *b*. Our mechanism proposes to forward data packets *a* and *b* with a different *V* parameter. Specifically, the *V* parameter is higher in the case of packet *a* than in the case of packet *b*. In particular, the increase of the *V* parameter depends on the number of

hops traversed by packet *a*. On the other hand, $HeNB_i$ uses the *V* parameter already calculated on a HELLO message basis to forward data packet *b*.

Therefore, we propose an additional modification to recalculate the *V* parameter on a per-packet basis. To distinguish between the different packets, we use the IP "time-to-live" (TTL) field, which specifies the maximum number of hops a packet can traverse within the transport network. The TTL is by default decreased by one at every hop traversed in the transport network. Thus, the TTL provides an idea of the time spent by a packet in the NoF. We propose to use the TTL to correct the *V(t)* value periodically calculated for a bunch of packets for a slot interval *(t,t+1)*. Specifically, the lower the TTL field the higher the increment experienced by *V(t)* for that packet.

$$V_{packet} = V(t) + f(Packet_{TTL})$$

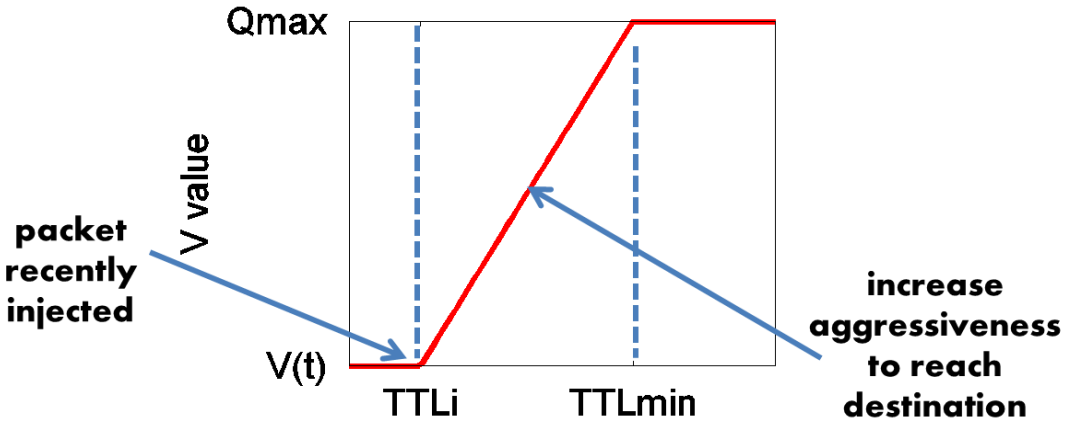

Figure 2-12 Per-packet V calculation as a function of TTL

The modification of the algorithm works as follows (see Figure 2-12). Prior to route a data packet, the Var-*V* algorithm looks at the IP packet header and gets its TTL value. If the TTL is lower than the TTL_i, the *V(packet)* algorithm modifies the value calculated by the variable-*V* algorithm *V(t)* as follows:

$$V(packet) = \frac{TTL_i - TTL_{packet}}{TTL_i} \cdot (Q_{MAX} - V(t)) + V(t)$$

In our specific case, the penalty function is tightly related with the end-to-end delay packets may experience. Additionally, the time packets have been in the NoF is directly related to the TTL field in the IP header. The lower the TTL, the higher the time spent in the NoF. As a result of this, we propose to bias *V(t)* as a function of the time the packet has been routed over the NoF. Specifically, we propose to increment the *V(t)* algorithm calculated every time slot and so the emphasis in the penalty function as the TTL field in the header of the packet decreases.

- TTL_i corresponds to the higher TTL a packet has to experience in order to apply the proposed algorithm to the packet. This is a parameter that can be configured by the routing protocol.
- TTL_{min} corresponds to the minimum TTL value accepted to include a queue load balancing in the routing decision. This is a parameter to be configured by the routing protocol. This parameter would come determined by the delay requirements of the NoF. Specifically, if the NoF specifies the maximum delay a data packet may experience.
- TTL_{packet} corresponds to the TTL value for the packet.

V(packet) is the *V* value used to forward data packet. The calculation of *V* on a per-packet basis is especially important for improving end-to-end delay in a NoF loaded with multiples flows, and hence with a high degree of TTL variability at HeNBs.

Finally, there are two observations we want to highlight, which may pose limitations on the proposed *V(packet)* algorithm :

- The first observation is that the total delay accumulated by a data packet in the NoF is not merely quantified by the number of hops traversed by a data packet. In addition to the number of hops traversed by a data packet in the NoF, a more precise *V(packet)* estimator should take into account the time spent by packets in data queues. A more complete study should be the one taking into account both queueing delay, and the number of hops traversed in the NoF. However, as a first approximation we opt the study which already shows important benefits in terms of delay, as will be shown in section 2.2.2.3.
- The second observation is the increase of the packet dropping probability due to queue drops with the increase proposed by the *V(packet)* algorithm. Under high congestion conditions, the *V(packet)* algorithm can force to forward a data packet to a HeNB neighbour quite congested, leading to queue drops. This is likely to happen in a circumstance in which the TTL of the forwarded packet is quite low. We propose to configure the TTL_{min} to a value in which the more important factor is to reach the intended destination than maintaining a degree of load balancing such that there are no queue drops at the expense of incrementing the queue drops in the network.

2.2.2.3 Practical Variable-V algorithm: Evaluation

Evaluation Methodology:

In all the experiments evaluating the variable-V algorithm, the injected traffic consists of unidirectional UDP with maximum packet size (i.e., 1472 bytes) at a CBR generated by the ns-3 OnOff application. The duration of each simulation is of 120 seconds. The data queue size limit assigned to the HeNBs is of 200 packets. Therefore, in this case, using a *V* parameter greater than or equal to 200 means using the shortest path in terms of Euclidean distance to the destination. On the other hand, the lower the *V* parameter (i.e., from 200 up to 0), the bigger the degree of load balancing offered by the backpressure routing protocol. The wireless link data rate used by all HeNBs in the backhaul is a fixed rate of 54Mbps.

We label the variable-*V* algorithm computing periodically the *V* parameter as *VarPrev-V*, and the variable-*V* algorithm computing the *V* on a per-packet basis as *Var-V*.

With regards to the configuration of the variable-V algorithms, the *VarPrev-V* algorithm calculates *V* every 100ms, and the *Var-V* computes the *V* parameter for each data packet. We configured the TTL_i to 60 in *Var-V* so that the data packets can traverse at least 4 hops in the NoF without giving importance to the calculation of *V* on a per-packet basis. Additionally, the TTL_{min} is configured to 50, meaning that if a packet traverses 14 hops the queue backlogs are not taken into account to compute forwarding decisions. In this case we consider the data packet requires to be received by the destination even at the expense of being dropped by a data queue.

A special case: Bidirectional Symmetric Traffic:

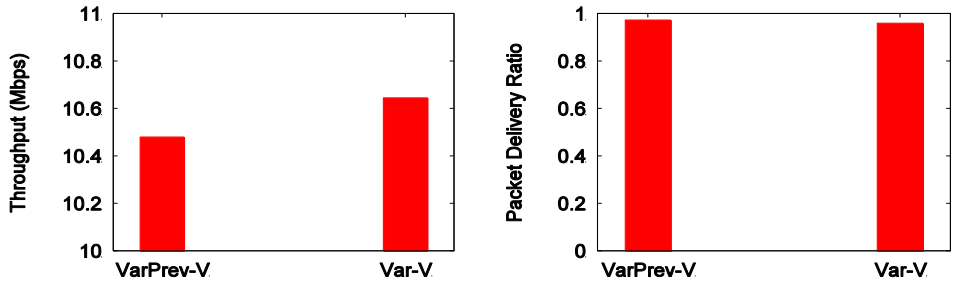

Figure 2-13 Throughput and Packet Delivery Ratio for VarPrev-V and Var-V algorithms

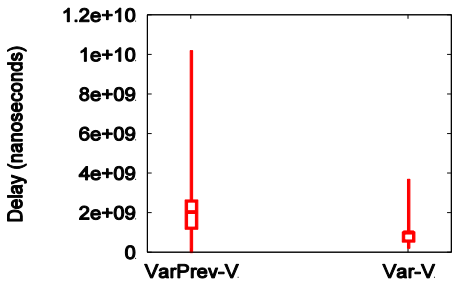

Figure 2-14 Comparison of Delay and Packet Delay Distribution for VarPrev-V and Var-V algorithms

This experiment already illustrates the potential improvement in the packet delay distribution in the NoF, comparing NoF performance metrics with the variable-V algorithm recalculating the *V* parameter every 100ms (i.e., *VarPrev-V*), and *Var-V* which includes the correction on a per-packet basis.

The experiment is based on sending bidirectional traffic between two HeNBs in the transport network. The minimum distance between both HeNBs is of 5 wireless hops.

In this case, Figure 2-13 shows that in terms of packet delivery ratio and throughput, both variable-*V* algorithms do not experience significant differences. Specifically, there is a slight decrease with the *Var-V* algorithm, since it drops certain packets with a low TTL, not dropped by *VarPrev-V*. On the other hand, Figure 2-14 shows that there are substantial differences between both Variable-V algorithms, with that calculating V as a function of TTL on a per-packet basis performing much better.

MultiFlow:

Data packets originated from different sources and directed towards different destinations can traverse on its way same HeNBs. Thus, it is likely that a HeNB has data packets accumulated in its queue with different TTL values.

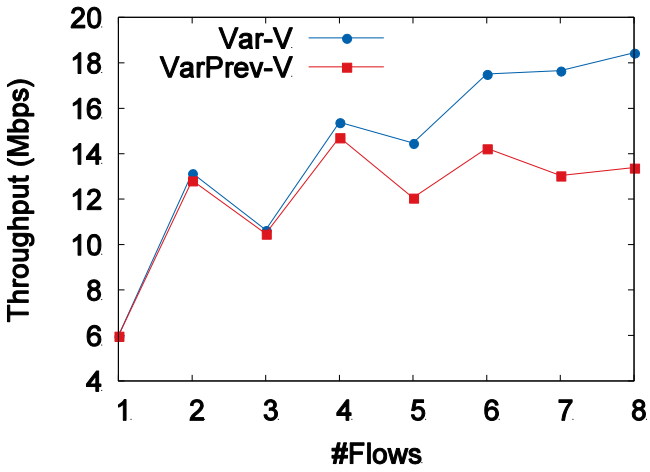

Figure 2-15 Throughput vs. load/number of flows for VarPrev-V and Var-V algorithms

The packets accumulated at data queues experience variability in their TTL as the number of flows in the NoF grows. Data packets in a data queue may belong to different flows. Therefore, it is likely to observe a higher variance of TTLs in a HeNB since they may be originated from different sources, and directed towards different destinations. It is in these usual cases (i.e., 5 flows in a NoF) when the variable-V algorithm calculating the *V* parameter on a per-packet basis demonstrates its potential for improving NoF metrics such as throughput, and delay. On the other hand, a periodical computation of the variable-V algorithm merely based on local congestion cannot attain this type of improvements, since it does not provide such a fine granularity calculating the *V* parameter.

The experiment consists of injecting several flows in the NoF crossing the same set of HeNBs towards different directions. Figure 2-15 provides throughput results of both variable-V algorithms with the increase of the number of flows in the NoF. We observe significant improvements from the injection of 5 flows with the computation of the *V* parameter on a per-packet basis (i.e., *Var-V*) compared to the periodical computation of the *V* parameter (i.e., *VarPrev-V*). Figure 2-16 provides delay results of both variable-V algorithms with the increase of the number of flows in the NoF, in which *Var-V* also gives better results.

We observe that adjusting the *V* parameter on a per-packet basis (i.e., *Var-V*) determines significant gains in terms of end-to-end delay as well as throughput with the increase of the number of flows injected in the NoF.

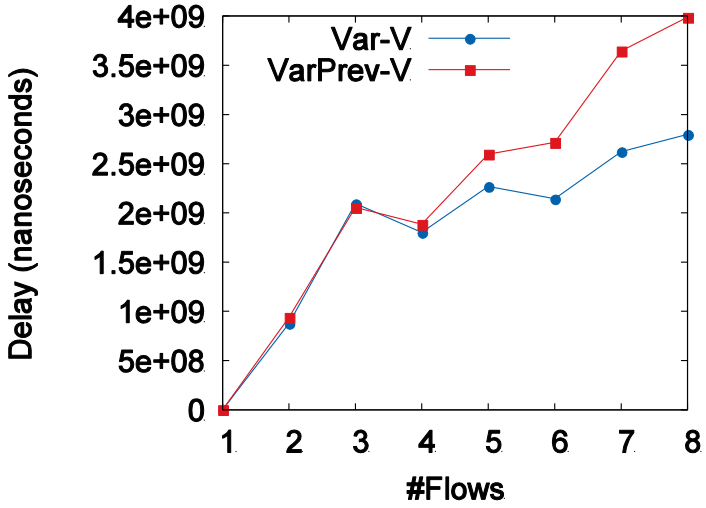

Figure 2-16 End-to-end delay vs. load/number of flows for VarPrev-V and Var-V algorithms

In the case of end-to-end delay, we observe a huge reduction in the packet delay experienced by *Var-V* (i.e., the variable-V recalculating the *V* on a per-packet basis) with respect to that in *VarPrev-V* routing policy. On the other hand, the end-to-end delay experiences improvements in the point in which at least 5 flows load the NoF, and increases from this point as the number of injected flows grow. In fact, the average delay is reduced by 2x (i.e., 1 second) with respect to *VarPrev-V* (i.e., the previous variable-V algorithm) for the case in which 7, and 8 flows load the NoF.

In the case of throughput, there is a significant improvement, especially when there are a high number of flows injected into the NoF. Throughput results are practically equivalent when there are not excessive flows loading the NoF. Specifically, in Figure 2-15 throughput results for both algorithms are similar when the NoF backhaul handles 1, 2, 3, and 4 flows. However, we start observing remarkable throughput improvements which are close to the 20% when 5 flows are injected in the NoF. Moreover, the throughput improvements increase up to a point of 30% in the case in which the NoF is loaded with 8 flows.

2.2.3 Multi Local Femto Gateway

The introduction of several LFGWs may potentially increase the feasibility region, that is, the set of all possible rates and flows that can be appropriately handled by the network. In fact, the capacity of wireless links of LFGW is a potential bottleneck, as it acts as interconnector of the HeNB with the core network. As a result, as the number of LFGWs capable of pulling packets from the NoF grows, the feasibility region might also potentially grow.

2.2.3.1 Idea behind Dynamic Anycast Backpressure Routing

So far, in the solution proposed we assumed there is only one LFGW in the all-wireless NoF. However, there might be several LFGWs for large-scale deployments. In an all-wireless NoF with multiple LFGWs, there are some critical issues to take into account:

- LFGW placement: The problem of LFGW placement is of primal importance in a NoF. The efficiency of the LFGW placement strategy to choose will highly depend on the traffic demands in that NoF, and also on the way the distributed routing protocol propose to do LFGW load balancing.
- Number of LFGWs: The more LFGWs are placed in the NoF, the more chances NoF performance metrics can be optimized.

The first issue to solve is how to deploy the LFGWs in the all-wireless NoF so that distributed backpressure routing can exploit LFGW load balancing. We propose a specific LFGW deployment suitable for both the constrained environment posed by the NoF, and for the characteristics of the distributed routing protocol.

The LFGW deployment follows. We deploy a single LFGW in the centre of the NoF in geographic terms. This LFGW is referred as the reference LFGW. The reference LFGW is the one whose geographic

location is known by all the HeNBs in the NoF. Then, the rest of LFGWs referred to as opportunistic LFGWs are deployed so that they are evenly distributed around the reference LFGW on a grid layout fashion. We define opportunistic LFGWs as those nodes with LFGW capabilities (i.e., they are able to pull uplink routing packets from the NoF) but whose location is not known by the HeNBs.

The intuition justifying this approach relies on the fact that the proposed variable-V distributes traffic whenever it finds congestion. All the uplink flows generated by HeNBs send traffic to the reference LFGW (whose geographic coordinates we assume are the only ones given by the local mobility management entity). If due to traffic distribution capabilities of the routing protocol, data packets cross an opportunistic LFGW (see Figure 2-17), this LFGW is also able to pull data packets from the NoF. The advantages of the proposed LFGW deployment follow:

a) HeNBs just require the location of one single LFGW in the NoF, hence reducing the state kept at each HeNB. Therefore, the amount of state stored in each HeNB does not vary.
b) Traffic distribution capabilities of the proposed distributed backpressure routing protocol exploit the proposed LFGW deployment.

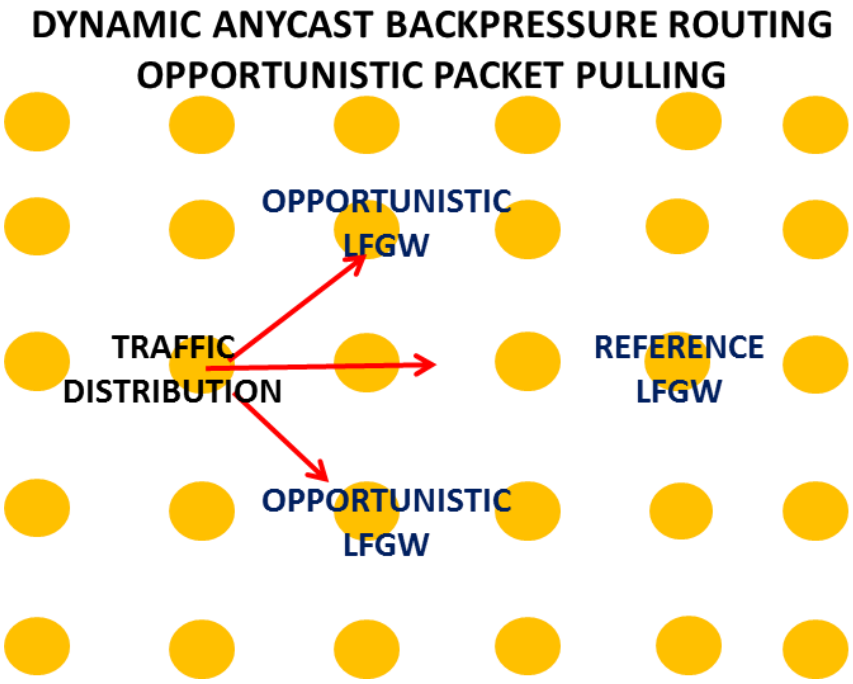

Figure 2-17 Multi Local Femto Gateway

On the other hand, we study throughout the evaluation section the improvement of the NoF performance metrics with the increase of the number of deployed LFGWs. Here, we illustrate through an example the gains introduced by adding an additional LFGW in the NoF.

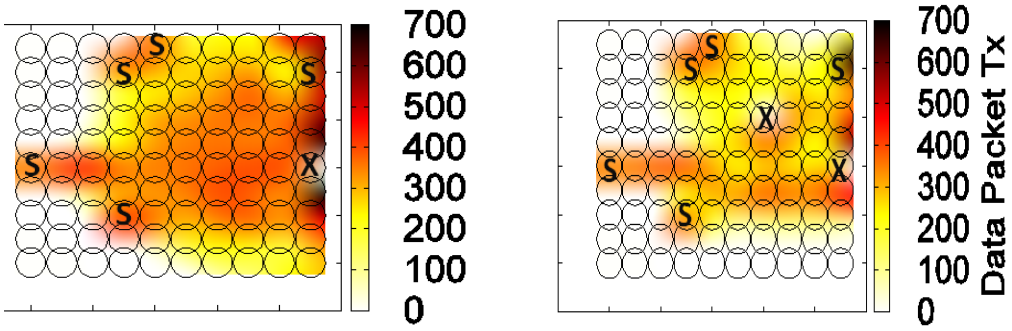

a) 1 LFGW **b) 2 LFGWs**

Figure 2-18 Reduction in terms of congestion introduced by adding an opportunistic LFGW

To do so, we carry out two experiments. In both experiments, the routing protocol variant used is the variable-*V* distributed routing protocol. Heatmaps in Figure 2-18a, and Figure 2-18b correspond to the

resulting data packet distribution injecting the same offered load to the NoF with 1 LFGW, and 2 LFGWs, respectively. Figure 2-18a, and Figure 2-18b plot the average number of data packets per second transmitted by every HeNBs. Notice that this figure is only for illustration purposes and the LFGW is not at the centre, as in the simulation results presented below.

The offered load for both heatmaps consists of six unidirectional UDP flows sent by six HeNBs labeled as "S" towards the LFGWs labeled as "X" (i.e., the reference LFGW).

The second heatmap illustrates the gains introduced by adding a second LFGW labeled as "X" (i.e., opportunistic LFGW) in the NoF. In particular, we observe a decrease of congestion in the transport network since the amount of data packets per second transmitted by every HeNB is considerably reduced. As can be shown in both figures, the predominant dark color in nodes transmitting packets in Figure 2-18a becomes lighter in Figure 2-18b due to the addition of an opportunistic LFGW close to the reference LFGW. Therefore, the addition of a second LFGW close to the reference LFGW is considerably relieving congestion in the NoF.

Since all HeNBs direct traffic to the reference LFGW, and the proposed variable-V distributed backpressure routing protocol distributes traffic just when it finds congestion, an opportunistic LFGW close to the reference LFGW can alleviate congestion in a high degree.

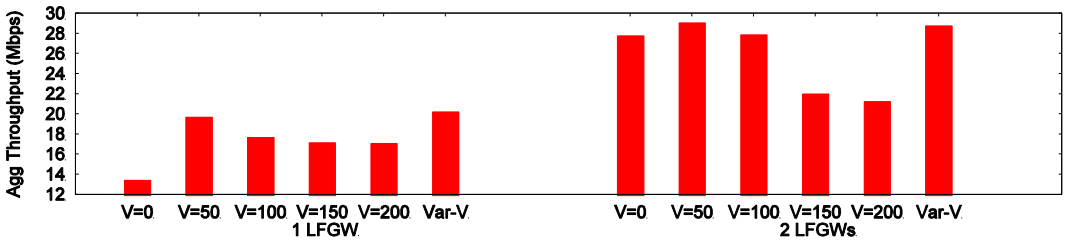

a)1 LFGW **b) 2 LFGWs**

Figure 2-19 Comparison between different routing variants (fixed-V and variable-V routing policies) in terms of Aggregated Throughput with 1 LFGW and 2 LFGWs

Going back to the simulation results (i.e., reference LFGW at the centre of the NoF), Figure 2-19 plots the gains experienced in terms of aggregated throughput by the addition of an opportunistic LFGW. Furthermore, Figure 2-19 provides the comparison between different variants of the fixed-V routing policy and the variable-V routing policy described in previous section.

We observe that fixed-*V* routing variants with low *V* values (i.e., *V*=0, *V*=50, and *V*=100) experience high throughput gains by the addition of an opportunistic LFGW. Recall that, as extensively evaluated in D5.2, low *V* values in a fixed-V routing policy imply a high degree of load balancing in the NoF. Therefore, for low *V* values an opportunistic LFGW close to the reference LFGW is exploited since a considerable amount of data packets are pulled by the opportunistic LFGW relieving congestion from the NoF. In contrast, for high *V* values (i.e., *V*=150, *V*=200) the addition of an opportunistic LFGW does not lead to such throughput gains as with low *V* values. This is consequence of the decrease in the use of the opportunistic LFGW for pulling packets from the NoF. Recall that, as extensively evaluated in D5.2, the increase of *V* in a fixed-*V* routing policy decreases the degree of load balancing in the NoF backhaul. As a consequence, with high *V* values (i.e., *V*=150, *V*=200) it is less likely packets cross an opportunistic LFGW given that the degree of load balancing is practically null.

On the other hand, the variable-V algorithm behaves similarly to the best fixed-V routing variant with 1 LFGW as well as with 2 LFGWs. Actually, the variable-V algorithm has the potential to adapt to both previously described LFGW layouts without any additional knowledge by the HeNBs.

As will be shown in next subsection, in addition to the specific LFGWs layout, the traffic patterns are of primal importance in order to determine the importance of the variable-V algorithm with respect to a fixed-V routing policy. Additionally, the specific location of the reference LFGW influences in the performance experienced by the fixed-V routing policy. In contrast, the variable-V routing policy maintains its stability. With the variable-V algorithm it does not matter where we locate the reference LFGW as long as the opportunistic LFGWs are not too far from the reference one.

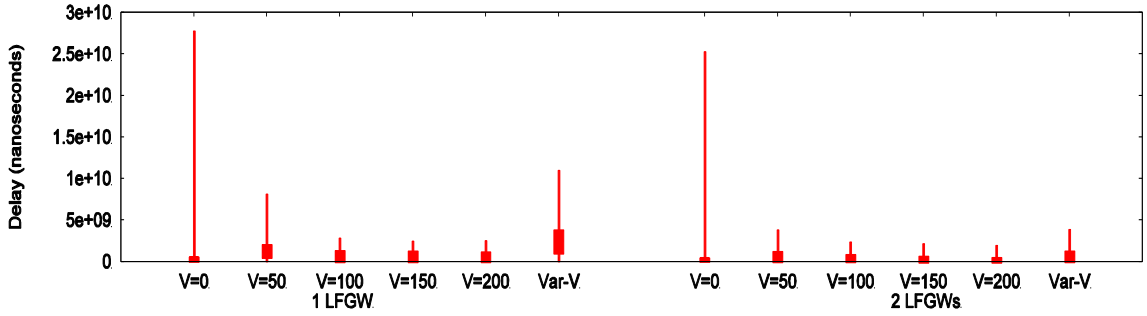

a) 1 LFGW **b) 2 LFGWs**

Figure 2-20 Comparison between different routing variants (i.e., fixed-V and variable-V routing variants) in terms of End-to-end delay with 1 LFGW and 2 LFGWs.

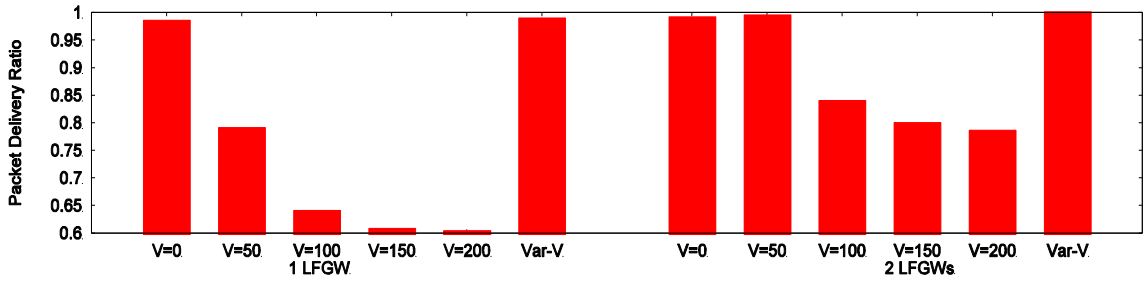

1 LFGW **b) 2 LFGWs**

Figure 2-21 Comparison between different routing variants in terms of Packet Delivery Ratio

With regards to end-to-end delay results evaluation results show the following features. Note that when evaluating end-to-end delay, as issue of primal importance is to take into account packet delivery ratio results. For instance, with a single LFGW, the variable-*V* algorithm experiences higher delay results than with some fixed-V policies such as *V*=100, *V*=150, and *V*=200. Nevertheless, in Figure 2-21 we observe that with the variable-V algorithm close to a 40% of more data packets arrive to the reference LFGW.

On the other hand, as can be shown in Figure 2-21, end-to-end delay decreases with the addition of an opportunistic LFGW in a different degree for all the routing variants under evaluation. The variable-V routing policy is the one experiencing the higher decrease of end-to-end delay.

2.2.3.2 Multi LFGW Evaluation

Methodology:

The experiments are based on injecting a high offered load to the NoF. Specifically, there are 8 flows injecting 6Mbps directed to one single LFGW (i.e., the reference LFGW). Moreover, we evaluate different routing policies (i.e., fixed-V and variable-V). With regards to the number and location of the LFGWs, we consider three different setups. In the first one, there is a single LFGW referred as the reference LFGW located in the centre of the 10*10 node square grid NoF. The geographic location of the reference LFGW is known by all the HeNBs in the NoF. The location of the reference LFGW is equivalent along the three setups under evaluation.

In the second setup, there are two additional opportunistic LFGWs around the reference LFGW. Specifically, the two opportunistic LFGWs are in the same row of the reference LFGW. In the third setup, there are four additional opportunistic LFGWs around the reference LFGW.

For each experiment, the NoF selects 8 HeNBs to inject traffic directed towards the LFGW in the centre of the grid. Furthermore, there might be also flows not directed to the LFGW in the centre but to another HeNB (i.e., local routing). We do this in order to evaluate the Multi-LFGW solution in a more generic traffic scenario. Specifically, there is a combination of uplink and local routing.

We measure the aggregated throughput attained by the LFGWs, the end-to-end delay attained in the LFGW, and the packet delivery ratio during a time interval of 100 seconds. We repeat simulations 10 times choosing a different set of source HeNBs to inject traffic in the NoF. Varying the position of HeNB sources 10 times provides a representative distribution of potential traffic sources in the grid NoF. All the traffic coming from the HeNB sources close in Euclidean distance up to a case in which all source HeNBs are evenly distributed in the NoF.

The evaluation compares the fixed-*V*, and the variable-*V* routing policies. Specifically, we choose as fixed-*V* the following instances: *V*=0, *V*=50, *V*=100, *V*=150, and *V*=200. The variable-V routing policy is the one computing the *V* parameter on a per-packet basis, explained in section 2.2.2.2.

Discussion of the Results:

The case of *V*=0 is very powerful in a many-to-one scenario but outside this case it experiences high throughput degradation. This fact can be observed in the minimum throughput values attained by such routing variant in Figure 2-22, Figure 2-23, and Figure 2-24. Those values correspond to a traffic pattern in the NoF different than the many-to-one traffic scenario, hence becoming difficult to create decreasing gradients towards the respective destinations.

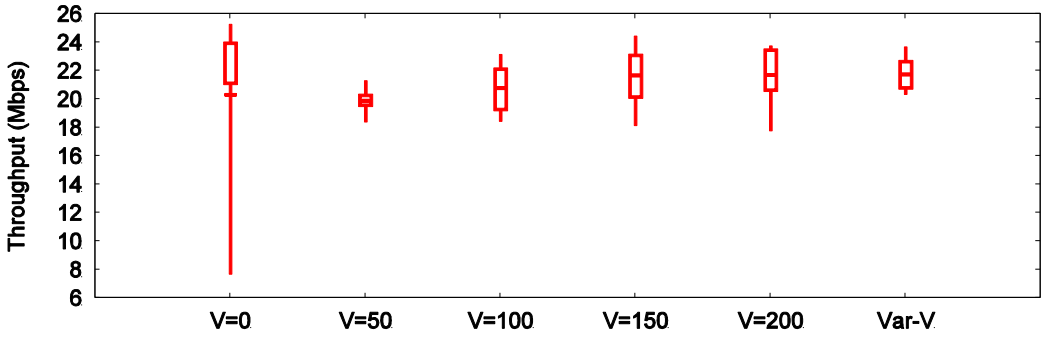

Figure 2-22 Different routing variants (i.e., fixed-V and variable-V) in terms of aggregated throughput with 1 LFGW

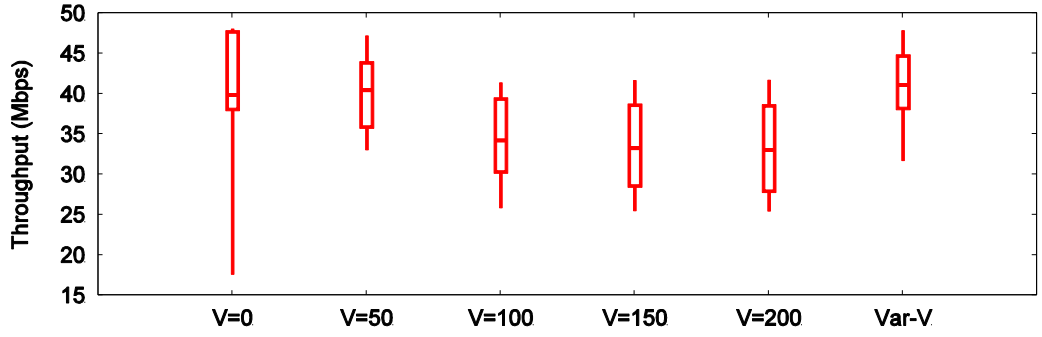

Figure 2-23 Different routing variants (i.e., fixed-V and variable-V) in terms of aggregated throughput with 3 LFGWs

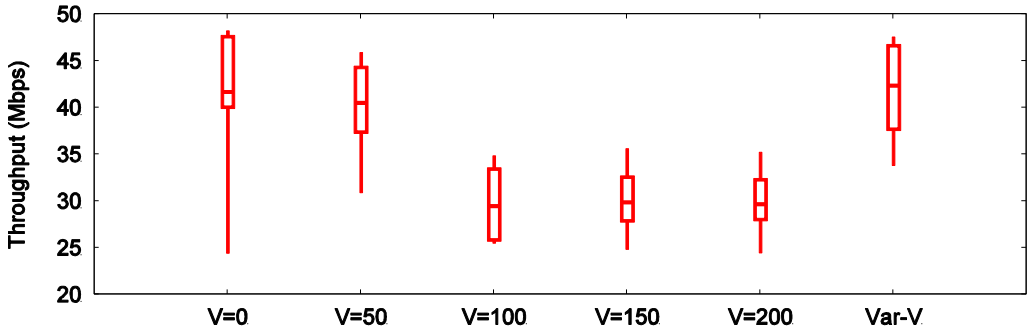

Figure 2-24 Different routing variants (i.e., fixed-V and variable-V) in terms of aggregated throughput with 5 LFGWs

Figure 2-23 and Figure 2-24 show that all routing variants experience throughput gains with the addition of opportunistic LFGWs with respect to throughput attained with a single LFGW (see Figure 2-22). On the one hand, we observe that with the fixed-*V* routing policy, the degree of load balancing decreases with the increase of the *V* parameter. The higher the *V* parameter the lower the chances data packets are pulled from the network by an opportunistic LFGW.

In contrast, the variable-*V* routing policy attains the maximum throughput in average compared with fixed-*V* routing policies.

As can be shown by throughput improvements observed in Figure 2-23 and Figure 2-24 with respect to Figure 2-22, the distributed routing protocol uses opportunistic LFGWs even though the HeNBs injecting traffic to the WiFi backhaul is not aware of the location of these opportunistic LFGWs. This is because data packets can be delivered to any of the available LFGWs due to the enabled anycast routing capabilities.

Variability increases with the number of LFGWs and minimum throughput attained increases with the increase in the number of LFGWs for the variable-*V* routing policy. Figure 2-23 shows that in average the offered load injected to the NoF is practically served with the Var-*V* routing policy.

High fixed-*V* policies (i.e., *V*=100, *V*=150, and *V*=200) exploit better the 3 LFGWs case than the 5 LFGWs case since in the 5 LFGWs layout, the opportunistic LFGWs are located physically slightly farther from the reference LFGW. Therefore, for fixed-*V* routing variants, the more emphasis in *V* implies a lower throughput gain with the addition of opportunistic LFGWs.

In the case of *V*=0, we observe that when the network scenario is merely composed by uplink traffic, the throughput attained is the best from all routing variants including the variable-*V* routing policy. The main issue with *V*=0 appears when the traffic is not only uplink but also local/downlink. In this case *V*=0 experiences a high throughput decrease. This is illustrated by minimum attained throughput values in boxplots from figures Figure 2-22, Figure 2-23, and Figure 2-24. Remarkably, the Var-*V* routing policy experiences the maximum values in terms of minimum aggregated throughput achieved at the LFGWs.

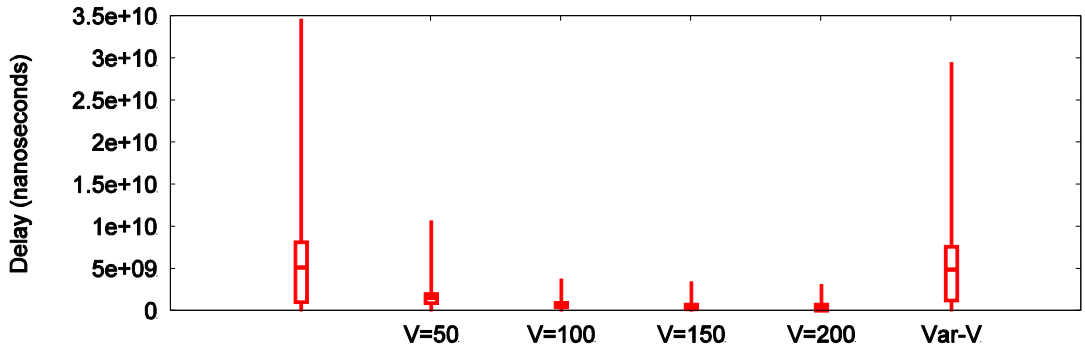

Figure 2-25 Different routing variants in terms of Delay 1 LFGW

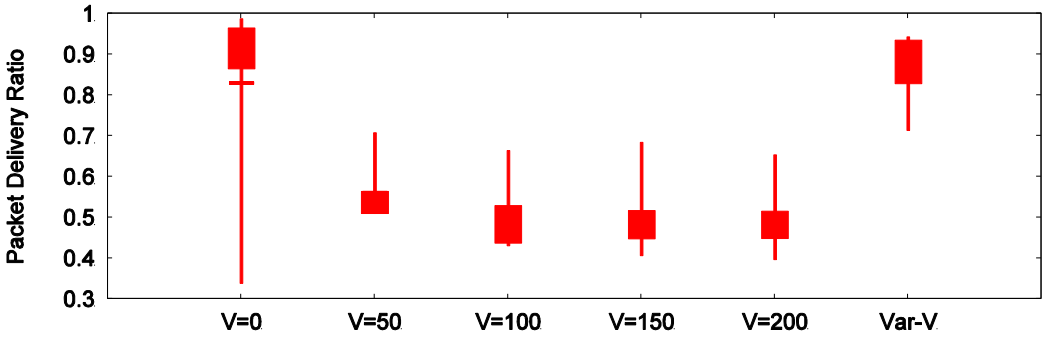

Figure 2-26 Different routing variants in terms of PDR 1 LFGW

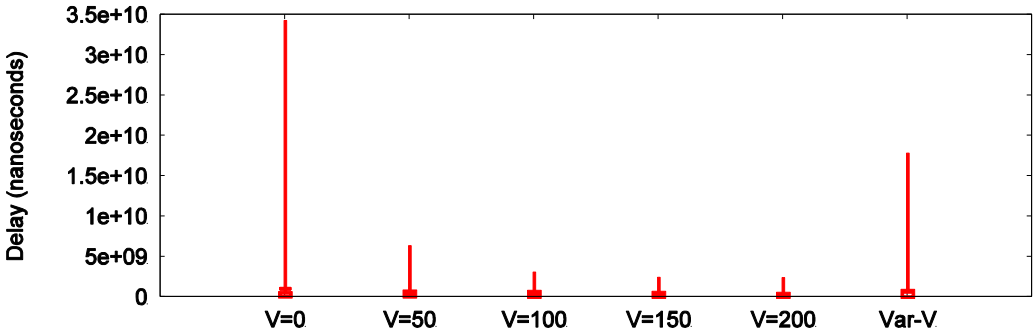

Figure 2-27 Different routing variants in terms of Delay 3 LFGWs

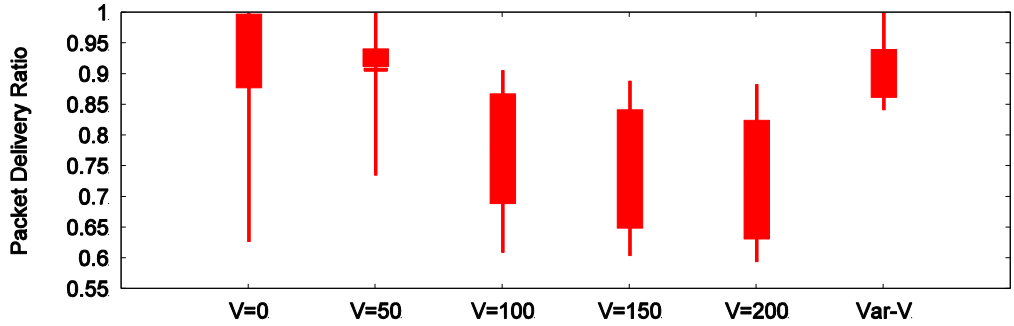

Figure 2-28 Different routing variants in terms of PDR 3LFGWs

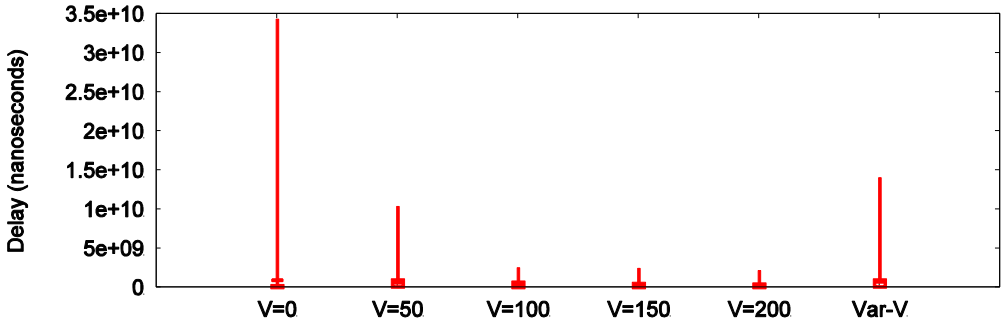

Figure 2-29 Different routing variants in terms of Delay with 5 LFGWs

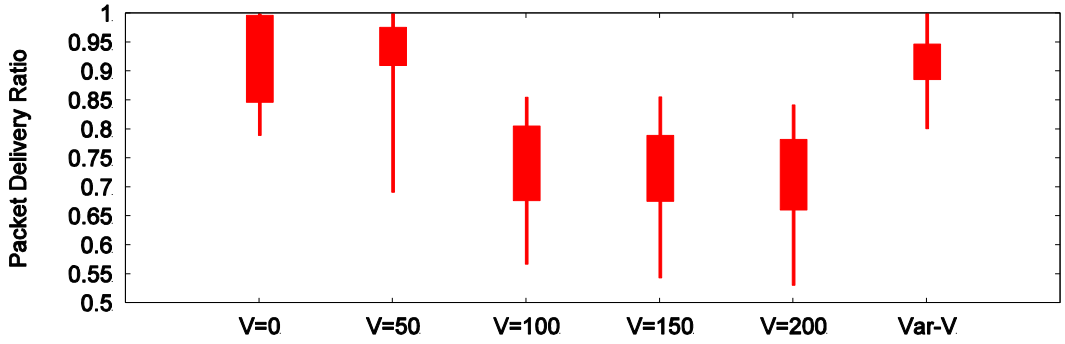

Figure 2-30 Different routing variants in terms of PDR 5 LFGWs

The distributed routing protocol also experiences end-to-end delay improvements using the *Var-V* variable algorithm. With the variable-V routing algorithm increasing the number of LFGWs in the NoF decreases the congestion experienced by the NoF. In particular, decreasing the congestion in the NoF turns into a decrease of the queuing and access delays, hence minimizing end-to-end delay in the NoF (see Figure 2-25, Figure 2-27, and Figure 2-29).

In contrast, for fixed-*V* routing policies and high *V* values, the fraction of packets that arrive experiences the lowest average end-to-end delay (i.e., with *V*=100, *V*=150, and *V*=200 in Figure 2-25, Figure 2-27, and Figure 2-29). However, a smaller fraction of packets arrives to the LFGWs (see Figure 2-26, Figure 2-28, and Figure 2-30). Therefore, these results can not be compared with the *Var-V* algorithm. In this case, the NoF drops data packets due to queue drops in HeNBs since the fixed-V routing policy configured with a high *V* increases the overall number of queue drops in the NoF. A fixed-V routing policy with a low *V* parameter experiences high delay variability in the NoF.

When there are two additional LFGWs in the NoF, delays decrease a 6.9x with respect to the single LFGW NoF setup showed in Figure 2-25. For fixed-V routing policies, the maximum average delay decrease experienced is of 3x. As Figure 2-29 shows, if there are four additional LFGWs in addition to the reference LFGW the maximum average delay decrease is also experienced by the *Var-V* algorithm. Precisely, the delay decrease experienced by *Var-V* is 6.2x, compared with the 5.45x experienced by *V*=0 (i.e., the maximum average delay decrease for the fixed-*V* routing policies).

2.2.4 Dead Ends

This solution explores the combination of backpressure routing with the use of geographic coordinates. One issue in the context of geographic routing, and so related with the proposed routing solution, is the dead end problem. The dead-end occurs when there is no neighbour closer to the destination in terms of Euclidean distance. An initial study to see how/whether the proposed distributed backpressure routing protocol could circumvent dead-ends in the NoFs was done in D5.2. In subsection 2.2.4.1, we provide a description of the final mechanism used to avoid dead-ends in a sparse all-wireless NoF. Subsection 2.2.4.2 evaluates the mechanism explained in previous subsections.

2.2.4.1 Backpressure Circumventing Dead-Ends

One key aspect of geographic routing techniques is the management of network holes, in which a node may find itself not the destination of a packet, but also discovers that there are no neighbours geographically closer to the destination, causing packet to remain trapped at the nodes. In an all-wireless NoF, this is an issue that could occur. But so far we have dealt with regular network deployments.

There are a high number geographic routing protocols proposing to circumvent dead-ends changing the behavior of the routing protocol, hence introducing additional complexity and keeping additional state at nodes. We emphasize that in contrast to other proposed routing procedures that switch to a different routing strategy when a packet reaches a dead-end, the proposed routing solution does not require any additional routing strategy than that presented in previous section. We posit that the distributed variable-V backpressure routing algorithm is able by itself to circumvent holes in an all-wireless NoF. The mechanism is based on the adaptive *V* calculation on a per-packet basis rather than using a dual routing mode. In fact, the routing protocol continues working on a distributed and stateless mode. This solution

requires no additional storage to keep track of the void such as in other proposals. There is no additional control overhead than that generated by HELLO messages. The proposed variable-V distributed backpressure algorithm, and the greedy strategy combining backpressure and geographic routing is able to deal with sparse deployments. In next section, we compare the potential to circumvent holes offered by the variable-V distributed backpressure algorithm with several instances of the fixed-V routing policy.

2.2.4.2 Evaluation

Methodology

To evaluate how the distributed routing protocol overcomes sparse deployments, we evaluate the behaviour of several routing policies under the same offered load conditions. The load consists of sending bidirectional and symmetric traffic between two HeNBs. Therefore, two HeNBs are senders and receivers of two flows. Specifically, two unidirectional UDP flows of 6Mbps load the NoF. The HeNBs marked with a cross in Figure 2-31, and Figure 2-35 are the ones sending and receiving traffic. The methodology consists of deleting HeNBs belonging to the set of direct paths between both HeNBs. We repeat the experiments increasing the number of HeNBs switched off from the NoF. Specifically, we repeat the same experiments turning off an increasing set of HeNBs. Specifically, we turn off 3 HeNBs, 9 HeNBs in two different manners, and 11 HeNBs in the reference 10x10 grid NoF. Every experiment supposes a different obstacle with a different form to overcome by the routing protocol. Moreover, we use different fixed-*V* routing variants (i.e., *V*=0, *V*=50, *V*=100, *V*=150, and *V*=200) and the variable-*V* to evaluate how they react with all the different dead-end forms.

Discussion

Figure 2-31 illustrates the data packet distribution attained by the Var-*V* in a sparse deployment. In this case, 3 HeNBs are switched off from the original grid NoF forming a linear obstacle for both HeNB exchanging traffic. Throughput, delay, and packet delivery ratio results illustrate that all the routing policies except *V*=0, and *V*=200 do not experience NoF performance degradation.

On the one hand, with *V*=0 any traffic scenario but the many to-one is a wrong choice with a single data queue per HeNB, since packets do not have any sense of direction. On the other hand, with *V*=200 data packets cannot reach the intended destination. This is because the distributed routing protocol requires a queue backlog difference of more than 200 packets to take into account the Lyapunov drift in their routing decisions. Since the maximum queue length of a HeNB is 200 packets, a queue backlog difference between the HeNBs of more than 200 packets is not possible. Therefore, in this setup, the fixed-*V* routing with *V*=200 cannot take routing decisions that imply forwarding data packets to HeNBs farther from the intended destination, yielding to null throughput (see Figure 2-32, Figure 2-33, and Figure 2-34).

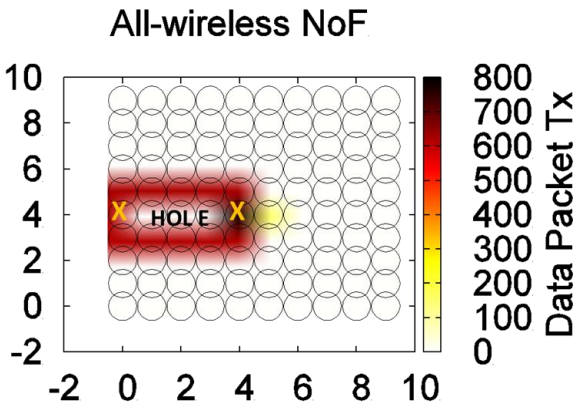

Figure 2-31 Heatmaps illustrating the light hole problem with the Var-V algorithm.

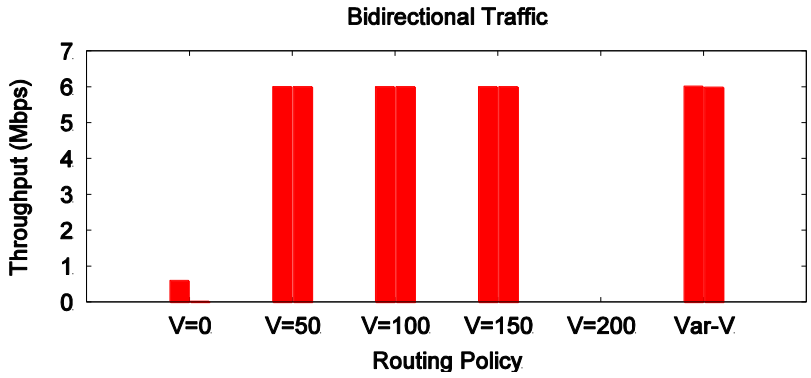

Figure 2-32 Attained throughput after switching off 3 HeNBs

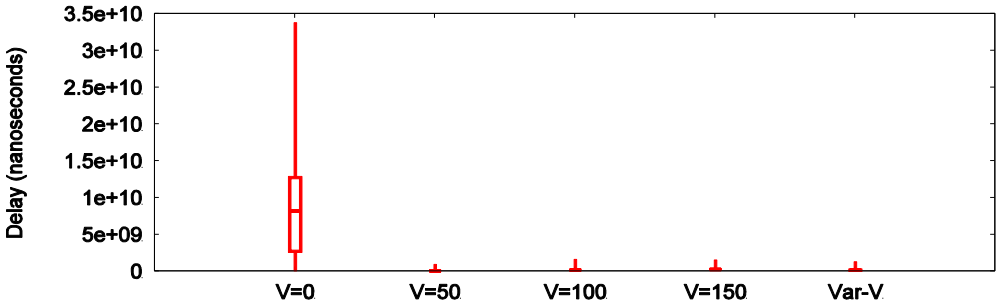

Figure 2-33 Delay Distribution of Packets for routing variants able to circumvent the hole

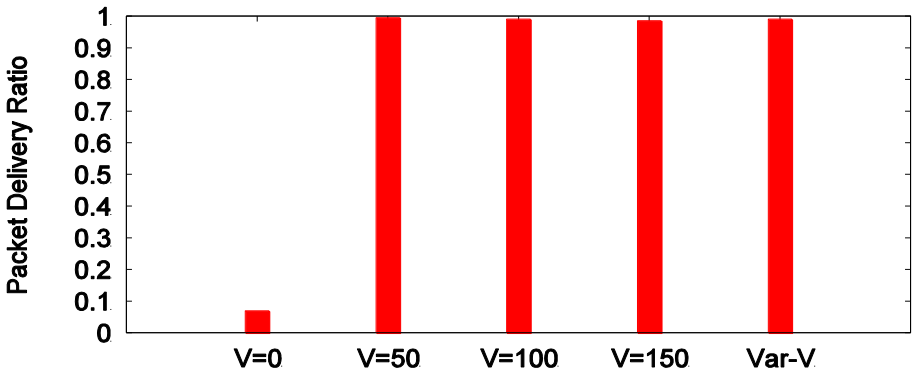

Figure 2-34 Packet Delivery Ratio for routing variants able to circumvent the hole

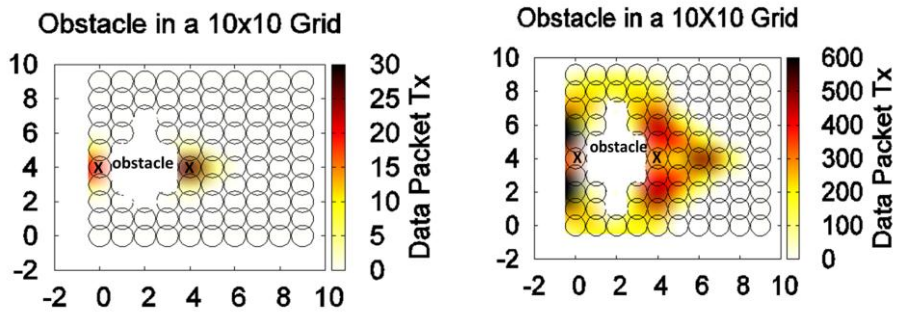

a) Fixed-V V=100 **b) Var-V**

Figure 2-35 Illustration of the operation of Var-V and fixed-V algorithms in the presence of obstacles

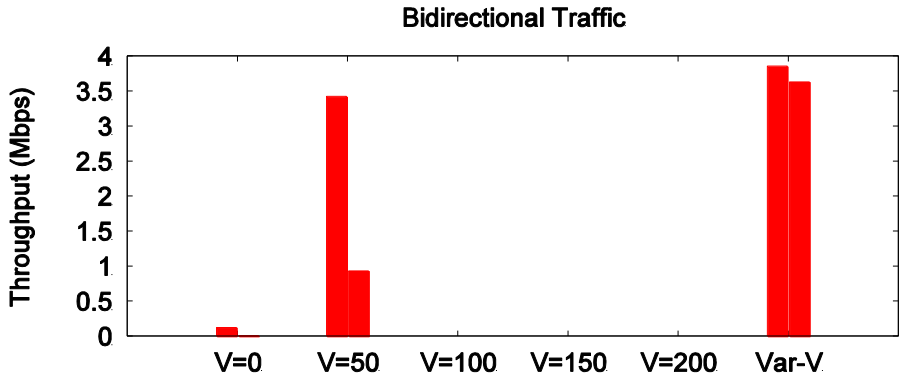

Figure 2-36 Achieved throughput with fixed V and var-V algorithms in the presence of obstacles

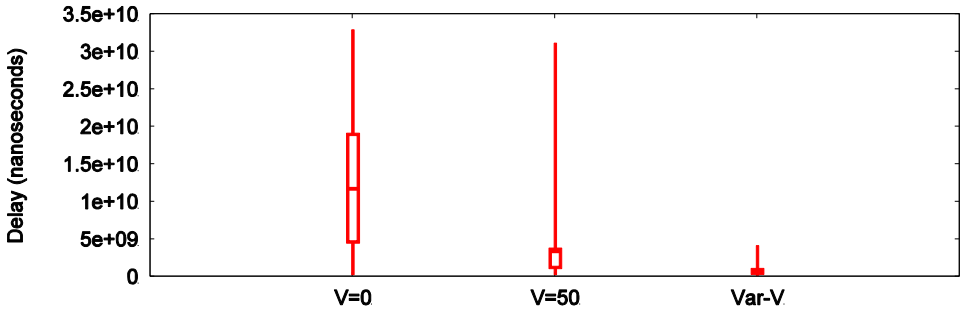

Figure 2-37 Packet delay distribution attained with fixed V and var-V algorithms in the presence of obstacles

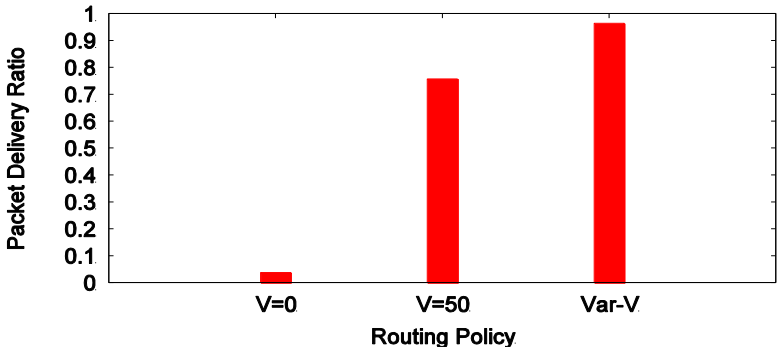

Figure 2-38 Packet delivery ratio with fixed V and var-V algorithms in the presence of obstacles

One observation to highlight from Figure 2-35 is that the bigger the structure of the void in the NoF, the more appropriate is the use of the variable-*V* algorithm computing decisions on a per-packet basis presented in section 2.2.2.2. We eliminate a set of HeNBs belonging to the set of HeNBs composing the more direct paths between the source-destination pairs. Figure 2-35a) depicts the data packet distribution with a fixed-V routing strategy (i.e., *V*=100), which is unable to circumvent the hole. On the contrary, Figure 2-35b) shows how the variable-*V* is able to circumvent the hole adapting the *V* parameter to attain a queue backlog difference between HeNB necessary to circumvent the hole.

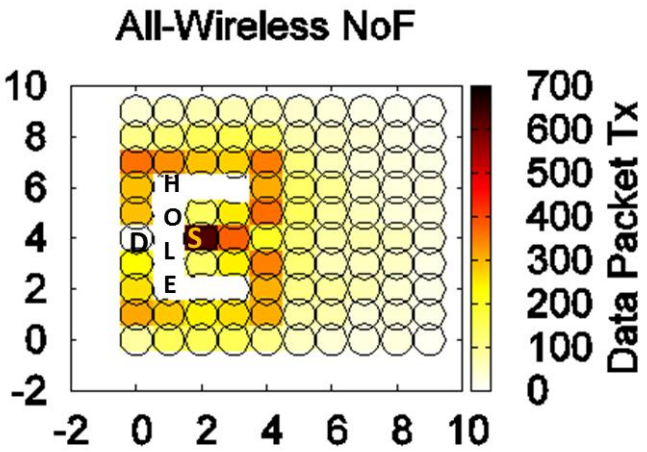

Figure 2-39 Illustration of the operation of Var-V algorithm with complex obstacles

In fact, with *V*=100 the routing protocol requires a difference of 100 packets between neighbours to take forwarding decisions that direct data packets farther from their intended destination. Since the maximum queue size in a HeNB is of 200 packets, they cannot advance farther of the first hop in Figure 2-35a. Therefore, the bigger the obstacle in the NoF, the lower the *V* parameter needed to overcome the hole.

The variable-V algorithm in every HeNB around the hole detects the accumulation of data packets, hence reducing the *V* parameter and overcoming the obstacle. Packets in the perimeter of the hole eventually reach the destination since HeNBs adapt their *V* so that a decreasing gradient is generated to reach the destination on a per-packet basis. The potential of the variable-*V* algorithm can be shown in the results obtained in terms throughput, delay, and packet delivery ratio. As can be shown in Figure 2-36, Figure 2-37, and Figure 2-38 there are only two routing configurations (i.e., fixed-*V* with *V*=50, and the variable-*V* routing algorithm) able to circumvent the hole. However, the Var-*V* algorithm obtains the best results in terms of throughput, delay, and packet delivery ratio.

The distributed routing protocol also shows its potential to circumvent complex holes such as the one depicted in Figure 2-39. In this case, data packets have to circumvent a hole with a "U" shape. In this unlikely sparse deployment in a NoF, the distributed backpressure routing protocol is also able to circumvent the hole. The protocol in this case requires to direct data packets in the opposite direction of the intended destination in order to circumvent the hole. It is able to achieve this by decreasing the *V* parameter at HeNBs around the shadow of the hole. At the same time, these HeNBs accumulate data packets at their queues, hence facilitating the decreasing queue backlog gradient towards the opposite direction of the destination.

2.2.5 Conclusions

The proposed distributed variable-*V* algorithm seems a promising strategy in a constrained scenario an all-wireless NoF poses. In particular, the routing protocol is able to obtain an interesting trade-off between throughput and delay even under dynamic topologies, and traffic scenarios. Specifically, we propose a variable-*V* algorithm that dynamically adapts the weight of Lyapunov drift-plus-penalty routing decisions on a per-packet basis. The specific *V* parameter is function of the traffic load around the HeNB, and the number of hops traversed by data packets. Furthermore, such weight (referred to as *V*) is independently calculated at each node based on local queue backlog information, and it is easy to implement. This variable-*V* algorithm aims at maximizing the relevance of the penalty function as much as possible while avoiding queue overflows in the network. The evaluation results (with a simple penalty function based on Euclidean Distance towards the destination) show an interesting trade-off between throughput and delay. On the one hand, the throughput attained with the variable-*V* algorithm is similar to the maximum throughput achieved with the best fixed-*V* algorithm. On the other hand, the proposed variable-*V* routing policy outperforms all fixed routing setups in terms of delay, as it reduces delay variation as well as the maximum delay. The proposed algorithm requires zero-configuration of the *V* parameter, no matter the changes in the offered load to the network. Additionally, the variable-*V* algorithm is agnostic of the particular penalty function used, since its calculation merely requires 1-hop queue backlog information and data packet information.

We have extensively studied the distributed routing protocol under several circumstances comparing the proposed variable-*V* algorithm with previous routing policies (fixed-*V* and variable-*V* routing policies). The overall study indicates an interesting trade-off between throughput and delay, since it takes forwarding decisions on a per-packet basis rather than on a periodical basis.

On the other hand, it has been shown to be appropriate in the multi-LFGW scenario, and to overcome holes in sparse deployments. We proposed an easy way to deploy multiple LFGW in a NoF so that the distributed backpressure routing protocol can exploit them without having knowledge of the location of the opportunistic LFGWs. The main advantage observed is the decrease of congestion in the NoF with respect to single LFGW NoF deployments, yielding to improvements in throughput, delay, and packet delivery ratio. Finally, we evaluated the distributed routing protocol under several sparse deployments. The study indicates the convenience of using the distributed routing protocol to circumvent holes compared to fixed-V routing policies.

2.3 Traffic Offloading

2.3.1 Introduction

Nowadays there is enormous growth of the number of a new generation of mobile devices like various smart phones (iPhone, Android-based), laptops, netbooks, etc. in the market. At the same time, mobile networks operators are incorporating actively Internet applications and services for the mobile devices. There are thousands of web data applications and services available now (e.g. YouTube, Facebook, Spotify, IM, mobile TV, etc.) that are becoming extremely popular in the mobile user environment. According to the Cisco VNI Global Mobile Data Traffic Forecast [10], overall mobile traffic is expected double every year from 2011 onwards.

As a result of these two factors, there is an explosion of both data and signalling traffic towards the core network of Mobile Network Operators (MNOs). As a consequence, congestion situations can arise in the core network. Thus, solutions to avoid unnecessary traffic load at network nodes are needed. One such solution is to apply a traffic offloading mechanism by means of femtocells. It can solve macro core network capacity crunch avoiding future upgrades of the network infrastructure.

From a network management perspective it is very important to correctly understand performance benefits (if any) of offloading in order to develop correct deployment strategies. Failing into doing so may lead to investing large efforts in installing costly offloading infrastructures that do not bring targeted benefits. In order to pursue these objectives it is important to characterize and model user behaviour and data hotspots from the viewpoint of offloading strategy that MNOs plan to use. As a result, one must assess if the gain in network resources obtained by means of traffic offloading is enough to avoid network congestions.

Thus, the objective of this study is to analyse which are the benefits, coming from the deployment of an offloading network in terms of performance.

In this study, we consider the traffic offloading process from the viewpoint of a MNO perspective. In this context it is important for the MNO to care about a traffic load that goes to its core network (e.g. 3G CN) after offloading. What is really needed for the MNO is to know what was before offloading and what happens after in the context of traffic parameters to adjust with them dimensioning characteristics of its network, e.g. to evaluate required system capacity after offloading.

Up to our knowledge, there has been no prior work analytically studying such offloading gains. An eventual analytical framework is expected to help in taking network design decisions when deploying offloading techniques. We make a contribution in this direction.

2.3.2 Work during Year 2

During the second project year, a model for the non-offloaded traffic of a single source that eventually reaches the network of the operator has been proposed.

Based on previous measurements [11], we characterize the duration of offloading periods as heavy-tailed. On the other hand, [12] and references therein present well-known models of the behaviour of single flow traffic, which describe traffic burstiness in terms of long-range dependence and heavy-tails. In the same way, we characterize user activity according to these models.

Thus, it assumes in our model that user activity periods Y(t) and periods characterizing offloading X(t) are heavy-tailed. We model them as strictly alternating independent ON/OFF processes. Therefore, the non-offloaded traffic Z(t) (i.e., that traffic still being served by the MNO on a regular basis) is modelled as the product of these two processes Z(t) = X(t)Y (t) as shown in Figure 2-40.

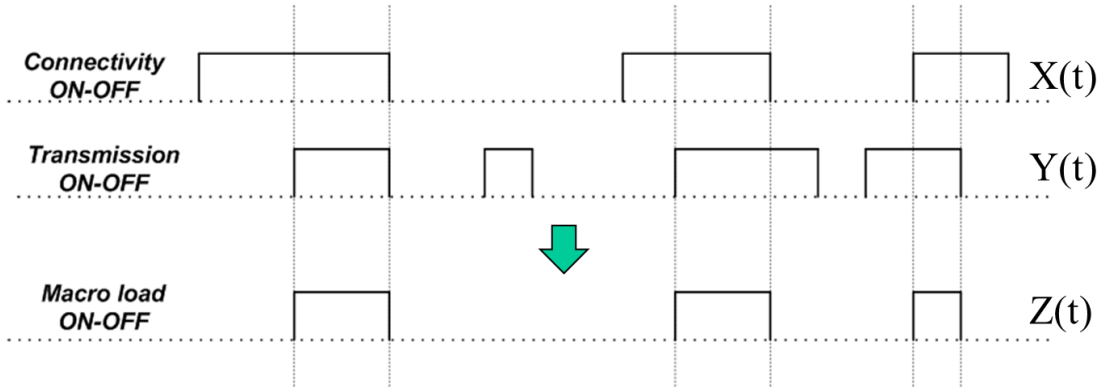

Figure 2-40: Non-offloaded traffic from a single source (Z(t)) modelled as product of two strictly alternating ON/OFF processes, X(t) and Y(t)

Operators are interested in the behaviour of the process modelling the aggregation of several Z(t) processes. Therefore, our problem is to obtain an analytical model describing the behaviour of such an aggregated traffic and the resource consumption it entails.

We have formed a high level view of the steps needed for solving the problem follows. Since, as explained above, Z(t) has ON and OFF periods that follow heavy tailed durations, this process is long-range dependent. Therefore, the aggregation of several such processes is self-similar and can be characterized by means of the Hurst parameter (H). This can be done by means of the same techniques presented in [13]. In turn, parameter H can be derived from the parameters characterizing the heavy-tailed behaviour of the ON and OFF periods of Z(t). Besides, such parameters can be obtained from those of processes of the original processes X(t) and Y(t). Therefore, once the parameters of the original processes are known, by following the above steps, we can characterize the behaviour of the aggregated non-offloaded traffic, and hence, the resources needed in the network of the MNO to serve it.

In this deliverable we present the main result of our research related to the main parameters characterizing the asymptotic behaviour of the non-offloaded traffic, we validate the main results by means of simulations, and we provide detailed analysis of performance evaluation issues related to resource consumption in the network of the MNO deploying an offloading strategy.

2.3.3 Main Results

Lemma 1. Let Z(t) be the process resulting from the product of processes X(t) and Y (t). Let these two latter processes have i.i.d. ON periods, i.i.d. OFF periods, and independent ON and OFF periods with heavy-tailed distributions. The complementary distribution function for the ON-periods of process Z(t) satisfies

$$F_{on}^{cz}(t) \sim \widetilde{c_1^z} t^{-\alpha_{on}^z} \widetilde{L_1^z}(t),$$

where

$$\alpha_{on}^z = \alpha_{on}^x + \alpha_{on}^y - 1,$$

and α^x_{on} α_{on}^z and α^y_{on} α_{on}^y are the parameters characterizing the heavy-tails of the ON and OFF periods of processes X(t) and Y (t), respectively. Hence, as $\alpha > 1$,

$$\alpha_{on}^z > max\{\alpha_{on}^x, \alpha_{on}^y\}.$$

Additionally, the complementary distribution function for the OFF-periods of process Z(t) satisfies

$$F_{off}^{cz}(t) \sim \widetilde{c_2^z} t^{-\alpha_{off}^z} \widetilde{L_2^z}(t),$$

where

$$\alpha^z_{off} = min\{\alpha^x_{off}, \alpha^y_{off}\}$$

In (1), (4) $c_j > 0$ is a constant and $L_j(t)>0$ is a slowly varying function at infinity.

Theorem 1. Let Z(t) be the process resulting from the product of two strictly alternating ON/OFF processes X(t) and Y (t) with i.i.d. ON periods, i.i.d. OFF periods, and independent ON and OFF periods with heavy-tailed distributions. Then, Z(t) is long-range dependent with covariance function:

$$\gamma_z(t) \sim \sigma_z^2 t^{1-\alpha^z_{min}},$$

where

$$\begin{aligned} \alpha^z_{min} &= min\{\alpha^z_{on}, \alpha^z_{off}\} = \\ &= min\{\alpha^x_{on} + \alpha^y_{on} - 1, \alpha^x_{off}, \alpha^y_{off}\}. \end{aligned}$$

Lemma 1 and Theorem 1 have been proved using proved using the probability theory laws and two fundamental results related to this type of processes from [13][14].

2.3.3.1 Validation of main results

Taking into account the fact that both processes X(t) and Y (t) are heavy-tailed, we use the Pareto distribution with parameters α and K (the scale parameter) to model both the ON- and OFF-durations of the processes. In our simulations we use the Hill's estimator [15] that provides a good way to estimate tail-index α of Pareto-like tails [16]. In accordance with the methodology presented in [16], the ON- and OFF-durations were simulated with 1010 states and 15000 largest sequences were considered out of them in the estimation procedure. For a case study initial data were formed on a basis of statistical information provided in the experimental studies on the performance of 3G mobile data offloading [13] (for the process X(t)) and the burstiness of web traffic caused by accesses of HTTP clients to the heterogeneous contents (text, images, PDF files, etc.) [17] (for the process Y (t)).

Thus, for the process X(t) we use the following initial data:

$$\alpha^x_{on} = 1.6,\ \alpha^x_{off} = 1.1,\ K^x_{on} = 12.5,\ K^x_{off} = 14.5,$$
$$p^x_{on} = 0.25,\ \mu^x_{on} = 40\ min,\ \mu^x_{off} = 120\ min.$$

For the process Y (t) the input data are:

$$\alpha^y_{on} = 1.51,$$
$$\alpha^y_{off} = 1.27,\ K^y_{on} = 6.1,\ K^y_{off} = 5.96,\ p^y_{on} = 0.39,\ \mu^y_{on} = 18\ s,\ \mu^x_{off} = 28\ s.$$

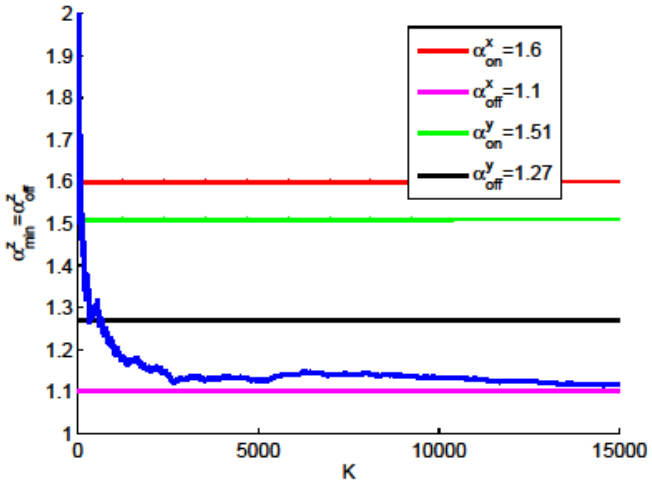

Figure 2-41: Estimation of the tail-index α^z_{min} by means of Hill's estimator when $\alpha^z_{min}=\alpha^z_{off}$

In accordance with the simulations the tail-index of the process *Z(t)* is α^z_{min}~1.1 as illustrated in Figure 2-41. This agrees with Theorem 1 according to which

$$\alpha^z_{min} = min\{\alpha^z_{on}, \alpha^x_{off}, \alpha^y_{off}\} = min\{2.11, 1.1, 1.27\}$$

In this case,

$$\alpha^z_{min} = \alpha^z_{off}$$

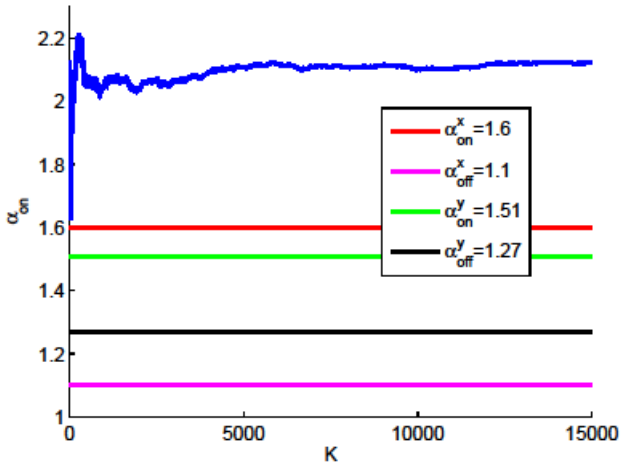

Figure 2-42: Estimation of the tail-index α^z_{on} by means of Hill's estimator

Figure 2-42 shows simulations to estimate the parameter α^z_{on}, which in accordance with Lemma 1 should be equal to 2.11 ($\alpha^x_{on} + \alpha^y_{on} - 1$). The result of the simulations matches well with the analytical result.

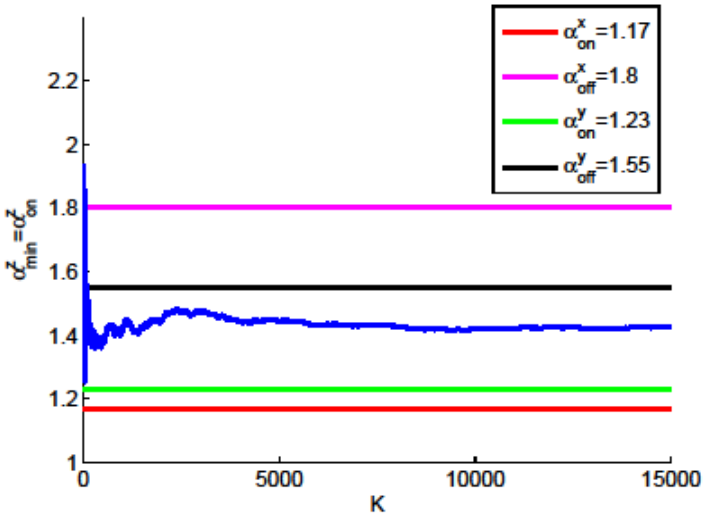

Figure 2-43: Estimation of the tail-index α^z_{on} by means of Hill's estimator when $\alpha^z_{min}=\alpha^z_{on}$

The extensive simulations using Hill's estimators were carried out for different sets of initial data and in all cases values of the tail-index α^z_{min} were estimated correctly in accordance with the main results of the analytical. As an example, for the data set $\alpha^x_{on} = 1.17$, $\alpha^x_{off} = 1.8$, $\alpha^y_{on} = 1.23$, $\alpha^y_{off} = 1.55$, we have a case when in accordance with Theorem 1 $\alpha^z_{min}=\alpha^z_{on}=1.4$. As seen from Figure 2-43 it is perfectly agree with the result of the simulations.

2.3.3.2 Performance bounds in offloading scenarios

We adopt the perspective taken in [18] and [19] in order to evaluate the system-wide implications of the Lemma 1 and the Theorem 1. Specifically, we study which are the large-scale implications of implementing an offloading strategy on the provisioning of resources in a mobile network.

In particular, Norros [19] derives an approximation of the capacity that a system requires under fractional Brownian traffic in order to provide a target level of QoS, expressed as a bound (ε) on the amount of traffic lost. Let us consider an arrival traffic model such as

$$A(t) = \lambda t + \sqrt{a\lambda} B_H(t),$$

where λ is the average amount of traffic that arrives to the network, *a* is a variance coefficient and $B_H(t)$ is a normalized FBM process with Hurst parameter H.

Given A(t), the capacity needed to guarantee that the probability of system buffer overflow is bounded P(W >w) < ε can be approximated by ([19]),

$$C \sim \lambda + (H^H (1-H)^{1-H} \sqrt{-2ln\epsilon})^{\frac{1}{H}} a^{\frac{1}{2H}} w^{\frac{-(1-H)}{H}} \lambda^{\frac{1}{2H}}$$

As Theorem 1 reveals, when applying offloading to a heavy-tailed ON/OFF source, the distribution of the resulting sequence of ON/OFF durations may still keep heavy-tail behaviour but with a different behaviour of the tail. At large scale, when aggregating a large number of sources, the result is that the burstiness of the arrival flow has changed.

Let us denote as H_z and H_y, the Hurst parameters of the aggregate arrival process to a system when we apply an offloading strategy (H_z) and when it is not applied (H_y).

Taking into account Theorem 1 and the relation $H = (3 - \alpha_{min})/2$ we make the following observations:

$$\begin{cases} H_z > H_y, & if\ \alpha^z_{min} = \alpha^z_{off} \text{ and } \alpha^x_{off} < \alpha^y_{min} \\ H_z \leq H_y, & otherwise \end{cases}.$$

From a network dimensioning perspective relation (10) has a high relevance. Specifically, the expression (10) states that special care should be taken to control the distribution of the duration of offloading periods. In particular, when disconnection (offloading) durations present higher heavy-tailness than the original system (i.e., $\alpha^x_{off} > \alpha^y_{min}$), the net result is that the offered load to the mobile network will present a higher degree of burstiness (i.e., $H_z > H_y$).

In order to illustrate this fact let us consider the following example. Assume we have a network without the offloading service dimensioned to support an offered load of λ_y = 200 Mbps with an outage probability of $\varepsilon = 10^{-5}$ given a buffering capacity of w = 100 kbytes. Assume further that the system aggregates heavy-tailed ON/OFF sources with Pareto-like ON and OFF durations with parameters α^y_{on} α^y_{on} = 1.3 and α^y_{off} = 1.8.

Now assume that we introduce an offloading strategy in the previous system. Taking into account relation (9) we can define a worst case scenario when $\alpha^x_{off} \to 1$. We can also define a best case scenario when both α^x_{off} and α^x_{on} do not have a heavy-tailed distribution (i.e., α^x_{on} = 2 and α^x_{off} = 2).

Applying (9), Figure 2-44 plots the amount of resources that the system needs to offer the quality of service specified ($\varepsilon = 10^{-5}$). Specifically, the figure shows the capacity needed in the original system together with the worst and best case scenarios when we offload a 50% of the traffic.

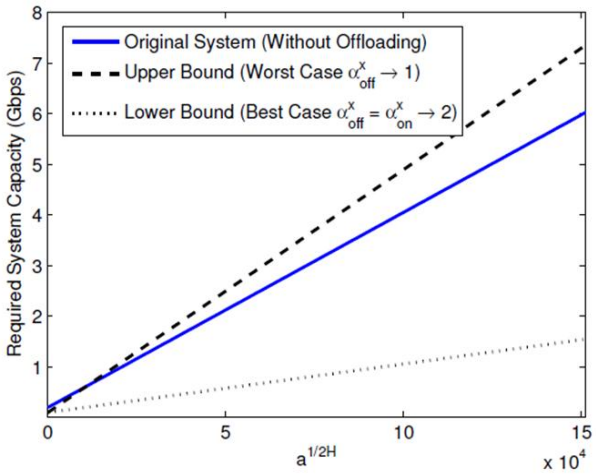

Figure 2-44: Bounds on resource needs vs. variance coefficient (*a*) with 50% of offloaded traffic

The figure illustrates two important observations. First, as explained above, the parameter α^x_{off} has a capital importance as we can end up in an extreme case where we start offloading data but we need to

increase the amount of resources of the network to maintain a certain level of QoS (due to an increase of data burstiness). Second, introducing a fine-grained control of the distribution of offloading periods can be highly beneficial as it can also lead to decreasing the burstiness of data traffic to the core of the network.

An alternative way to present this last observation is computing the amount of overprovisioning that the system needs to keep up with a target QoS. In this context, overprovisioning is understood as the resources beyond the average load that the operator must put in place to serve bursts of traffic. Figure Figure 2-45 plots this for the same scenario as in the previous figure. In particular, it plots, for a fluid model, the excess of resources over the total capacity that the network operator needs to implement to maintain the objective probability of loss (ε). As the figure shows, in the worst case scenario even though we reduce the amount of load to the system, we need to increase the overprovisioning margin to keep up with the QoS. The contrary happens in the best case scenario where in addition to data traffic reduction the operator can also relax overprovisioning needs.

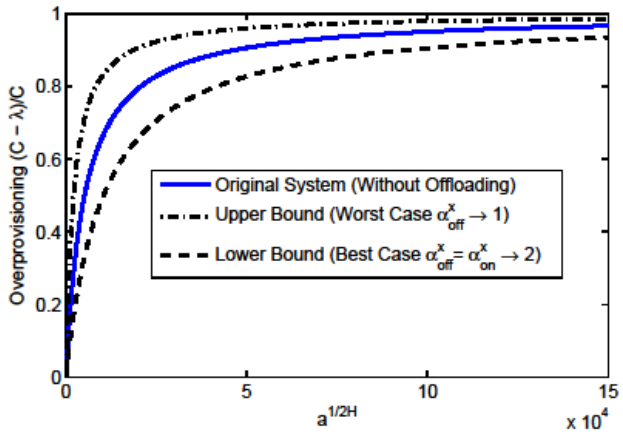

Figure 2-45: Normalized overprovisioning of the system taking a fluid model approximation

Finally, let us consider Figure 2-46, which plots the relation C_z/C_y between the resources needed after and before offloading with respect to the tail index of offloading periods (α^x_{off}). The figure illustrates the influence of the different design parameters on the dimensioning of the network after applying offloading. In particular, the figure focuses on illustrating the strong dependence of the effectiveness of offloading on the actual distribution of offloading periods.

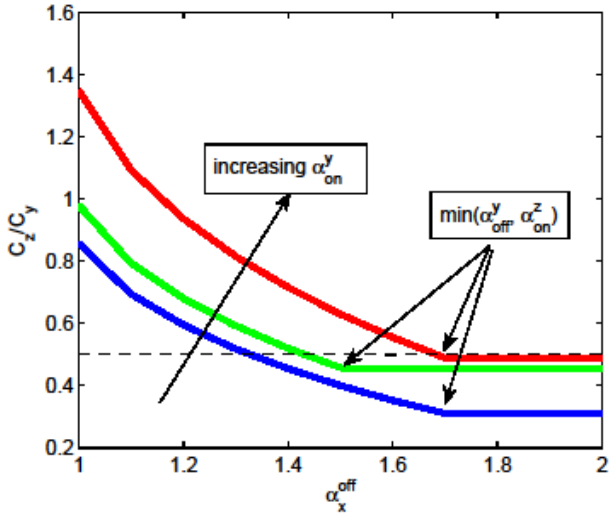

Figure 2-46: Illustration of the relation between the parameters of the system and the required capacity before and after implementing offloading

Taking as a reference the dashed line in the figure indicating the amount of traffic offloaded (i.e., P(X(t) is in ON state), it can be seen that when the distribution of offloading periods exhibits large tails (i.e., α^x_{off} is low) there is a high probability that the network operator needs to increase resources to maintain QoS.

Another interesting observation is that the reduction on the number of resources is best (and cannot do better than) when $\alpha_{off}^{x} \geq \min(\alpha_{off}^{y}, \alpha_{on}^{z})$.

As a summary, these facts illustrate that the main consequence of Theorem 1 is that the distribution of offloading periods turns out to be the main design parameter in order to implement effective offloading strategies in mobile network.

2.3.4 Conclusion

Operators are interested in benefits (if any) that traffic offloading implemented by means of femtocell deployments can give for its network in terms of resource consumption. We proposed a theoretical framework for studying mobile traffic offloading, in which both user activity and offloading periods are modelled by means of strictly alternating ON/OFF processes whose ON and OFF durations are characterized by heavy-tailed distributions. Furthermore, the process describing the non-offloaded traffic (i.e., that traffic still needing to be served by the MNO on a regular basis) is modelled as the product of the two previous processes. This framework is agnostic of the specific offloading technique applied as well as the node where offloading is applied. We derived the exact parameters describing the asymptotic behaviour of the non-offloaded traffic, which is shown to be long-range dependent with ON/OFF durations following a heavy-tailed distribution. We also obtained the parameters characterizing this process as a function of those of the original processes. Based on the characteristics of the aggregated non-offloaded traffic, we provided performance bounds of resource consumption in the network of the MNO when deploying offloading strategies. Furthermore, we illustrated the influence of the different design parameters on the dimensioning of the network before and after applying offloading. We concluded that offloading does not always entail a gain in terms of network resources and that the appropriate design of offloading periods is key in network dimensioning. We validated the analytical results by means of simulations.

3. Mobility Management

Mobility management mechanisms to support seamless handover with minimal signalling cost and enable efficient location management for femtocells are developed in this section. For topics already studied in previous deliverables, a subsection presents a summary of the work done. Section 3.1 further develops the concepts already studied in previous deliverables on local location management in networks of femtocells. In particular, this section focuses on describing a scheme for minimizing the impact of paging control traffic over an all-wireless local backhaul. Section 3.2 introduces a new mechanism for reducing the impact in terms of packet loss and service disruption time when handing over between macrocells and femtocells.

3.1 Local Location Management

3.1.1 Introduction

This section describes an integrated solution for Local Location Management (LLM) in the context of large-scale, all-wireless networks of femtocells (NoFs).

Traditionally, Mobility Management has been classified into Handoff Management and Location Management. The former focuses on the provision of session continuity for voice and data calls during a handover between neighbouring cells. The latter provides the necessary mechanisms to update the location of a User Equipment (UE) within the NoF, and to page a mobile terminal when a voice or data call is to be established. Formally, LLM deals with the extension of Location Management challenges to the specific context of large-scale, all-wireless NoFs.

Standard 3GPP Location Management mechanisms have been designed with macrocell scenarios in mind. Therefore, their performance in large-scale NoFs is far from optimal due to the overhead generated by frequent handovers and cell reselections. Thus, NoF scenarios require specific Location Management mechanisms in order to track UEs efficiently whilst keeping location signalling traffic under control. This applies to both Tracking Area Update (TAU) (i.e., updating the location of a UE in the NoF) and Paging procedures (notifying a UE in idle mode that a voice or data call needs to be established).

In the context of large-scale, all-wireless networks of femtocells, LLM provides a mechanism that enables network entities to map a subscriber's identity to the address and location of the HeNB where the UE is currently camped on. On the one hand, standard 3GPP identifiers (such as the International Mobile Subscriber Identity (IMSI) and/or the Serving Temporary Mobile Subscriber Identity (S-TMSI)) are used to identify users within the cellular network. On the other hand, the serving HeNB address varies as the destination UE moves throughout the NoF. This address is used by the underlying transport network to route packets towards the destination UE. In order to avoid interoperability problems with current HeNB-GWs and signalling traffic overload of the Evolved Packet Core (EPC), LLM mechanisms should only affect the network elements in the NoF (i.e., the local network) and not the network elements of the Evolved Packet Core (EPC).

3.1.2 Work during Years 1 and 2

The work carried out during the first two years has focused mainly on the definition of a distributed LLM scheme (along with its associated protocol architecture) that is capable of providing LLM functionalities in the context of a large-scale, all-wireless NoF. The LLM scheme is based on VIMLOC [20], a distributed, wireless mesh network-oriented location management mechanism in which location information is distributed across all HeNBs in the network of femtocells.

In order to integrate native 3GPP location management procedures with VIMLOC, modifications to the protocol architecture of HeNBs were needed. As a result of this, a 2.5 protocol layer (also referred to as geosublayer) was inserted between the network and access layers. One of the main functions of the geosublayer was to intercept all 3GPP control-plane location management messages in order to trigger the corresponding VIMLOC procedures in the network of femtocells. This work is described in detail in [1].

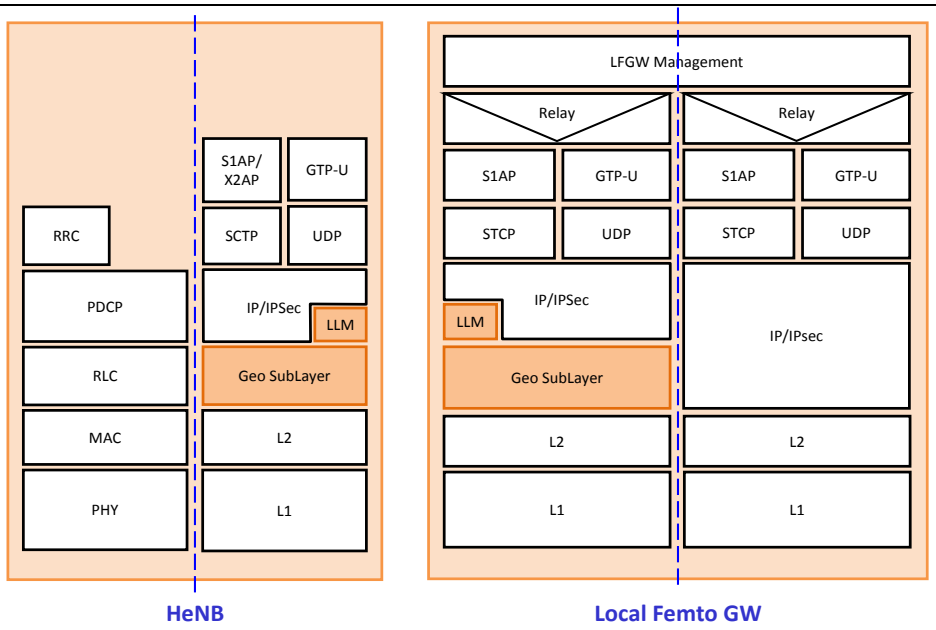

Figure 3-1: The 2.5 Layer (Geosublayer) in the LLM Protocol Architecture.

VIMLOC relies on native 3GPP user location mechanisms in order to determine the IP and geographic addresses of the HeNB where the destination UE is currently camped on. In order to do so, 3GPP Location Management mechanisms must be able to determine, with the granularity of a single femtocell, the current location of the destination UE within the NoF. Since standard 3GPP mechanisms can only determine the location of a UE with the granularity of a Tracking Area (TA), a first approach to the problem of fine-grained user tracking could be to reduce the size of all TAs in the NoF to that of a single femtocell. However, this solution is far from optimal, as it requires UEs to perform Tracking Area Update procedures every time they reselect/handover between neighbouring femtocells.

In order to address this problem, we proposed a self-organized Tracking Area List (TAL) mechanism built on top of the standard 3GPP TAU procedure. This was done to comply with 3GPP Technical Specifications. First, the Proxy Mobility Management Entity (P-MME) monitors the arrival rate of TAU Request messages from the UE in order to determine its mobility state. Secondly, the P-MME updates the UE-specific TAL by increasing, keeping, or reducing the number of cells in the TAL according to the mobility state and the paging arrival rate. Finally, the MME sends the new TAL to the UE in the TAU Accept message.

The self-organized mechanism combines static and dynamic TAL management depending on the UE mobility state. Thus, TALs are kept static until the location signalling traffic reaches a certain threshold. Past this activation point, the P-MME enables dynamic TAL management in order to reduce the overall location signalling traffic in the network.

A detailed description of the self-organized TAL mechanism, along with some analytical results, has been presented in [21].

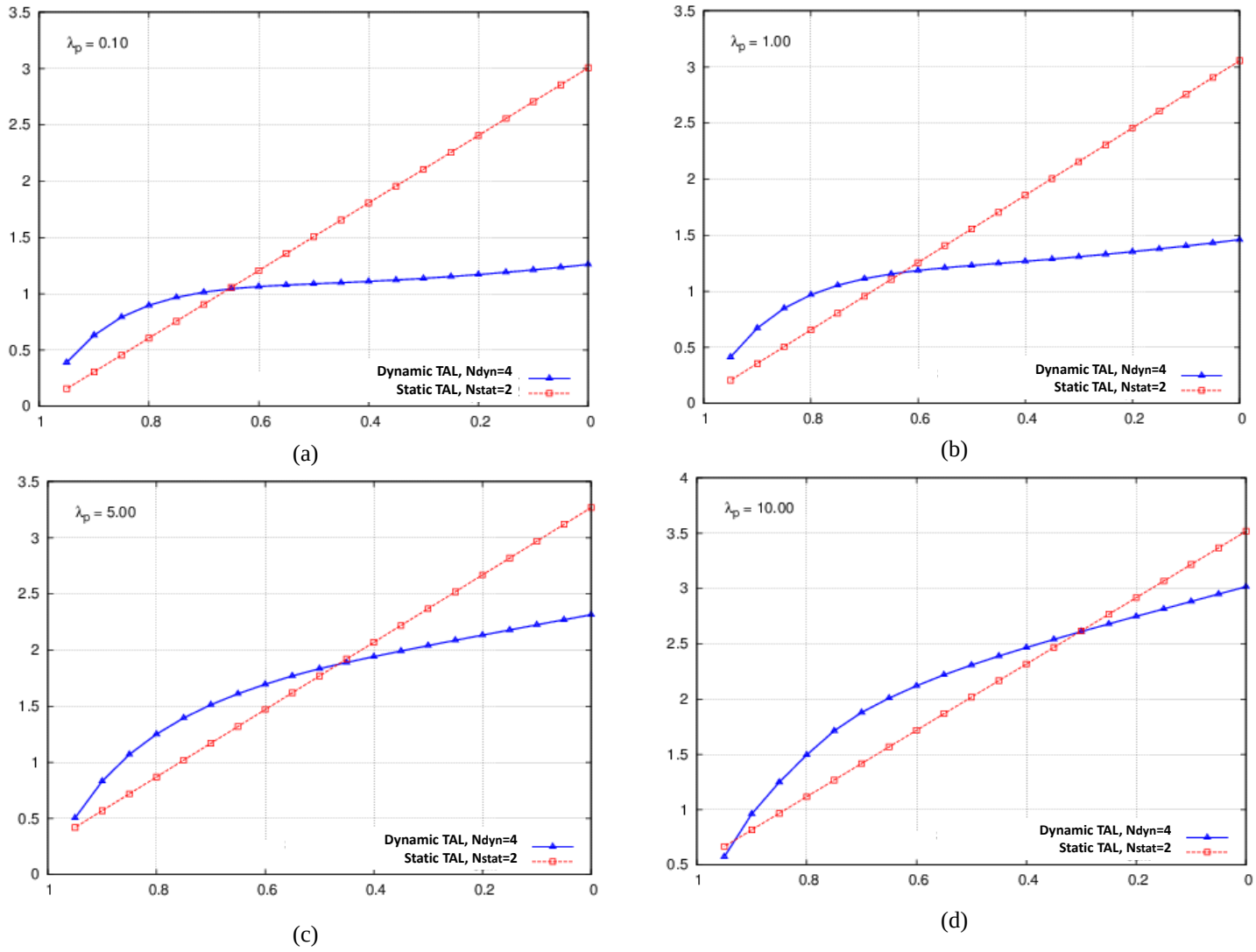

Figure 3-2: Impact of UE speed on location signalling traffic (static vs. dynamic TALs)

Figure 3-2 shows the impact of UE speed on the normalized signalling cost function for different paging arrival rates (λ_p). The normalized signalling cost function is a metric that captures both TAU and paging signalling. In general, dynamic Tracking Area Lists generate less location signalling traffic than static TALs for medium- to high-speed UEs. This reduction is significantly higher when UEs are subject to moderate paging arrivals. Since the cost of a single TAU operation is tenfold that of a paging operation [22], the self-organized TAL mechanism aims at minimizing the normalized signalling cost function by reducing the probability of TAU arrival for each UE.

The intersections of the two curves in each figure determine the activation points of the self-organized mechanism. Thus, at speeds where static TALs generate less location signalling traffic than dynamic TALs, the self-organized mechanism keeps the TAL size constant. Once the activation point has been reached, the P-MME enables dynamic TAL management, hence reducing the overall location signalling traffic in the network. This switching strategy yields a significant reduction in location signalling traffic per UE, as shown in Table 3-1.

λ_p	**Location signalling traffic reduction**
0.1	39.45%
1	33.53%
5	13.21%
10	4.45%

Table 3-1: Reduction in location signalling traffic per UE.

3.1.3 Enhancements to Proposed Schemes

One of the main drawbacks of the self-organized Tracking Area List mechanism is the cost (in terms of signalling traffic) of paging a UE that has been registered to a large TAL (i.e., a UE in high-mobility state). In the standard 3GPP Paging procedure, the (P)-MME sends an S1-AP Paging message (containing the UE ID) to each cell in the TAL where the UE is currently registered. The impact of this scheme on over-the-air signalling traffic is particularly relevant in large-scale, all-wireless NoFs.

In order to reduce the number of S1-AP Paging messages over the wireless multihop backbone, we propose a distributed paging mechanism that structures the 3GPP Paging procedure in two stages. First, it performs unicast paging from the P-MME to the closest HeNB in the destination TAL. Secondly, it performs an efficient paging broadcast within the destination TAL by forwarding an optimal number of Paging messages between neighbouring HeNBs over the X2 interface. This is described in details in the sections below.

3.1.3.1 Description of the Distributed Paging Mechanism over the X2 Interface

The following sequence takes place during the execution of the distributed paging algorithm:

- The P-MME receives a control-plane message from the MME (S1-AP Paging) or the P-SGW (GTP-C Downlink Data Notification) indicating that an incoming voice/data call needs to be established towards a certain UE in the NoF.
- The P-MME looks up the destination UE ID (e.g., S-TMSI) in its internal location database and determines the Tracking Area List ID where the UE is currently registered.
- Once the destination TAL ID has been retrieved, the P-MME determines the closest HeNB (to the P-MME) in the destination TAL. The P-MME stores the geographical location of each HeNB in its internal location database. This information is obtained from the geosublayer at each HeNB through O&M procedures.
- The P-MME derives an optimal paging broadcast tree (in terms of number of over-the-air Paging messages) for the destination TAL. The closest HeNB to the P-MME is the tree root.
- The P-MME encapsulates the paging broadcast tree in the payload of an S1-AP Paging message and sends it to the closest HeNB in the TAL. Note that a single S1-AP Paging message is sent from the P-MME to the destination TAL over the all-wireless multihop backbone.

- The closest HeNB to the P-MME in the TAL receives the S1-AP Paging message, performs a L1 paging procedure over the LTE-Uu interface, and sends an X2-AP Paging message to its one-hop neighbours as per the information contained in the broadcast paging tree.
- Upon receipt of an X2-AP Paging message, any HeNB in the destination TAL performs a L1 paging procedure over the LTE-Uu interface and sends an X2-AP Paging message to its one-hop neighbours as per the information contained in the broadcast paging tree.
- The destination UE is paged.

Figure 3-3 illustrates the operation of the standard paging and the distributed paging mechanisms in terms of control-plane messages over the all-wireless multihop backbone.

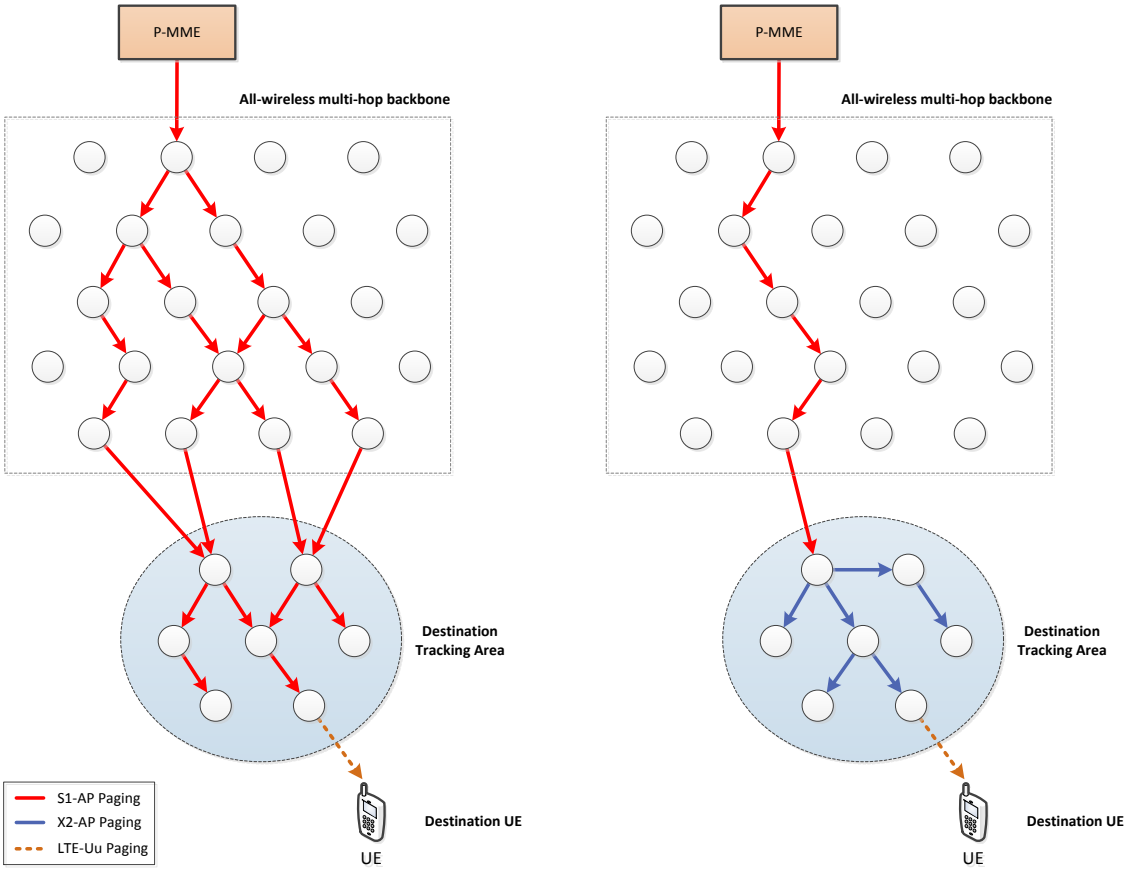

Figure 3-3: Operation of the Standard vs. Distributed Paging Mechanisms

3.1.3.2 Implications in the 3GPP Protocol Architecture

The following implications in the 3GPP protocol architecture must be considered durign the design of the distributed paging mechanism:

- **Geographic information availability at the P-MME:** the P-MME must know the physical location of each HeNB in the NoF in order to determine the closest femtocell in the destination TAL. This information can be obtained from the geosublayer at each HeNB through O&M procedures.
- **New Information Element (IE) in the S1-AP Paging message:** an additional IE (*PagingTree*) must be added to the structure of the S1-AP Paging message in order to encapsulate the optimal paging broadcast tree for the destination TAL. The size of this IE must be kept bounded in order to avoid large S1-AP Paging messages traversing the all-wireless multihop backbone.
- **New X2-AP Paging message:** a new Paging message needs to be defined in the X2-AP protocol. This message encapsulates the paging broadcast tree and is intended to allow Paging notifications amongst neighbouring HeNBs.

The following tables summarize the modifications that need to be added to the corresponding 3GPP Technical Specifications in order to provision the new S1-AP and X2-AP Paging messages.

Modifications to 3GPP TS 36.413: "Evolved Universal Terrestrial Radio Access Network (E-UTRAN); S1 Application Protocol (S1AP)"

Additions to the Technical Specification are highlighted in green.

9.1.6 S1-AP PAGING

This message is sent by the MME and is used to page a UE in one or several tracking areas.
Direction: MME → eNB

IE/Group Name	Presence	Range	IE type and reference	Criticality	Assigned Criticality
Message Type	M		3GPP TS 36.423, 9.2.13	YES	ignore
UE Identity Index value	M		3GPP TS 36.413, 9.2.3.10	YES	ignore
UE Paging Identity	M		3GPP TS 36.413, 9.2.3.13	YES	ignore
Paging DRX	O		3GPP TS 36.413, 9.2.1.16	YES	ignore
CN Domain	M		3GPP TS 36.413, 9.2.3.22	YES	ignore
List of TAIs		*1*		YES	ignore
>TAI List Item		*1 to <maxNoOfTAIs>*		EACH	ignore
>>TAI	M		3GPP TS 36.413, 9.2.3.16	-	
CSG Id List		*0..1*		GLOBAL	ignore
>CSG Id		*1 to <maxNoOfCSGId>*	3GPP TS 36.413, 9.2.1.62	-	
Paging Broadcast Tree		*0..1*		YES	ignore
>List of HeNBs		*1 to <maxNoOfHeNBsInTree>*		EACH	ignore
>> E-UTRAN Cell Identifier	M		BIT STRING (28)	-	
Paging Priority	O		3GPP TS 36.413, 9.2.1.78	YES	ignore

Range bound	Explanation
maxNoOfTAIs	Maximum no. of TAIs. Value is 256.
maxNoOfCSGId	Maximum no. of CSG Ids within the CSG Id List. Value is 256.
maxNoOfHeNBsInTree	Maximum no. of HeNBs in the Paging Broadcast Tree. Value is 256.

Modifications to 3GPP TS 36.423: "Evolved Universal Terrestrial Radio Access Network (E-UTRAN); X2 application protocol (X2AP)"

Additions to the Technical Specification are highlighted in green.

9.1.2.23 X2-AP PAGING

This message is sent by the (H)eNB and is used to page a UE in one or several tracking areas.
Direction: (H)eNB → (H)eNB

IE/Group Name	Presence	Range	IE type and reference	Criticality	Assigned Criticality
Message Type[1]	M		3GPP TS 36.423, 9.2.13	YES	ignore
UE Identity Index value	M		3GPP TS 36.413, 9.2.3.10	YES	ignore
UE Paging Identity	M		3GPP TS 36.413, 9.2.3.13	YES	ignore
Paging DRX	O		3GPP TS 36.413, 9.2.1.16	YES	ignore
CN Domain	M		3GPP TS 36.413, 9.2.3.22	YES	ignore
List of TAIs		*1*		YES	ignore
>TAI List Item		*1 to <maxNoOfTAIs>*		EACH	ignore
>>TAI	M		3GPP TS 36.413, 9.2.3.16	-	
CSG Id List		*0..1*		GLOBAL	ignore
>CSG Id		*1 to <maxNoOfCSGId>*	3GPP TS 36.413, 9.2.1.62	-	
Paging Broadcast Tree		*0..1*		YES	ignore
>List of HeNBs		*1 to <maxNoOfHeNBsInTree>*		EACH	ignore
>> E-UTRAN Cell Identifier	M		BIT STRING (28)	-	
Paging Priority	O		3GPP TS 36.413, 9.2.1.78	YES	ignore

Range bound	Explanation
maxNoOfTAIs	Maximum no. of TAIs. Value is 256.
maxNoOfCSGId	Maximum no. of CSG Ids within the CSG Id List. Value is 256.
maxNoOfHeNBsInTree	Maximum no. of HeNBs in the Paging Broadcast Tree. Value is 256.

9.2.13 Message Type

The *Message Type* IE uniquely identifies the message being sent. It is mandatory for all messages.

[1] As stated in 3GPP TS 36.423, section 9.2.13, the *Procedure Code* IE must be se to "16" (*Paging*).

IE/Group Name	Presence	Range	IE type and reference	Semantics description
Procedure Code	M		INTEGER (0..255)	"0" = Handover Preparation "1" = Handover Cancel "2" = Load Indication "3" = Error Indication "4" = SN Status Transfer "5" = UE Context Release "6" = X2 Setup "7" = Reset "8" = eNB Configuration Update "9" = Resource Status Reporting Initiation "10" = Resource Status Reporting “11” = Private Message "12" = Mobility Settings Change “13” = Radio Link Failure Indication “14” = Handover Report “15” = Cell Activation “16” = Paging
Type of Message	M		CHOICE (Initiating Message, Successful Outcome, Unsuccessful Outcome, …)	

3.1.4 Performance Evaluation

Early results obtained with ns-3 show that the proposed scheme can achieve up to an 85% reduction of over-the-air paging transmissions and an 80% of end-to-end paging delay reduction.

3.2 Seamless Macro-Femto Handover Based on Reactive Data Bicasting

3.2.1 Introduction

When a user moves from a macrocell to a femtocell or vice versa, seamless mobility should be supported by the employed handover procedure such that the handover is not perceptible to the users. Two main Key Performance Indicators (KPIs) during handover are Service Interruption Time (SIT) and packet loss. In current 3GPP standard, the same hard handover procedure as for inter-macro mobility is used for macro-femto mobility. A data forwarding procedure is used to forward the Downlink (DL) packets from the source cell to the target cell during handover to enable lossless packet delivery. Whereas this procedure works well for the handover between macrocells, it may be inappropriate for the handover between macrocells and femtocells. In most deployment cases, the fixed broadband operators will have no contractual agreements with the mobile network operators to provide guaranteed backhaul performance. Thus, remarkable DL SIT up to several hundreds of milliseconds may be perceived by the users in handover due to the data forwarding latency along the delay-prone residential backhaul.

Data bicasting or multicasting schemes have been widely used in literature to enable seamless handover by pre-buffering the data at the potential target cells before handover. Conventionally, a candidate set of the potential targets is dynamically updated based on the radio signal level and speed of a user. Duplicate data is transmitted and buffered at all the cells in the candidate set [23][24]. However, given that the hard handover is the only handover procedure supported by LTE so far, the maintenance of the candidate set may require considerable modifications to the standard. Furthermore, the size of the candidate set may be large due to the dense deployment of the femtocells. Proactively multicasting the data to all the cells in the candidate set may consume numerous backhaul and buffer resources at these cells.

To enable seamless mobility while keeping minimal changes to the 3GPP standard, we propose a reactive data bicasting scheme to reduce the DL service interruption time during HO by making "standard-friendly" modifications to the 3GPP LTE HO procedure. Compared to the conventional schemes which proactively trigger the data bicasting before the HO is initiated, the proposed scheme triggers the data bicasting after the HO is initiated by the source cell. An optional drop-head buffering mechanism only requiring a very small buffer size can be used at the S-GW to eliminate the packet loss during the HO procedure. The proposed scheme can significantly relax the resource requirements compared to the proactive data bicasting schemes.

3.2.2 Proposed Handover Procedure

A simple but effective modification based on the standard 3GPP HO procedure to enable seamless handover when users move from a macrocell to a femtocell or vice verse is proposed. The modified handover procedure is shown in Figure 3-4. When the MME receives the *HO Required message* from the source cell, the MME will determine the target cell by checking this message and send a *Data Bicasting Request* to the S-GW. When the S-GW receives this request, it will duplicate the downlink data packets and bicast them to both the source and the target. The target cell maintains a receiving buffer for the bicasted data. The other actions from the MME and the target cell are the same as the standard procedure until the source cell receives the *HO Command* message.

Instead of sending the *SN Status Transfer* message to the target cell via the MME and forwarding the downlink data to the target cell via the S-GW, the source cell will include the SN status in the *RRC Connection Reconfiguration* message and send it to the UE. The data that arrives at the source cell after the UE has been detached will be simply discarded. When the UE is synchronized with the target cell, the UE will send the *RRC Connection Reconfiguration Complete* message with the SN status to the target cell. Based on the SN status, the target cell can immediately determine the sequence number of the next data packet to be transmitted to the UE and start both DL and UL data transmissions. The target cell then sends the *Path Switch Request* including *Bicasting Cancellation* command to the MME. The MME will send the *UP Update Request* to the S-GW to switch the downlink path from the source cell to the target cell and at the same time cancel the bicasting. It is noted that most modifications can reuse the existing messages defined in the standard. Therefore, the proposed scheme keeps minimal changes to the standard procedure.

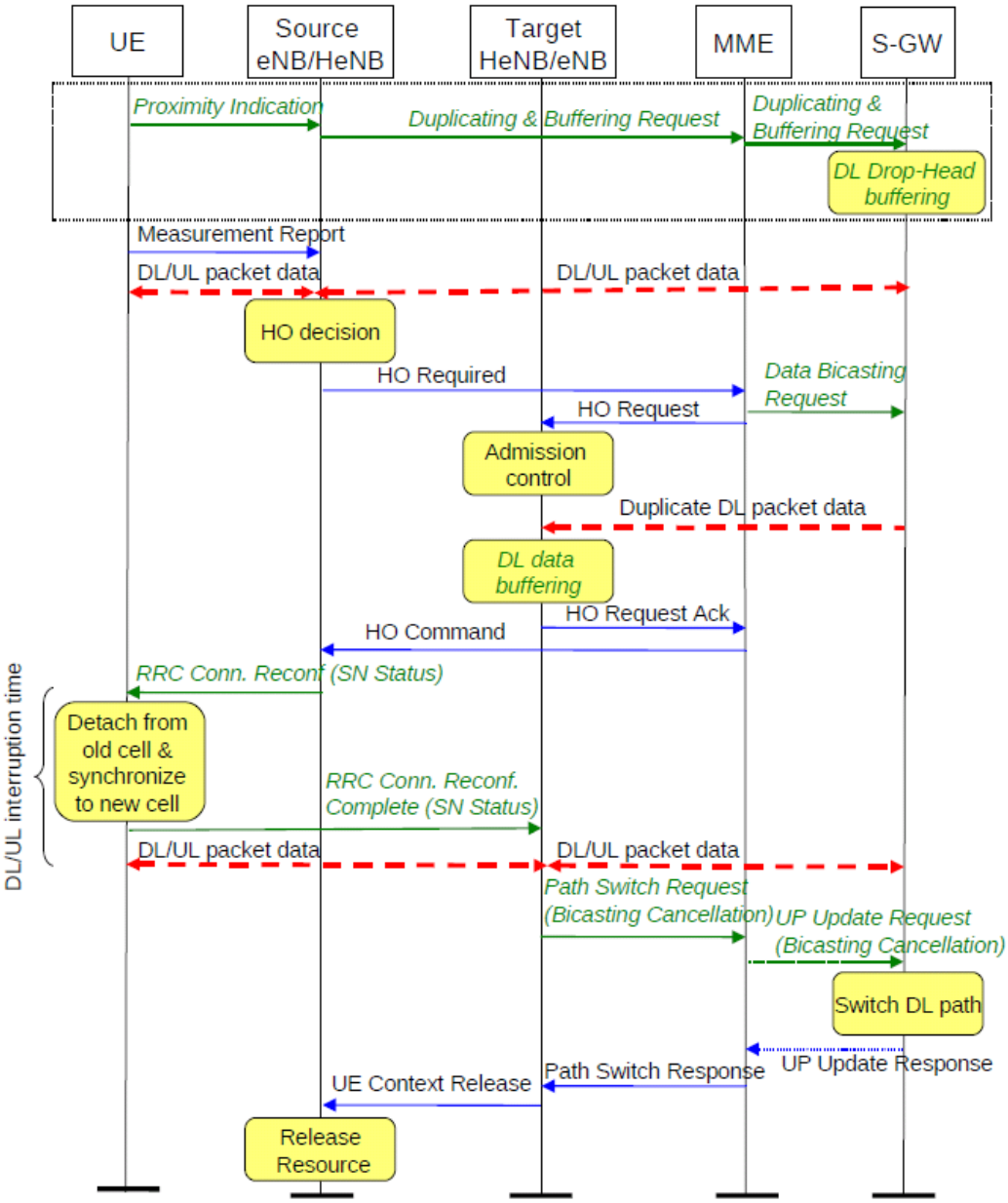

Figure 3-4: Proposed handover procedure

Since there is no data forwarding process from the source cell to the target cell during the HO, the data packets will be lost if they arrive at the source after the UE is detached and are also not buffered at the target. It will be shown in the following that the number of lost packets is very small. Actually, this loss can be simply ignored for the real-time traffic such as VoIP. However, if lossless handover is required, an optional drop-head buffering mechanism can be used to avoid the packet loss. Just before the HO, the UE may send a *Proximity Indication* to the source cell if it determines that it is near a target cell. Note that the proximity estimation method has already been proposed by 3GPP [25] to facilitate the HO to Closed Subscriber Group (CSG) or hybrid cells. A *Duplicating and Buffering Request* will be sent by the source cell and forwarded by the MME to the S-GW. A drop-head buffer with a size of *N* will be activated. Any DL packet arriving at the S-GW will be duplicated before the original one is sent out. The duplicate copy will be put into the drop-head buffer. The buffer will drop the packets from the front if it reaches its maximum capacity, in other words, the buffer will always keep the latest *N* packets. When the S-GW receives the *Data Bicasting Request*, it will first empty the drop-head buffer and send the packets in the buffer to the target cell. A small buffer size will be enough to avoid the packet loss as will be shown in the following.

3.2.3 KPI Analysis

In this section, the proposed handover procedure will be analyzed in terms of the two KPIs mentioned before: expected DL service interruption time and expected number of lost packets. For the packet loss, we analyze the case that there is no drop-head buffering at the S-GW. Thus, we can estimate the required buffer size *N* if we want to avoid the packet loss during the HO. The similar analyzing methods can be used for the handover from a macrocell to a femtocell and the handover from a femtocell to a macrocell. In the following, we will take the former case for description purpose. The latencies incurred during the handover procedure are denoted as follows:

- $D_{eNB,MME}$: The transmission latency between the eNB and the MME.
- $D_{eNB,SGW}$: The transmission latency between the eNB and the S-GW. Without loss of generality, we assume that $D_{eNB,MME}$ and $D_{eNB,SGW}$ have the same distribution and can be denoted by the random variable x.
- $D_{HeNB,MME}$: The transmission latency between the HeNB and the MME.
- $D_{HeNB,SGW}$: The transmission latency between the HeNB and the S-GW. Without loss of generality, we assume that $D_{HeNB,MME}$ and $D_{HeNB,SGW}$have the same distribution and can be denoted by the random variable y.
- D_{HO_exec}: The HO execution latency from the time that the UE receives the *RRC Connection Reconfiguration* message to the time that the target cell receives the *RRC Connection Reconfiguration Complete* message. It can be denoted by the random variable h.

The latency between the MME and the S-GW via S11 interface is very low (1 ms as stated in [26]). Thus, we ignore this latency in the analysis.

We assume that x, y, and h have mixed-Erlang density functions [27]:

$$f_d(t) = \sum_{j=1}^{N_d} \alpha_{d,j} \frac{(\lambda_{d,j}t)^{k_{d,j}-1}}{(k_{d,j}-1)!} \lambda_{d,j} e^{-\lambda_{d,j}t}$$

where d represents x, y, or h. N_d, $\alpha_{d,j}$, $k_{d,j}$, and $\lambda_{d,j}$ determines the shape and scale of the distribution and $\sum_{j=1}^{N_d} \alpha_{d,j} = 1$. The mixed-Erlang distribution is selected here because it can achieve a good approximation for many other distributions and real-world measurement traces [28]. Its corresponding Laplace transform is given as:

$$F_d(s) = \sum_{j=1}^{N_d} \alpha_{d,j} \left(\frac{\lambda_{d,j}}{s+\lambda_{d,j}}\right)^{k_{d,j}}$$

3.2.3.1 Expected DL Service Interruption Time

For the 3GPP scheme, the data forwarding latency is $D_{eNB,SGW} + D_{HeNB,SGW}$, which can be represented by the random variable $U = x + y$with density function $f_U(t)$. The DL SIT is determined by the maximum value between U and h. Note that the packet inter-arrival duration is not considered in the SIT since this is not related to the handover procedure. Thus, the expected DL SIT can be derived as:

$$E[DL\_SIT]^{3GPP} = \int_{U=0}^{\infty} \int_{h=0}^{U} U f_h(h) f_U(U)\, dh\, dU + \int_{U=0}^{\infty} \int_{h=U}^{\infty} h f_h(h) f_U(U)\, dh\, dU.$$

For the first term on the right side of the above equation, we have:

$$\int_{U=0}^{\infty}\int_{h=0}^{U} U f_h(h) f_U(U)\, dh\, dU$$
$$= \int_{U=0}^{\infty} U f_U(U) \int_{h=0}^{U} \sum_{j=1}^{N_h} \alpha_{h,j} \frac{\lambda_{h,j}^{k_{h,j}} h^{k_{h,j}-1}}{(k_{h,j}-1)!} e^{-\lambda_{h,j} h}\, dh\, dU$$
$$= \int_{U=0}^{\infty} U f_U(U) \Bigg\{ \sum_{j=1}^{N_h} \alpha_{h,j} \cdot \Bigg[1 - \sum_{n_j=0}^{k_{h,j}-1} \frac{(\lambda_{h,j} U)^{n_j}}{n_j!} e^{-\lambda_{h,j} U} \Bigg] \Bigg\} dU$$
$$= \sum_{j=1}^{N_h} \alpha_{h,j} \Bigg\{ \int_{U=0}^{\infty} U f_U(U)\, dU - \sum_{n_j=0}^{k_{h,j}-1} \frac{(\lambda_{h,j})^{n_j}}{n_j!} \cdot \Bigg[\int_{U=0}^{\infty} U^{n_j+1} f_U(U) e^{-\lambda_{h,j} U} \Bigg] dU \Bigg\}$$
$$= \sum_{j=1}^{N_h} \alpha_{h,j} \Bigg\{ \sum_{j=1}^{N_x} \alpha_{x,j} \frac{k_{x,j}}{\lambda_{x,j}} + \sum_{j=1}^{N_y} \alpha_{y,j} \frac{k_{y,j}}{\lambda_{y,j}} - \sum_{n_j=0}^{k_{h,j}-1} \frac{(\lambda_{h,j})^{n_j}}{n_j!} \cdot \Bigg[\frac{(-1)^{n_j+1} d^{n_j+1} F_U(s)}{ds^{n_j+1}} \Big|_{s=\lambda_{h,j}} \Bigg] \Bigg\},$$

where $F_U(s)$ is the Laplace transform of $f_U(t)$. Based on the convolution theorem, it can be denoted as:

$$F_U(s) = F_x(s) F_y(s)$$
$$= \Bigg(\sum_{j=1}^{N_x} \alpha_{x,j} \Big(\frac{\lambda_{x,j}}{s+\lambda_{x,j}} \Big)^{k_{x,j}} \Bigg) \Bigg(\sum_{j=1}^{N_y} \alpha_{y,j} \Big(\frac{\lambda_{y,j}}{s+\lambda_{y,j}} \Big)^{k_{y,j}} \Bigg)$$

For the second term on the right side, we have:

$$\int_{U=0}^{\infty}\int_{h=U}^{\infty} h f_h(h) f_U(U)\, dh\, dU$$
$$= \int_{U=0}^{\infty} f_U(U) \int_{h=U}^{\infty} h \sum_{j=1}^{N_h} \alpha_{h,j} \frac{\lambda_{h,j}^{k_{h,j}} h^{k_{h,j}-1}}{(k_{h,j}-1)!} e^{-\lambda_{h,j} h}\, dh\, dU$$
$$= \int_{U=0}^{\infty} f_U(U) \sum_{j=1}^{N_h} \alpha_{h,j} \cdot \sum_{n_j=0}^{k_{h,j}} \frac{k_{h,j} \lambda_{h,j}^{n_j-1} U^{n_j}}{n_j!} e^{-\lambda_{h,j} U}\, dU$$
$$= \sum_{j=1}^{N_h} \alpha_{h,j} \sum_{n_j=0}^{k_{h,j}} \frac{k_{h,j} \lambda_{h,j}^{n_j-1}}{n_j!} \Bigg[\frac{(-1)^{n_j} d^{n_j} F_U(s)}{ds^{n_j}} \Big|_{s=\lambda_{h,j}} \Bigg].$$

For the proposed scheme, if the buffer for storing bicasted data at the target cell is not empty when the user gets connected, the communication session can be resumed immediately. Otherwise, the session will be resumed when the bicasted packets arrive. When data bicasting is initiated at the S-GW, it takes $D_{eNB,SGW}$ to arrive at the target cell. The duration from this moment to the time that the UE initiates the detachment from the old cell and synchronization to the new cell is represented by the random variable $y+y'+x$. The DL SIT is determined by the maximum value between h and $y''-(y+y'+x)$. y'' and y' have the same distribution as y. Let $L = y''-(y+y'+x)$ with density function $f_L(t)$. Thus, the expected DL SIT can be derived as:

$$E[DL\_SIT]^{Prop} = \int_{L=-\infty}^{0}\int_{h=0}^{\infty} h f_h(h) f_L(L)\, dh\, dL + \int_{L=0}^{\infty}\int_{h=L}^{\infty} h f_h(h) f_L(L)\, dh\, dL + \int_{L=0}^{\infty}\int_{h=0}^{L} L f_h(h) f_L(L)\, dh\, dL.$$

There is no simple expression available for the solution of the above equation. The derivation process is omitted here.

3.2.3.2 Expected Number of Lost Packets without Drop-Head Buffer at S-GW

Suppose that the S-GW receives the *Data Bicasting Request* message at time t_0, the duration from this moment to the time that the UE receives the *HO Command* message and is detached from the source is represented by the random variable $y+y'+x$. The data packets will be lost if they have been sent to the source before t_0 but arrived after the UE receives the *HO Command* message. It is assumed that the data packets arrive at the S-GW according to a Poisson process with the arrival rate λ_p following the assumption widely adopted in literature. Let t_i denote the time at which the *i*th packet was sent from the S-GW to the source cell tracking back from t_0. $T_i = t_0 - t_i$ has an Erlang distribution with the density function:

$$f_{T_i}(t) = \frac{(\lambda_p t)^{i-1}}{(i-1)!}\lambda_p e^{-\lambda_p t}$$

Its corresponding Laplace transform is given as:

$$F_{T_i}(s) = \left(\frac{\lambda_p}{s+\lambda_p}\right)^i$$

The transmission latency of the *i*th packet can be represented by the random variable x_i that has the same distribution as x. Let N_L denote the number of lost packets at the source cell during the HO procedure. Let $W_i = y + y' + x + T_i$ with density function $f_{W_i}(t)$. The expected number of lost packets is given as:

$$\begin{aligned} E[N_L] &= \sum_{i=1}^{\infty} Pr[W_i < x_i] \\ &= \sum_{i=1}^{\infty}\left\{\int_{W_i=0}^{\infty}\int_{x_i=W_i}^{\infty} f_{W_i}(W_i) f_{x_i}(x_i)\, dx_i\, dW_i\right\} \\ &= \sum_{i=1}^{\infty}\sum_{j=1}^{N_x}\alpha_{x,j}\sum_{n_j=0}^{k_{x,j}-1}\frac{\lambda_{x,j}^{n_j}}{n_j!}\left\{\frac{(-1)^{n_j} d^{n_j} F_{W_i}(s)}{ds^{n_j}}\bigg|_{s=\lambda_{x,j}}\right\} \end{aligned}$$

where $F_{W_i}(s)$ is the Laplace transform of $f_{W_i}(t)$. Based on the convolution theorem, it can be denoted as:

$$\begin{aligned} F_{W_i}(s) &= F_y(s) F_{y'}(s) F_x(s) F_{T_i}(s) \\ &= \left(\sum_{j=1}^{N_y}\alpha_{y,j}\left(\frac{\lambda_{y,j}}{s+\lambda_{y,j}}\right)^{k_{y,j}}\right)^2 \\ &\quad\cdot\left(\sum_{j=1}^{N_x}\alpha_{x,j}\left(\frac{\lambda_{x,j}}{s+\lambda_{x,j}}\right)^{k_{x,j}}\right)\left(\frac{\lambda_p}{s+\lambda_p}\right)^i \end{aligned}$$

3.2.4 Numerical Results

Numerical examples are evaluated in this section to investigate the two KPIs. Without loss of generality, we use the setting $\alpha_{d,j} = 0.5$ and $k_{d,j} = 2$ for $j = 1, 2$, and $\lambda_{d,1} = 2\lambda_{d,2}$, where d represents x, y, or h [27]. By referring to [29], we set $E[x]$=10 ms and $E[h]$=20 ms. For real-time applications such as VoIP and video streaming, the packet inter-arrival time typically ranges from 10 to 40 ms. Thus, the packet arrival rate λ_p ranges from 1/10 ms-1 to 1/40 ms-1.

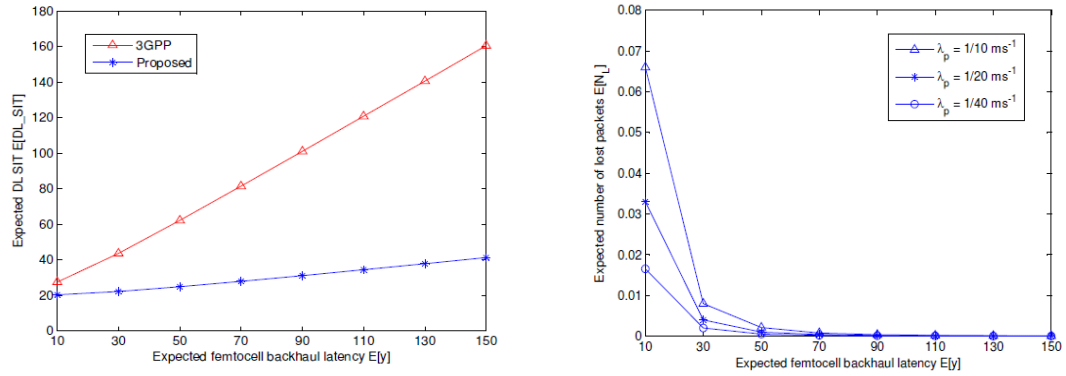

(a) Expected downlink service interruption time (b) Expected number of lost packets without S-GW buffering

Figure 3-5: Handover from macrocell to femtocell.

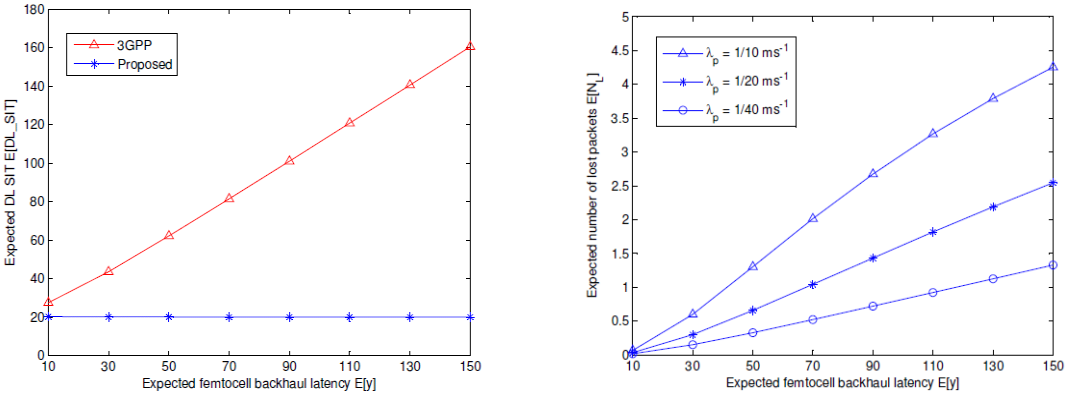

(a) Expected downlink service interruption time (b) Expected number of lost packets without S-GW buffering

Figure 3-6: Handover from femtocell to macrocell.

Figure 3-5 and Figure 3-6 show the KPIs for the handover from macrocell to femtocell and from femtocell to macrocell with respect to the expected femtocell backhaul latency, respectively. With the increase of the femtocell backhaul latency, the expected DL SITs during both handovers will significantly increase for the standard 3GPP handover procedure due to the data forwarding operation. On the contrast, the proposed scheme only slightly increases the expected DL SIT for the handover from macrocell to femtocell and keeps it almost constant for the handover from femtocell to macrocell. In the proposed scheme, the DL data is bicasted to the target cell during the HO without requiring the data forwarding any more. Therefore, the DL SIT is mainly determined by the inherent radio HO execution latency.

The expected number of lost packets when using the proposed scheme is negligible for the handover from macrocell to femtocell. For the handover from femtocell to macrocell, it will increase as the femtocell backhaul latency increases but still under 5 packets even when the femtocells backhaul latency is up to 150 ms. This implies that additional S-GW buffering mechanism is actually not necessary for the real-time traffic such as VoIP where a small amount of lost packets are acceptable. In case that a lossless handover is required, a small drop-head buffer at the S-GW will be enough to avoid the packet loss.

3.2.5 Conclusion

A novel handover procedure for LTE macro-femto networks based on reactive data bicasting is proposed. The proposed scheme can significantly reduce the downlink service interruption time compared to the standard 3GPP scheme while still avoiding the packet loss with the help of a small drop-head buffer at the S-GW. The data will be bicasted to the source cell and the target cell only when the HO is actually

initiated, and thus, only a small receiving buffer is required at the target cell. The simplicity, effectiveness, and limited resource requirements make it a promising solution to support seamless macro-femto mobility.

4. Network Management

4.1 Energy Saving Network Management and Performance in HetNets

The current trend towards heterogeneous networks (HetNet), where a layer of macrocells for blanket coverage co-exist with a layer of femtocells for providing capacity, will offer an improved spectral efficiency per area, but it can also offer an opportunity to improve the energy efficiency, measured as the power consumption needed to provide a certain throughput in a given area. We are going to analyze, two network performance indicators, the aggregated throughput and the energy efficiency, in two network architectures; a traditional deployment based on outdoor macro base stations for the provision of outdoor and indoor coverage, which will be used as a benchmark scenario, and a deployment where some of the indoor traffic is supported by femtocells.

Performance simulations and energy calculations have shown that the introduction of a femtocell layer, complementing the macrocell layer, greatly improves the system performance and the energy efficiency, when compared with current indoor coverage based on outdoor macro and micro base stations, even though some procedures must be implemented to reduce the total power consumption of the femtocell layer.

4.1.1 Current macro-only deployment limitations

Current mobile networks provide radio coverage by means of layers of base stations, based on a first layer of high power macrocells, and a second layer of medium power microcells. In general these layers are intended to provide simultaneous outdoor and indoor coverage, and thus are installed in outdoor locations. This standard procedure has worked fine as long as the traffic has been mostly originated from outdoors, but with the introduction of data-related services the scenario has reversed and the main traffic demand comes now from indoors.

In this indoor traffic demand scenario, an approach where the coverage is provided from indoors becomes preferable. The former solution incurs in high external walls penetration losses, and the latter is a natural evolution of the cellular concept, reusing resources in ever smaller cells, and can make a better use of the radio power as the femtonode and the user are located near each other, with minimal radio transmission losses that translate in a higher spectral efficiency.

4.1.2 Macrocell coverage analysis from the energy efficiency point of view

Urban macro network deployments characteristics

The macrocell urban scenario is usually intended to provide a good outdoor coverage and a sufficient indoor service, and its performance in dense urban deployments is usually interference-limited, because the unwanted power from neighbouring cells becomes noticeable, as there is a high degree of overlapping between small urban neighbouring macrocells. As a reference, 3GPP uses for a dense urban reference scenario an inter site distance (ISD) of only 500 metres, and the average inter-site distance of currently running networks in a dense urban scenario is around 200-300 metres.

LTE macrocell urban scenario simulation

A macrocell reference scenario with 18 LTE eNodeBs (54 cells) has been selected as an example of a real urban deployment, where all the traffic is served with macrocells. This reference scenario is a dense urban area in Madrid's city centre (Salamanca district), with an area of 2.86 km^2 and an average inter-site distance of 250 metres.

The eNodeBs transmit a power of 46 dBm (40 watts) per sector, their operation frequency is 2.1 GHz, their bandwidth is 10 MHz, and diversity is used in the eNodeB receivers. The overall capacity of this scenario is calculated considering 10 active users per cell, i.e. 540 active users are randomly distributed over the whole scenario, outdoor and indoor.

For the energy requirements analysis, the most favourable situation for the macro deployment has been selected; assuming outdoor base stations that do not need any shelter or air conditioning, thus the maximum consumed power per site, with three cells, is 790 W (based on actual eNodeB vendors' data). On the other hand, an eNodeB has always a minimum power level consumption, even when no traffic is served, that is approximately a 40% of the full traffic load situation. In the intermediate traffic situations, the power consumption is interpolated.

The macrocell reference scenario has been evaluated by means of a static radio planning tool (a Telefónica's proprietary tool) that calculates the signal level by means of a ray tracing tool core (Siradel) using as an input a 3D cartography of Madrid's city centre. Then the signal to noise ratio is calculated in a

grid of points in the reference scenario, and in a subsequent step the throughput in each point is calculated using a LTE look up table (SINR – throughput). Finally the scenario's average capacity is computed.

Macrocell scenario total throughput, total radiated power and total consumed power

The next figure shows the available throughput map. The aggregated average capacity for the 18 sites is 437 Mbps.

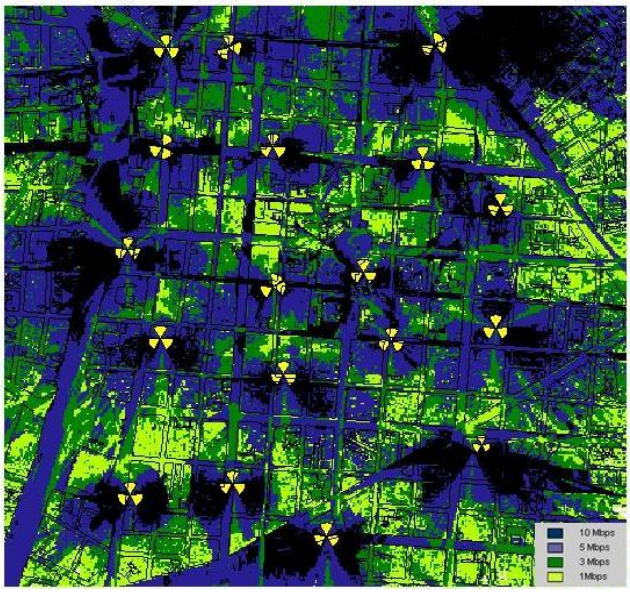

Figure 4-1. Available throughput map in the reference scenario

The total radiated power is 2,160 watts (40 watts/cell multiplied by 54 cells) and the total consumed power is 14,220 watts (790 watts/site multiplied by 18 sites).

Macrocell scenario Figures of Merit

In order to give a clear insight of the energy efficiency of this scenario, we will use some figures of merit, i.e. Mbps per watt, Mb/W. In the proposed reference scenario, when only the radiated power is considered, Mb/W equals 0.203, and this value decreases to 0.031 when the total consumed power is taken into account.

4.1.3 Combined macro and femto coverage analysis from the energy efficiency point of view

Multilayer macro and femto urban scenario simulation

We are going to analyze the same geographical area described previously, but considering that a fraction of the houses will install a femtonode. For this study it was used an 8 metre × 10 metre reference apartment (see next figure), with brick exterior walls and plasterboard partitions, which is typical of Madrid's Salamanca district simulated area.

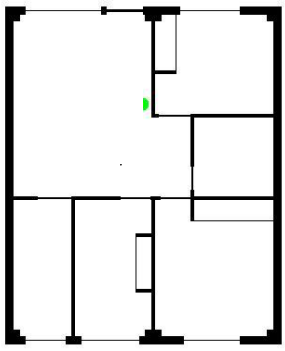

Figure 4-2. Reference 80 m2 apartment scenario with a central femtonode

In this scenario, the in-building area has a ground floor extension of 975,188 m^2, and taking into account that the average number of stories per building in the district is five; the total indoor area is 4,875,942 m^2, and there should be 60,949 reference apartments in this area.

The indoor section of the reference scenario has been evaluated by means of a Telefónica's proprietary indoor propagation tool based on COST 231 multi-wall model that characterizes indoor path losses by a fix path loss exponent, plus additional path loss factors related with the empirical attenuation introduced by all the walls crossed by the by the radio waves (considering the type of materials and their thickness). It is assumed that femtocells and macrocells are using different frequencies; therefore there is not significant interference between the macrocell and the femtocell layers.

In this exercise, 18% of the apartments, 10,971, have installed a femtocell. This 18% figure is one of the femtocell penetration options that have been studied and selected as representative for a moderate deployment scenario. Most of the apartments will enjoy a higher throughput than what could be provided from a macro, improving the aggregated throughput in the reference scenario, and at the same time they will offload the traffic and coverage requirements on the macro layer. For example, if an 18% of the indoor area is served by femtonodes, the operator can afford to reduce every macro site power and tolerate an indoor coverage gap (served from the macro layer) of the order of 18%. In our reference scenario, the simulations performed indicate that macrocell radiated power per eNodeB can be reduced from 46 dBm to 38 dBm (an equivalent result could be obtained reducing the number of sites), which renders a macro site power consumption reduction from 790 W to 391 W.

Given this new reference scenario, the next step is to analyze the aggregated throughput and power consumption. This exercise is deliberately pessimistic and therefore it is not considering femtocells without interferences from neighbour femtocells, and thus most of the femtonodes are highly interfered. The femtonodes are divided into four categories:

- Type 0 – Without an interferer femtocell. Not considered in this study.
- Type I –Serving Femtocell surrounded by one interferer femtocell, surrounded meaning that there is a neighbour apartment where a femtocell is installed too. The simulation scenario sets that a 10% of femtocells fall into this class (1,097).
- Type II – Serving Femtocell surrounded by two interferer femtocells. 40% of the scenario femtocells are classified Type II (4,388).
- Type III – Serving Femtocell surrounded by five interferer femtocells. 50% of the femtocells are considered to be Type III (5,486).

The percentages proposed for the distribution of the different types of femtonodes are an estimation, based on the homes distribution in a densely populated area as Madrid's Salamanca District. Every femtocell is located at a height of 1 meter and radiates 15 dBm from a 6 dB gain omni directional antenna. The consumed power per femtocell is 8 watts (data obtained from commercial 3G femtocells). The operation frequency is 2.6 GHz and the bandwidth is 10 MHz.

The average cell throughput for each femtocell type is: 27.5 Mbps for Type 0, 19.1 Mbps for Type I, 17.9 Mbps for Type II and 17.5 Mbps for Type III.

There is not a noticeable performance degradation increase between Type II (two neighbour interferers) and Type III (five interferers), because in Type III two of the interferers are located at the other side of a corridor, separated with additional walls). This is the reason for not considering some intermediate "Types", for example a serving femtocell surrounded by 3 or 4 interfering femtocells. The next figure shows the capacity results for a Type III femtocell.

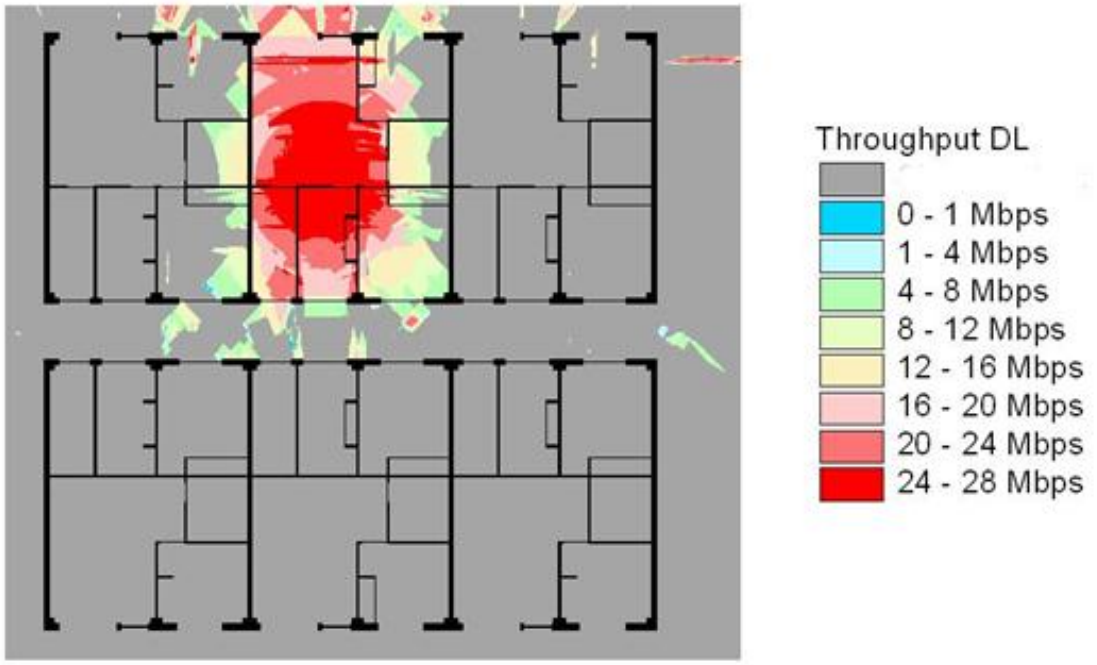

Figure 4-3. Femtocell Type III throughput map

Total throughput, total radiated power and total consumed power

The simulations that have been done to evaluate the aggregated capacity of the 10,971 femtocells and the 54 macrocells in the reference scenario, taking into account the type of femtocells, indicate a total aggregated average throughput for the whole scenario of 195,884 Mbps, from which 195,534 Mbps are provided by the femtonodes, and 350 Mbps by the macrocells.

Regarding energy, the total radiated power is 687 watts (346 W from the femtonodes, and 341 W from the macros) and the total consumed power is 94,806 watts, the femtonodes being responsible of 87,768 W, and the macros consuming 7,038 W.

Figures of Merit calculation

In the macro plus femtonodes scenario, the figure Mb/W equals 285 Mbps/W when only the radiated power is considered and 2 Mbps/W when the total power consumption is taken into account.

Comparison with the current macrocell approach

The energy efficiency comparison is clearly favourable to the macro plus femto approach. The next table summarizes and compares the figures of merit of both deployment solutions.

Figures of Merit	**Macro-only deployment**	**Macro & Femto deployment**
Mb/W (total power)	0.031	2
Mb/W (radiated power)	0.203	285

Table 4-1. Macrocell vs. Femtocell energy efficiency comparison

It can be observed that the hybrid macro and femto approach is about 65 times more efficient in terms of total consumed power than the macrocell approach and about 1,400 times more efficient in terms of radiated power.

These figures show that femtocells can improve not only indoor coverage and throughput, but also greatly improve indoor mobile service energy efficiency. However, it must be taken into account that the hybrid scenario absolute power consumption has been multiplied by 6.6 with respect to the reference one, thus making it mandatory to implement some femtonode switching-off procedures when they are not providing service.

4.1.4 Strategies to reduce energy consumption and interference in the femtonode layer

It must be taken into account that the femtonode users will not be at home during an important fraction of the day, and then the femtonodes can be switched off, rendering a potential sharp reduction of the aggregated power consumption described in the previous section, and also a reduction of the interference generated by these femtonodes, at least that due to the control and broadcast channels which are always transmitted regardless the presence of any UE.

Some implementations have been proposed for switching off the radio section of a femtonode when the user is not in the neighbourhood of the femtonode. They detect when the UE is camped in the nearest macro cell to the femtonode in order to decide when switching on or off the femtonode. When the User Equipment is not camped in a predefined macrocell it is assumed to be far away from home and the femtonode is switched off

The most efficient approach is to actually detect when the users are not at home, and thus switch off the radio section of the femtonode, reducing interference and improving energy saving. A possible solution is to detect the customer presence by means of a low-power radio interface activated in the UE, for example a Bluetooth Low Energy, or Wi-Fi, which could be always active in the UE but whose low power characteristic does not degrade significantly the battery lifetime. When the user arrives at home, a short range radio connection between the UE and the femtonode is established, and the latter can switch-on its radio section accordingly (the opposite is done when the user leaves the home and the short range connection is lost). Currently, this strategy is under evaluation in 3GPP [30].

It must be taken into account that the standard cell reselection and handover procedures could not work properly when the UE is moving from the coverage area of a macrocell to that of a femtocell whose radio section has been switched off when no UE is camping in it, in particular when the femtocell switch on procedure is performed only when the UE approaches to a very short distance of it. In the case the UE is leaving the macrocell coverage and it is getting into the vicinity of the still switched off femtocell, the UE will not have stored the femtocell cell RSRP among its reselection and handover candidate cells list.

When the UE is in idle mode, this will mean that there will be a period of time, from the moment it leaves the coverage area of the macrocell, until it detects the RSRP of the femtocell once it has been switched on, during which the UE will not be camping in any cell, and will be thus disconnected from the mobile network.

On the other hand, when the UE is in connected state, the hand over procedure between the macrocell and the femtocell could not be performed on time to keep the connection between the UE and the core network active, because the UE will leave the coverage area of the macrocell and it will have to wait for the femtocell to switch on, spend a certain period of time to measure its RSRP, and request to the MME to start the handover procedure.

Some work has been done to improve the UE measurement process for cell reselection and handover between standard LTE base stations that do not implement a radio section switch on/off procedure, for example, dedicating more time and accuracy for the measurement of certain preferred base stations. However, no work has been done to solve the specific problem of cell reselection and handover to a femtocell whose radio section is off and thus the UE cannot measure any parameter of the target cell. This is an open issue that will require further study.

5. Security

5.1 Local access control in networks of femtocells for multi-operator scenarios

5.1.1 Introduction

The scheme presented provides a solution to the problem of access control to local services in the NoF (e.g., those offered to users visiting some company premises). The problem and also the solution are divided into two different aspects: the access control part under the control of the mobile network operator (MNO), and the access control to local services of the network of femtocells, which is under the control of the local network operator (LNO) (e.g., the IT department of a company). The former is about allowing UEs attaching to a femtocell that operates in the licensed spectrum of the MNO. The latter is about providing a fine-granular control on what local services offered by the LNO can be accessed by what UE and during what period of time.

Therefore, the LNO must have the ability to control which user equipments (UE) can have access to the local network and to decide what resources it wants to share and which UE can use these resources. Given the architecture defined in BeFEMTO for NoFs, the LFGW plays a key role in this respect, as explained below. The standard mechanism used by BeFEMTO to share control between the MNO and the LNO is the CSG [31]. In fact, both operators can control what UEs are allowed attaching to a given closed subscriber group by appropriately managing the lists stored in core network servers in charge of managing CSGs. When accessing CSGs, there are two scenarios to consider. In the first one the UE and the femtocells in the NoF belong to the same HPLMN. The regular servers for CSG management (i.e., CSG Lists Server and CSG Admin Server) can be used in this case. This scenario was discussed in D5.2. In the second one, when a roaming agreement is in place, the UE may access femtocells belonging to a VPLMN. This is the focus of D5.3 in terms of access control.

In the multi-operator scenario, UEs from different MNOs are allowed to access local services offered by the LNO. In this case, there is still the need for CSG membership management and two options exist, namely HPLMN CSG Roaming (HCSG) and VPLMN Autonomous CSG Roaming (VCSG) [31]. VPLMN Autonomous CSG Roaming has been chosen instead of HPLMN CSG Roaming because of its flexibility due to reduced administrative exchanges with the HPLMN. On the other hand, in case there is the need for a fine-granular control by the HPLMN of what CSGs can be accessed by each UE in each VPLMN, HPLMN CSG Roaming should be used instead [31], when supported. In fact, as stated in [32], the following limitation appears when HCSG is used:

> "The visited network needs to access the HSS/HLR in the home network of the subscriber in order to update the CSG information for the subscriber. In some cases the visited network may not have access to this function in the home network, for example, if the home network does not support CSGs when the home network is Rel-7."

This is the main reason why VCSG was introduced and it is still under discussion as of the time of writing this deliverable. One way or the other, this allows that UEs that are not subscribers of the VPLMN have access to CSGs defined by the VPLMN and jointly managed (through allowed and operator CSG lists) by the MNO of the VPLMN and the LNO. However, since access to local services is a feature of interest to the LNO, the VCSG approach offers a control as confined as possible in the LNO (and partially in the VPLMN). In any case, the VPLMN must disable VCSG on a per HPLMN basis if so requested by the home operator [31]. Therefore, home operators still keep the control of their UEs.

5.1.2 Work during Year 2

The main focus of the work on access control to local services during Year 2 was on single operator scenarios in which the UE and the femtocells in the network of femtocells belong to the same Home Public Land Mobile Network (HPLMN).

The same procedures as the ones presented below were studied in a single operator scenario, namely CSG provisioning, access control enforcement at the MME based on CSG subscription information, and local access control list provisioning. The message sequence chart of the interaction of the UE with local services was also presented. In addition to that, the generic procedures for handling network security in networks of femtocells were also studied.

The introduction of the CSG Subscription Server (CSS) in the work presented below allowed us to follow the same general principles as those of year 2 for roaming UEs. However, some modifications are needed for access control at the MNO level. On the other hand, access control at the local network level has been simplified to allow for IT departments to apply their regular data networking access control policies also

for roaming UEs. Furthermore, in case the CSS is also used for UEs in the HPLMN of the femtocells, as suggested in [33], the solution presented below would handle access control in a homogeneous manner for both roaming and non-roaming UEs.

5.1.3 Relevant building blocks and interfaces

In addition to the building blocks mentioned in D5.2 for the single operator case, for the multi-operator case, we exploit a new optional building block introduced in release 11 for storing CSG membership information of roaming users: the CSG Subscription Server (CSS).

5.1.3.1 CSG Subscription Server (CSS)

According to TS 23.401 [34]: the "CSG Subscriber Server (CSS) is an optional element that stores CSG subscription data for roaming subscribers. The CSS stores and provides VPLMN specific CSG subscription information to the MME. The CSS is accessible from the MME via the S7a interface. The CSS is always in the same PLMN as the current MME." That is, the CSS performs the same function as the HSS but only for handling CSG subscription data and procedures.

CSG Subscription information

According to TS 23.002 [35] and TS 23.008 [36], the CSS is responsible for holding the following user related information:

- User Identification;
- CSG membership granted to the subscriber during his stay in the VPLMN, i.e. list of CSG IDs and associated expiration dates; more specifically, TS 23.008 states that "If a mobile subscriber has a Closed Subscriber Group (CSG) subscription, the HSS shall store Closed Subscriber Group Information which is a list of up to 50 CSG-Ids per PLMN and for each CSG-Id optionally an associated expiration date which indicates the point in time when the subscription to the CSG-Id expires and optionally corresponding APNs which can be accessed via Local IP access from this CSG identified by the CSG-Id". In the same way, the CSS should also follow these rules.
- User Location information: the CSS stores the location information of the subscriber for subsequent update of the CSG subscription information at the MME upon subscription change.

The CSS consists of the following functionalities:

- Download of the CSG subscription information upon request from the serving MME through the S7a interface, to enable roaming subscribers to access to the packet switched domain services via CSG cells;
- Service provisioning, including updating the appropriate serving entities (i.e. MME) with modifications of the CSG membership granted to the subscriber.

The interface between the MME and the CSS is S7a. There two main procedures defined through these interface between these two entities, namely "insert CSG subscriber data" and "update CSG location" that are initiated by the CSS and the MME, respectively. They are explained below in the context of CSG provisioning and Access Control at the MNO level.

5.1.4 Relevant procedures

5.1.4.1 CSG provisioning

The procedure for adding, removing, or modifying the subscription of users is almost the same as that presented in [37] except for the presence of the CSS. Therefore, in case the UE being registered does not belong to the HPLMN, the administration server will contact the CSS instead of the HSS. The following figure presents the message sequence chart for roaming UEs.

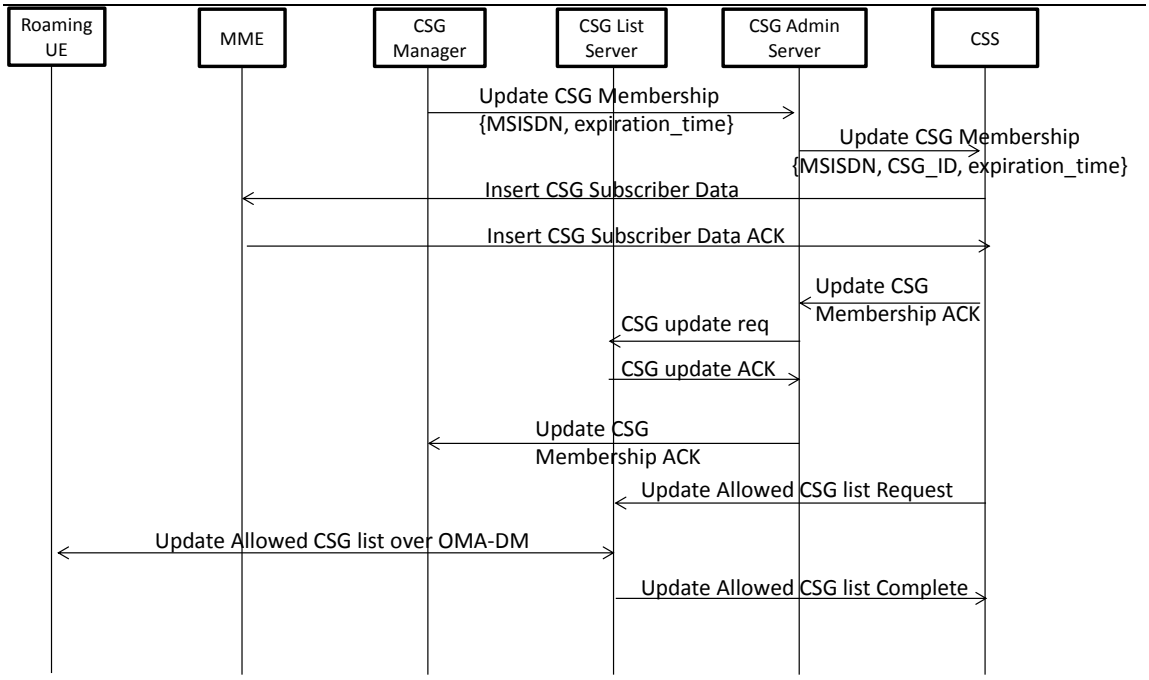

Figure 5-1: CSG provisioning for roaming UEs involving the CSS

The LNO network manager (e.g., the system manager of the company) logs on to the administration server and adds the new UE to the CSG that is already in place for providing access to local services to guest UEs. The UE is identified by means of the MSISDN. If the modification is approved by the MNO, the administration server then updates the CSS with the MSIDSN and CSG ID to which the UE is allowed access. If the UE is currently attached to an MME, the CSS initiates the insert CSG subscriber data procedure to modify the CSG information stored at the MME for this UE. This is done through the S7a interface. After that, the CSS updates the allowed or operator CSG lists (depending on the operator policy) in the CSG list server. Then, the CSG list server updates the UE with the new lists via OMA DM.

5.1.4.2 **Access control at the MNO level**

Once it has been registered, the UE is allowed to attach to femtocells belonging to a given CSG ID in the visited network. Access control at the MNO level to control the attachment (and other NAS procedures) to the appropriate CSG is described in the following figure. It is quite similar to that described in [37] except for the presence of the CSS. The presence of the P-MME could be made transparent (however, see the following subsection for some remarks on this).

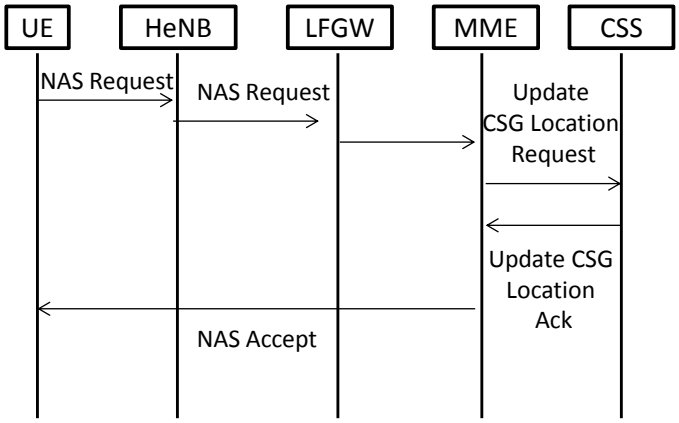

Figure 5-2: Access control at the MNO-level based on CSG subscription information retrieved from the CSS

When the UE initiates a NAS procedure (e.g., attach, tracking area update), it is first sent to the HeNB through an RRC message. The HeNB adds CSG related information to the message and sends the corresponding S1-AP message towards the MME. If there is no subscriber information on the UE, the MME will request it to the CSS as part of the roaming UE subscription profile in the form of an Update

CSG Location Request message. This will be ACK'ed by the CSS in the form of an Update CSG Location ACK message. A prior interaction with the home HSS may be needed to retrieve roaming UE subscription profile information. If the UE is not allowed to access this CSG, the MME sends a NAS reject message with the cause value #25 (not authorized for this CSG). Otherwise, the MME sends the NAS accept message.

5.1.4.3 **Remarks on MNO-level operation**

It is not needed that P-MME gets an update of subscriber information. This could still be handled by MME in the core. However, if such update is feasible (i.e., allowed by MNOs via interfaces equivalent to S6a or S7a), the operation would be more efficient, since access restrictions (if applicable) would be applied closer to the UE, hence saving resources.

The procedures hitherto described handle the first part of the problem, that is, how does the MNO (of the VPLMN or HPLMN), jointly with the LNO manager, grant access to a given CSG over licensed spectrum of the MNO. Therefore, they allow the UE to initiate NAS procedures (e.g., attach, tracking area update, service request) without being rejected.

The CSS only contains information on roaming UEs related with CSG management, all the rest of state information (e.g., that stored in the HSS) and procedures (e.g., those related with other kind of subscriber information exchange with the HSS) are not modified. Alternatively, one of the options mentioned in [33] is that the CSS could also contain all CSG subscription information (that is, also for non-roaming UEs). In this way, the HSS would not be overloaded with control information that is subject to temporary subscriptions, and hence, potentially generating control information quite often.

5.1.4.4 **Local Access Control List provisioning**

On the other hand, the procedures described below solve the second part of the problem, that is, granting access to the allowed local services.

In our solution, the MNO still has control on whether the roaming UE is allowed to have access to local services through a "home APN". In fact, it is expected that the MNO provides high-level offloading policies only and the more fine-granular ones are fully under the control of the LNO. As explained in D5.1 (section 2.2.4.2), the MNO could convey such policies by a TR069 management interface.

This control is enforced when the UE requests a PDN connection to the "home APN" that is received by the MME, as part of the subscription information transferred by the HSS to the MME. On the other hand, the fine-grained control of what services inside the local network are allowed to the roaming UE is under the control of the LNO by applying regular data networking access control policies. This would allow having homogeneous access control in the network of the company for all kinds of devices and networking equipment (including mobile phones).

The main idea is that the LNO manager maintains a local AAA server with information on each roaming UE indexed with its MSISDN. The allocated IP address for each UE is also stored in each record. Therefore, the LGW will ask this server for the IP address to be assigned to the UE when it establishes the PDN connection to the "home APN" [38]. As for access control lists, they could be manually configured in the networking equipment of the company. Alternatively, there are schemes in which Access Control Lists (ACLs) could also be stored for each UE in the local AAA in the form of downloadable ACLs. In this case, when there is the first attempt from the UE to access a local service, the firewall would contact the local AAA server for user authentication and for downloading the associated ACL if not already enforced [39].

5.1.4.5 **Remarks on LNO level operation**

The LNO manager (e.g., the system manager of the company) configures the ACLs in the AAA server of the LNO. Since ACLs will be applied based on fields of the IP data packet sent by the roaming UE (see MSC of the next section), entries in the AAA server will contain MSISDN and IP address (as well as expiration time). In this way, an appropriate mapping between the 3GPP identifiers and data networking ones, in use in the local network, could be done. Notice that the roaming UE will be assigned an IP address of the local network, which is fully under the control off the LNO manager.

The number of entities involved in the above MSC has been simplified by assuming that only the LNO manager can grant access to roaming UEs. If any employee of the company could grant access to roaming UEs, a new Local networked Femtocell ACL Administration Server entity (to which employees would log on) could be introduced. In this way, the final approval before configuration in the AAA server would still be given by the LNO operator.

5.1.5 Updated MSC of local access control for multi-operator scenario

The procedure for establishing a PDN connection for a local APN (or "home APN") through a CSG provisioned in a VPLMN is shown in the following figure. It is exactly the same as figure 2-26 of D5.1, though some comments are in order. A slightly modified version of the figure is pasted here for convenience (Figure 5-3).

For detailed explanation of each of the steps, please refer to D5.1 [1] section 2.2.4.3. Below, we just focus on issues related with access control.

In Figure 5-3, there is no interaction represented between the MME and the CSS, because we assume there was a previous interaction in the attach procedure and the subscription information is already available at the MME. Therefore, enforcement of CSG membership can readily be applied at the MME.

In step 5, we assume that the address is assigned by the local network (acting as an "external PDN network"). Since, the MSISDN is stored in the P-GW context, it will be sent in the tunnel establishment request message towards the L-GW (through the S-rat interface). Then, the L-GW includes the MSISDN in the AA-request message towards the local AAA server, which is then used as key for retrieving the IP address assigned by the LNO manager to the roaming UE. This is in accordance with TS. 29.061 in the sense that "The information delivered during the Diameter authentication can be used to automatically correlate the users identity (the MSISDN or IMSI) to the IPv4 address and/or IPv6 prefix, if applicable, assigned/confirmed by the GGSN/P-GW or the authentication server respectively."

There is a feature called downloadable ACLs from Cisco, with which a firewall can download ACLs associated to a given user from a RADIUS AAA server. This could be the same local AAA server configured by the LNO manager that contained other subscriber information used when assigning the IP address to the user based on its MSISDN. Alternatively, the LNO manager could use any other data networking configuration in the local network networking equipment according to company policies. One way or the other, eventually, ACLs are configured in regular data networking equipment of the local network and access control to local services can be done following the same procedures as for any other user in the network.

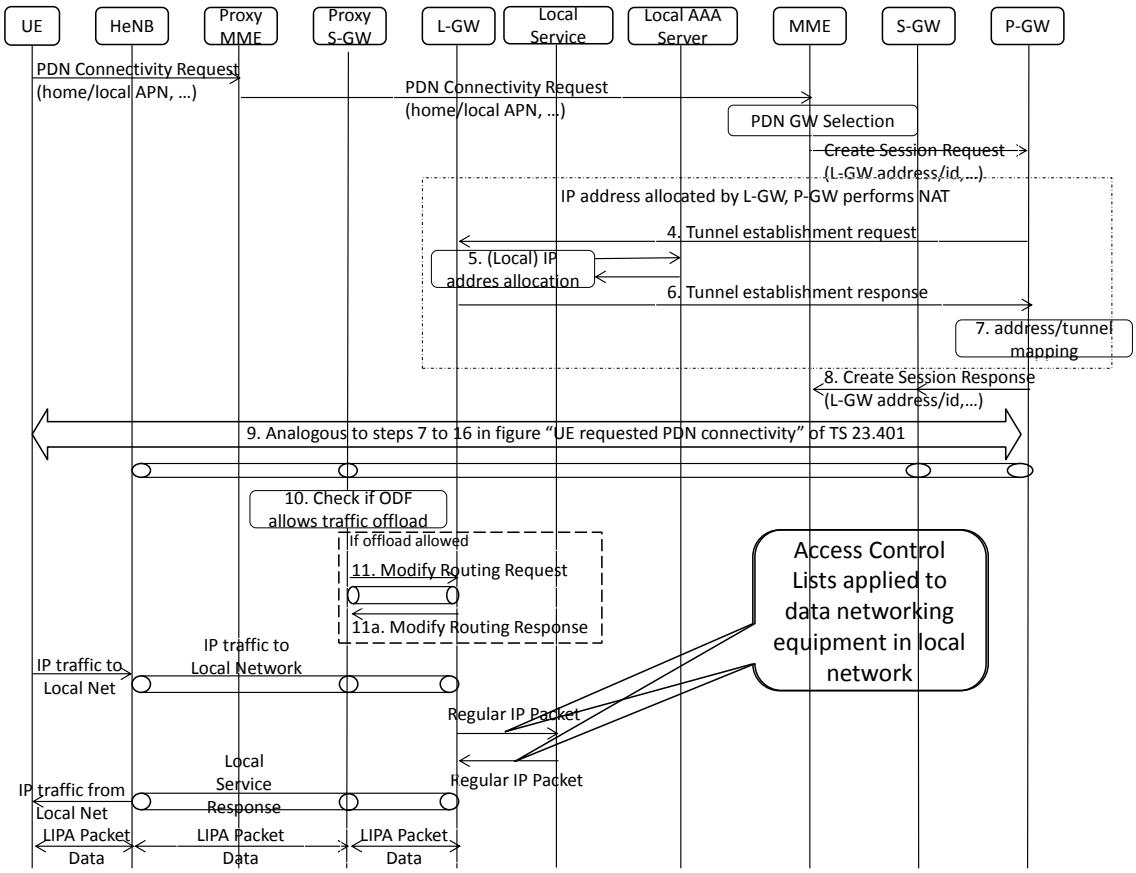

Figure 5-3: MSC for establishing PDN connectivity with LIPA/SIPTO support and local access control

5.1.6 Comments on local access control options

An alternative way of offering access control to local services with such control being shared by the MNO and the LNO is by applying filters in the ODF. As mentioned above, TR069 could be used by the MNO to apply high level offloading rules in the ODF of the PSGW. Since such filters are based on fields of IP packets, similar forwarding procedures as the ones mentioned above for the ACL option could be applied there. However, a new option as forwarding decision should be added, that is, not allowing the packet to go through it neither to the PGW nor to the LGW. That is, the packet may be discarded if the UE is not allowed to access a certain local service. This requires the LNO manager to be able to access the ODF configuration in some way. Nevertheless, this would imply that the LNO manager should adapt to a new environment specific for UE access control and thus, the regular data networking access control policies could not be used.

6. Summary of WP5 Findings

This chapter summarizes all the innovative concepts and mechanisms developed by BeFEMTO in WP5 during the whole project phase and their main achievements. These concepts and mechanisms contribute to the BeFEMTO system concept.

6.1 Traffic Forwarding and Resource Sharing

6.1.1 Centralized Traffic Management for Cooperative Femtocell Networks

Cooperative femtocells, which will be deployed in enterprises or public spaces, will have to be connected over the existing network infrastructure and will share the communication resources with existing services. Under this context, both the mobile operator(s) and the provider(s) of local network services do not want to see the Quality of Experience of their services affected by the presence of other stakeholder's traffic. Hence it would be desirable to monitor the performance of the respective networks to ensure service level agreements are met.

To ensure that local network resources are used efficiently and fairly, we analyse the effects of co-existing traffic in a cooperative femto network. To realize this, a hypercube enterprise network is designed consisting of OpenFlow switches which are connected to a controller which installs the routes on the switches. The end nodes connected to the OpenFlow switches act as femto and non-femto traffic sources. This entire network design was implemented in ns-3 network simulator. The analysis was carried out on the following scenarios: Baseline, VLAN with Priority queuing**,** traffic management is based on Valiant load balancing.

The baseline scenario assisted in understanding the effects on the co-existing traffic. Here we found that the video and voice traffic experience a significant degradation in QoS and very few parallel flows can be supported. The analysis of second scenario, laid the foundation for understanding the overheads involved in such cases and if traffic management can be achieved through a simple approach. The results show that through priority queues the voice quality is significantly improved, however the video stream still observed a degraded performance. This meant that there is a need for a better load balancing technique in a cooperative femto network. The final scenario, facilitated to study the performance enhancement which can be achieved for different stakeholders in a networked femto cell scenario using VLB method. VLB when combined with OpenFlow switches can significantly improve the QoS for voice and video and also support more parallel flows of traffic from different stakeholders.

The key inference of our analysis is that, different stakeholders in a networked femto scenario need to be supported by load balancing techniques to ensure the QoS. This can be ensured through the use of OpenFlow switches which are connected to a centralized load balancing controller.

6.1.2 Distributed Routing

An all-wireless NoF requires a specific routing protocol able to cope with the challenges posed by this constrained scenario. The protocol should try to find an appropriate trade-off between NoF performance metrics, such as throughput, packet delivery ratio, and delay. Additionally, the performance experienced by different UEs may be highly asymmetric, favouring UEs close to the LFGWs. Finally, the protocol should try to minimize its state information stored at nodes in order to be implemented in practice in HeNBs, and minimize its required control overhead considering that it is sent through an all-wireless local backhaul.

To address these challenges, we propose a routing protocol for an all-wireless NoF motivated by stochastic network optimization theory. The resulting protocol trades off decisions based on distributing the load in the NoF using backpressure routing strategies, and minimizing the distance to reach the intended destination using geographic information. The protocol trades-off these decisions on a per-packet basis based on the current congestion in the 1-hop neighbourhood in the NoF, and the characteristics of the specific data packet (i.e., the TTL). The decisions are taken on a distributed fashion using 1-hop neighbourhood information, and have low processing and state in each HeNB.

In a NoF with multi-LFGWs we have proposed a simple LFGW deployment that benefits from the load balancing characteristics of the distributed routing protocol, hence obtaining significant gains on NoF performance metrics. The deployment is based on adding LFGWs close to those LFGWs whose location is known by the HeNBs.

On the other hand, we have also explored the routing protocol under sparse NoF deployments without changing its default behaviour. Specifically, results show that by trading off between congestion (i.e., backpressure) and proximity to the destination, the protocol can circumvent complex obstacles.

Extensive results show it outperforms state of the art single-path routing protocols up to 100% in terms of aggregated packet delivery ratio, and aggregated throughput under a high variety of situations. In terms of end-to-end delay, the protocol is able to outperform state of the art solutions by achieving up to 50% of improvements. Additionally, it experiences a lower degree of variability with NoF performance metrics, hence showing a higher degree of fairness between the UEs no matter their respective proximity to the LFGWs.

One of the main conclusions derived from our research is that the proposed routing protocol highly improves NoF performance metrics in constrained wireless backhaul scenarios in which a low control-overhead, distributed, and scalable routing solution is required. Additionally, the presented distributed routing strategy is agnostic to the underlying layer-2 technology, hence facilitating its use in any wireless backhaul.

6.1.3 Voice Call Capacity Analysis of Long Range WiFi as a Femto Backhaul Solution

A frequent challenge in small cell deployments is that wired backhaul connectivity is not readily available at the most suitable small cell installation site and that installing wired connectivity or resorting to microwave-based wireless solutions is neither practical nor cost-efficient. This has motivated many operators to begin looking for alternative lower cost wireless backhauling solutions. This work studied the use of long range WiFi as alternative to current copper, optical fibre or microwave based technologies for backhauling outdoor small cell traffic.

Specifically, this work analysed the number of high quality circuit switched AMR voice and packet switched AMR VoIP calls that can be supported via femtocells using long range WiFi backhauling. It also proposes a QoS-based AMR codec rate adaptation mechanism to replace the current radio access link quality based adaptation. The QoE metric used is the MOS and is computed using a real time implementation of ITU-T's E-Model, a standardised computational model for subjective call quality assessment. Each VoIP application continually monitors its downlink QoS in real time based on delay, jitter, loss and the AMR codec mode. When the MOS score falls below a predefined threshold the application sends a CMR request using the AMR header of outgoing packets to the source application, on reception of this the source application will change the source coding rate to the requested mode.

Our findings show that this mechanism effectively adapts to changes of the backhaul connection's capacity and load. Without the proposed scheme, saturation of the backhaul link does not cause AMR codec adaptation, resulting in serious call quality degradation despite excellent radio conditions on the access link. With the proposed scheme, saturation of the backhaul link instead leads to much more graceful call quality degradation as the voice applications slowly decrease their AMR codec rate and a higher call capacity at good call quality levels. For example, a 5km long IEEE 802.11a backhaul link can support around 40 AMR over Iuh voice calls at the highest modulation rates. It can also be observed that with the proposed adaptation the call quality recovers much faster as calls begin to end and link capacity becomes available.

6.1.4 Local Breakout for Networked Femtocells

Local IP Access (LIPA) and Selective IP Traffic Offload (SIPTO) are two 3GPP architecture features that allow traffic to be "broken out" of the 3GPP domain at or near the femtocell and forwarded to/from the local IP network and the Internet, respectively. BeFEMTO started its work on local breakout for *networked* femtocells during the time of 3GPP's initial studies on breakout for *standalone* femtocells. Based on an analysis of the different solution proposals discussed in 3GPP and their relative advantages and drawbacks, BeFEMTO proposed a hybrid approach that combines the strengths of the solutions and is also better suited for networked femtocell scenarios. It provides the same features as the now standardized solution for standalone femtocells, but extends it in two important aspects:

- It uses a *single, centralized breakout point* on a new network element, the Local Femtocell Gateway (LFGW), rather than one on each femtocell, which allows local mobility for breakout sessions, facilitates management and control of these sessions and provides consistent breakout with legacy femtocells. This is done in a standard-compatible way, such that it works with non-proprietary femtocell solutions as well.

- It adds support for *hand-outs and hand-ins of breakout sessions to/from the macro network as well as (re-) of LIPA sessions from the macro network*, and it does so with a *single mechanism* instead of the currently two different ones, such that the user experience is more uniform.

The proposed approach has been specified in detail (message sequences, message contents, etc.) and the performance has been studied based on numerical simulations.

BeFEMTO's work on the LFGW with centralized local breakout has been presented at Femto Forum (now Small Cell Forum). BeFEMTO partners also sourced the 3GPP SA2 Work Item "LIPA Mobility and SIPTO at the Local Network" (LIMONET) for Rel-11 (now postponed to Rel-12). In a Technical Report of LIMONET, BeFEMTO 's approach of locating the breakout point on-path of the S1 interface is included as one of the candidate solutions.

6.1.5 Traffic Offloading

The increasing demand of mobile data traffic is starting to stress the networks of mobile network operators (MNOs). Techniques for offloading traffic (partially or totally) from the network of the MNO are currently being designed and deployed at various points of the network, including femtocells or femto GWs. Such techniques divert traffic to offloading networks or directly to the Internet.

We propose a generic analytical approach for modeling traffic in mobile networks implementing offloading. The model is generic in the sense that it is independent of the specific offloading technology used and may be of use to provide bounds on network dimensioning.

Based on previous measurements found in the literature, the proposed model assumes that user activity periods and periods characterizing offloading are heavy-tailed. We model them as strictly alternating independent ON/OFF processes. Therefore, the non-offloaded traffic (i.e., that traffic still being served by the MNO on a regular basis) is modelled as the product of these two processes. We proved that the resulting process is long-range dependent, with heavy-tailed ON/OFF-period durations, and its characteristic parameters can be derived from those of the initial processes.

We also evaluated the network resources required to serve the traffic resulting from the aggregation of many such sources. In particular, by studying the characteristics of the aggregation of several sources of non-offloaded traffic, we provide performance bounds of the core network resource consumption, which can be used when dimensioning the network. Furthermore, we quantitatively evaluate the benefits of offloading by comparing the required resources before and after deploying offloading for providing a given quality of service.

One of the main conclusions of our research is that offloading does not necessarily entail less resource consumption in the network of the operator. Under certain conditions, and due to an increase of the burstiness of the non-offloaded traffic, the amount of network resources to offer a given level of QoS is increased. In this context, the tail-index of offloading periods is the most important design parameter to make non-offloaded traffic less heavy-tailed, hence reducing the resources needed in the network of the operator.

Extensive simulations, in which the Hill's estimator was used to obtain the main parameters of the resulting process, confirm the results of our analytical study.

6.1.6 A QoS based call admission control and resource allocation mechanism for LTE femtocell deployment

Femto voice traffic is tagged by the femtocell with a DiffServ Code Point (DSCP) in the IP header that allows the DSL Access Multiplexer (DSLAM) to identify it as voice and forward it through the Expedited Forwarding (EF) queue. The EF queue provides the highest service level and is utilised for low latency and low bandwidth intensive services such as voice; however in typical deployments it has a fixed and relatively limited bandwidth. As the number of FAP deployments increases, the EF queues on DSLAMs will become increasingly congested, which will lead to increased packet delays, jitter and loss with a corresponding impact on the voice call quality. Therefore, the quality of the call depends on both the radio link from the customer's mobile device to their HeNB *and* the level of congestion on the backhaul link.

This work has developed and studied a method to enable both Quality of Service (QoS) aware Call Admission Control (CAC) and bandwidth negotiation in the backhaul links. It assumes that MNOs would have Service Level Agreements (SLA) in place with the fixed broadband access provider that ensure

maximum and minimum bandwidths at each DSLAM dedicated for their femtocell VoIP traffic, but that these bandwidths would be dynamically re-negotiable to allow control of cost for bandwidth reserved at the DSLAM while maintaining high voice call quality for their customers.

The proposed scheme is based upon the quality of ongoing voice calls passing through the HeNB-GW. A voice monitor application residing in the HeNB-GW maintains a list of ongoing calls, measures in real-time the voice call quality, determines when problems occur and employs the admission control and dynamic resource allocation mechanisms to restore/maintain the quality.

Our findings show that without the proposed mechanism and algorithm, new calls are still accepted when the provisioned bandwidth limit for the DSLAM's EF queue has already been reached as there are still resources available on the radio access. The resulting queuing means extra delay and eventually dropped/lost packets, which rapidly degrades the MOS values of on-going calls.

With the proposed scheme, we find that when the overall MOS drops, the feedback mechanism leads to rejection of new call requests to restore the overall MOS for all calls to a high level. Next, the voice monitor application triggers an increase of the bandwidth of the DSLAM's EF queue, which allows it to accept further calls.

6.2 Mobility Management

6.2.1 Local Mobility Management

In networked femtocells, no matter whether closed-access like in the enterprise femtocell network use case or open-access like in the airport terminal use case, the higher femtocell density compared to macro- or picocellular deployments and the high number of served users mean that the handover rate increases and with it the signalling load on the mobile core network. One can further expect a larger amount of traffic that is exchanged between mobile devices attached to the same local femtocell network, which means data traffic burdens the backhaul connection and mobile core network as it unnecessarily makes the round-trip from a local femtocell over the local backhaul to the P-GW in the core network and back.

This work proposes a local mobility management solution for femtocell networks that avoids unnecessary user data and mobility signalling traffic over the core and backhaul networks, while maintaining full compatibility and minimizing the impact on the EPC, the HeNBs and the UEs to facilitate adoption. To provide this functionality, BeFEMTO's new LFGW, which is transparently inserted into the S1 interface between the HeNBs and the EPC, integrates two additional functions:

- The Proxy MME function acts as local mobility control point on the control plane. It intercepts mobility-related signalling messages on the S1-MME interface and manipulates them such that towards the EPC UEs appear "frozen" to the HeNB they have initially attached or handed-in to, whereas towards the HeNBs it handles mobility signalling like the MME.
- The Proxy S-GW function is controlled by the Proxy MME and acts as GTP-level router that redirects data plane traffic from the EPC towards a UE's initial HeNB to its current HeNB, rewriting headers as necessary. It also short-cuts traffic between UEs of the same femtocell network that are communicating with each other, such that it does not need to make the round-trip via the core network. Finally, it can be re-used for traffic breakout (see Section 6.1.4).

The proposed approach has been specified in detail (message sequences, message contents, etc.), and its performance has been studied based on numerical simulations. The LFGW with local mobility management support has also been presented at Femto Forum (now Small Cell Forum).

6.2.2 Local Location Management

Frequent handovers and cell reselections in a network of femtocells scenario have a negative impact on the amount of location signalling traffic over the wireless backhaul. In order to tackle this issue, two LLM contributions have been considered. On the one hand, we have designed a self-organized Tracking Area List mechanism that allows P-MMEs to register UEs in individual TALs. The size of these TALs is set according to the UE mobility state, which enables a reduction on location signalling traffic of up to 39% per UE. On the other hand, we have devised a distributed paging mechanism over the X2 interface in order to reduce the amount of S1-AP Paging messages traversing the NoF upon voice/data call arrivals. This mechanism enables a unicast paging operation from the P-MME to the destination TAL, followed by an optimized broadcast paging within the TAL.

6.2.3 Mobility Management for Networked Femtocells Based on X2 Traffic Forwarding

Frequent handover among femtocells may cause significant signalling cost to the core network for data path switch operations. Two local mobility management schemes for networked femtocells based on X2 traffic forwarding are proposed. Instead of switching the data path after each handover, the target femtocell can use the local path between the previous serving femtocell and itself for ongoing session communications without sending the path switch request to the core network entities. A traffic forwarding chain will be established from the original local anchor point to the current serving femtocell. Since the local traffic forwarding may increase the end-to-end communication latency and consume the local resource, a threshold of the forwarding chain should be defined to balance the trade-off between the path switch cost and traffic forwarding cost. The first scheme, namely *Traffic Forwarding with Cascading Path* (TF_CP), cascades the target femtocell to the previous source femtocell via the local path after a handover. The second scheme, namely *Traffic Forwarding with Shortest Path* (TF_SP), implements local path switch if the target femtocell has a shorter path to the original local anchor point than the cascading path. To adapt to the self-deployment nature of the femtocells, fast session recovery mechanisms are also proposed to deal with the unavailability of a forwarding node when it is switched off or failed.

As shown by both analysis and simulation, remarkable signalling cost saving can be achieved compared to the 3GPP scheme with reasonable extra data delivery cost, especially when the core path switch cost and the mobility rates are high. In particular, the TF_SP scheme has less signalling cost and a little more data delivery cost than the TF_CP scheme when the threshold of the forwarding chain is small while it has more signalling cost and less data delivery cost when the threshold is large. In addition, both schemes can recover the communication session within a short period and only incur limited packet loss in case that a HeNB on the forwarding chain is switched off or failed. The proposed schemes are transparent to the EPC and the UEs and no upgrade is required from either side.

6.2.4 Inbound/Outbound Mobility Optimization

A scheme enabling fast radio link failure recovery for hand-in and hand-out mobility is proposed. The handover failure may frequently occur when a mobile is moving from an eNB to a HeNB or vice versa due to the large handover preparation delay over the Internet backhaul, the rapid signal degradation resulting from the wall loss and the co-channel interference. A UE-based forward handover with predictive context transfer is proposed to allow UE start RRC connection re-establishment procedure quickly without waiting for the completion of handover preparation at the target cell. Meanwhile, on detection of a failure, the source cell can send the UE's context to the potential target cells according to the prediction based on the latest received measurement report. The session can be resumed when the UE successfully establishes the connection with a new cell and that cell receives the UE's context. The UE's context is fetched from the source cell to the new cell as a fallback if it is not received within a certain amount of time.

By applying the proposed scheme, the service interruption time in case of handover failures can be significantly reduced compared to the current 3GPP procedure. The general latency requirement of real-time traffic (150 ms) can be met even when a handover failure occurs. However, to apply the proposed scheme the base stations (both eNB and HeNB) need to be upgraded to enable fast detection of the radio link failures for each UE and context fetch capability.

6.2.5 Seamless Macro-Femto Handover Based on Reactive Data Bicasting

Different from the macro cellular networks, the femto base stations are usually deployed by users at their own premises and connected to a mobile operator's network via latency-prone residential broadband access. The current 3GPP handover procedure may cause large downlink service interruption time when users move from a macrocell to a femtocell or vice versa due to the data forwarding operation.

To tackle this problem, a simple but effective handover procedure is proposed to enable seamless handover by reactively bicasting the data to both the source cell and the target cell after the handover is actually initiated. An optional drop-head buffering mechanism only requiring a very small buffer size can be used at the S-GW to eliminate the packet loss during the HO procedure.

Numerical results show that the proposed scheme can significantly reduce the downlink service interruption time while still avoiding the packet loss with only limited extra resource requirements compared to the standard 3GPP scheme.

6.2.6 Mobile Femtocells based on Multi-homing Femtocells

This work studied an alternative approach to Mobile Relays, which is to turn a normal femtocell into a Mobile Femtocell. The Mobile Femtocell works in an overlay manner by establishing the IP connectivity to its mobile operator's Femtocell Gateway over a mobile cellular access. By extending such overlay solution to multiple IP backhaul links, i.e. by making the femtocell *multi-homing capable*, several mobile access links can be bundled for higher reliability, quality, and capacity. It is even possible to use mobile accesses of different vendors and to use any combination of radio access technologies. A further advantage of Mobile Femtocells compared to Mobile Relays is that they allow Local IP Access, e.g. for providing value-add services on the bus or train the Mobile Femtocell is installed in.

There are several ways to provide multi-homing support for such Mobile Femtocells. In this work, we studied replacing the existing protocol combination of GPRS Tunnelling Protocol (GTP) over User Datagram Prototcol (UDP) on the data plane between the mobile femtocell and its femtocell gateway with SCTP. SCTP is already used on the control plane and has a number of key features like transport layer multi-homing, multi-streaming, concurrent multi-path transfer and partial reliability that are useful in this context.

The mapping of GTP/UDP to SCTP (e.g. sequence numbers and bearer ids) has been studied and the performance overhead evaluated. Our findings show that the proposed approach is not even less efficient in most cases: SCTP's overhead is 12 bytes for the common header and 16 bytes for the data chunk header. In comparison, UDP and GTP add 8 and 12 bytes, respectively, so in the worst case the SCTP overhead is 8 bytes higher per packet. However, unlike UDP, each SCTP packet can contain multiple data chunks. Thus, the additional overhead can be amortized over the number of voice or data packets that can be bundled into one SCTP packet.

6.2.7 Deployment, Handover and Performance of Networked Femtocells in an Enterprise LAN

A network of femtocells supported by a LAN can significantly reduce the cost of the femtocell backhauling in an enterprise scenario, and at the same time improves its reliability, thanks to the reuse of the enterprise's wired infrastructure.

A networked femtocells in an LAN pilot was deployed in the ground floor of a Telefónica I+D building. Femtonodes from two manufacturers were installed in the same locations in order to allow a consistent performance comparison. Also two femtonodes subsystems were used in this pilot to provide service to the corresponding femtonodes. The femtonodes were connected to TID's LAN, and connected through a IPSEC tunnel to each respective femtocell subsystem located in Telefónica's radio labs in Pozuelo (Madrid). The pilot was not connected to the general mobile core network that provides service to Spain's customers, but to an evaluation core network used for testing purposes and used a different frequency and PLMN ID that the commercial mobile network, to avoid uncontrolled interactions with real customers.

The generic elements that composed the femtonode subsystem were:

- Security GW (IPSec Gateway).
- IP Clock Server, that provides a reference clock for femto synchronization.
- Configuration Server (Femtocell Manager), which configures the femtonodes radio parameters.
- Femto Manager (Femtocell Home Register).
- Femto subnetwork manager, controller of the femtonode subsystem network.
- AAA Server (Authentication, Accounting and Authorization Server).
- Femto Gateway (Access Gateway).

During the tests, different femtocell's power control techniques were evaluated, along with handover analysis and solving IP connectivity issues from the enterprise's network to the core network.

6.3 Network Management

6.3.1 Distributed Fault Diagnosis

Fault diagnosis is necessary to identify femtocells status in a networked environment, isolating the problems derived from the backbone network from those whose origin are the femtocells themselves. The scheme must operate in a scenario where the femtocells are provided by different vendors, and also ensure their supervision and fault management when the mobile operator has no control on the backbone network, usually an enterprise's local area network.

Fault Diagnosis focuses on the enterprise networked femtocells scenario and is designed as a distributed framework that allows local management capabilities inside the femtocell network. In order to implement this distributed framework, a multi-agent approach is followed. Fault diagnosis is therefore cooperatively conducted by a set of cooperation agents distributed in different domains which share their knowledge about network status. In particular, Fault Diagnosis targets the diagnosis of problems related to the use of video services while being under the coverage of an enterprise femtocell network. Diagnosis knowledge is modelled as a Bayesian Network (BN) which relates causes and symptoms by means of probabilities. This approach is well suited to deal with uncertainty and lack of full status information. Furthermore, diagnosis knowledge can be split up and appropriately distributed to the different domains involved.

6.3.2 Energy Saving and Performance in HetNets

Heterogeneous networks, where a layer of macrocells for blanket coverage co-exist with a layer of femtocells for providing capacity, offer an improved spectral efficiency per area and an improved energy efficiency, measured as the power consumption needed to provide a certain throughput in a given area. Performance simulations and energy calculations show that the introduction of a femtocell layer, complementing the macrocell layer, greatly improves the system performance and the energy efficiency, when compared with current indoor coverage based on outdoor macro and micro base stations. In a dense urban reference scenario, the hybrid macro and femto approach is about 65 times more efficient (measured as a ratio between supported traffic and power, Mb/W) in terms of total consumed power than the macrocell approach and about 1,400 times more efficient in terms of radiated power.

However, some procedures must be implemented to reduce the total power consumption of the femtocell layer, because the hybrid scenario consumes about 7 times more power than the macro-only network deployment.

One solution is to take into account that the femtonode users will not be at home during an important fraction of the day, and then the femtonodes can be switched off, rendering a potential sharp reduction of the aggregated power consumption of the femto layer, and also a reduction of the interference generated by these femtonodes, at least that due to the control and broadcast channels which are always transmitted regardless the presence of any UE. Some energy-reduction strategies are based on switching off the radio section of a femtonode when the user is not in the neighbourhood of the femtonode, for example detecting when the UE is camped in the nearest macro cell to the femtonode in order to decide when switching on or off the femtonode. Another approach is to actually detect when the users are not at home, for example detecting the customer presence by means of a low-power radio interface activated in the UE, for example a Bluetooth Low Energy, or Wi-Fi, which is always active in the UE but whose low power characteristic does not degrade significantly the battery lifetime. When the user arrives at home, a short range radio connection between the UE and the femtonode is established, and the latter can switch-on its radio section accordingly.

6.3.3 Enhanced Power Management in Femtocell Networks

The proposed scheme aims to reduce the amount of energy wasted in enterprise femtocell networks when femtocells are active during office hours at times and in locations when no user is present in the respective femtocell's coverage area. It is based on the observation that individual users often follow a strict daily routine but that this routine can vary significantly amongst the employee base. It thus considers individual user activity and routine patters like the sequence of incoming and leaving users as well as electronic calendar entries for meeting appointments and absences, combined with user specific traffic demands, working locations and mobility patterns to only maintain the minimum set of femtocells powered-on to serve a particular group of users.

Three energy management strategies that consider an increasing amount of user context information have been devised and compared in efficiency to a baseline, schedule-based strategy that simply switches on

all femtocells in a given building during office hours and switches them off in the evening as the building closes for business: 1) a location-based strategy that detects a given user's presence and connection state and activates the femtocells in that user's office and path to the office, 2) a location-coverage intelligence-based strategy that additionally uses cell coverage information to minimize switching on additional cells if existing cells can accommodate an arriving user, and 3) an information-centric strategy that additionally considers usage statics created from previous observations as well as user calendar entries.

The results show that more context information (like femtocell locations, typical user mobility and meeting and absence information) can be effectively converted into higher overall energy savings by reducing the time individual femtocells are powered on. The information-centric strategy thereby showed 30% more energy efficiency than the location-intelligence strategy. The difference can even increase with the number of scheduled absences. It has also shown to be relatively robust to small errors in the predictions.

6.4 Security

6.4.1 Secure, Loose-Coupled Authentication of the Femtocell Subscriber

Current fixed access networks, regardless of the access technology, are natural heirs of traditional PSTN lines. This is probably the reason why the subscriber identification is based, generally, on parameters directly linked with physical elements of the access network. The usage of these identification schemes for femtocell deployments leads to highly complex systems implying heavy workflows for service provision.

A new authentication procedure for the femtocell subscriber is proposed using a UICC card in order to store the subscriber credentials. This UICC card supporting EAP-AKA authentication is inserted in a femtocell triggering the subscriber authentication mechanism towards the backhaul. At the network side, NASS and RACS subsystems resolve the EAP challenge identifying the subscriber, granting his access and configuring the access network nodes according to the services subscribed.

The development of this new authentication procedure and the real time access network configuration enable the speed up of the service delivery until the very moment of the service purchase. The selection of a UICC card to store subscriber credentials provides also some advantages related with mobility scenarios because a subscriber could extract the UICC card from a femtocell node and insert it in another, triggering an authentication process in which the backhaul would be configured identically than if he were at home.

It is important to note that the set of protocols and architectures selected for subscriber authentication are independent of the access network technology (xDSL, FTTH), and that this model can be applied both in an integrated femtocell node (in which a single box provides femto and broadband router functions) or in a two-box model (in which two different boxes, one for the femtocell node and other for the broadband router, exist).

In conclusion this new subscriber authentication mechanism has enabled the identification of the subscriber to the fixed access line that acts as a backhaul for the femtocell node, in a way that is decoupled from the physical elements of the access network infrastructure, secure, compatible with current standards, and near the market fostering the paradigm of service mobility.

6.4.2 Access Control to Local Network and Services

The Local Network Operator must be able to restrict femtocell and local network resources usage to members of the household and selected visitors. This problem is more relevant in a multiple operator scenario, i.e., UE from different MNO are allowed to access local services offered by LNO.

The proposed solution is divided in two parts: a) the UE attachment to the NoF and b) the access control to local services of the LNO.

Regarding the first part, the adopted solution for CSG membership management is based on VPLMN Autonomous CSG Roaming (VCSG). This mechanism allows UEs that are not subscribers of the VPLMN attaching to a given CSG, which is defined by the VPLMN and jointly managed by the MNO, VPLMN, and LNO. This solution requires the introduction of the CSG Subscription Server (CSS), which is responsible for storing roaming subscribers' CSG-related subscription data. The necessary procedures include the CSG provisioning and the access control at the MNO level.

Regarding the second part, the LNO maintains a local AAA server with information on each roaming UE indexed with its MSISDN. The Local Access Control List could be manually configured in the networking equipment of the LNO, or could be stored in the local AAA.

In conclusion, an access control mechanism has been provided with such control being shared by the VPLMN, the home MNO, and the LNO. The adopted solution allows fine-grained control of what services inside the local network are allowed for different UE by applying regular data networking access control policies.

6.4.3 Architecture and IP Security

Security of Femto solutions is a vast problem and only select issues were targeted mainly as a highlight for implementers and evaluators. Architecture of a solution consisting of systems and devices distributed in controlled and uncontrolled areas is a challenging task. For most intensive purposes devices or elements connected in uncontrolled environment must be treated as external and all communication, exchange of data or configuration details must be secured appropriately. Some measures applied by manufacturers like secure booting are certainly needed, because they do protect most of the devices from the less knowledgeable attackers. However, those who have the know-how and sufficient incentive would possibly be able to overcome such obstacles. Considering the fact that mobile devices are being used for access to all kind of systems, including financials, attackers may seek every kind of opportunity to intercept such communication. Femto solutions at least in theory are not free from possible vulnerabilities. While BeFEMTO project is not focused on security issues this topic could not be omitted. As a result of our work (in D5.2 [2]) on security issues that appear in femtocell networks, we provide high level recommendations that are based on practical tests of selected solutions and devices. While these are not revolutionary, they certainly should provide a strong message that implementation of IPSec alone is not sufficient to secure Femto environments.

6.5 Revenue Sharing in Multi-Stakeholder Scenarios

Revenue sharing process takes place when more than one party participates in a service delivery process, provides some value the service delivery chain, receives some revenue or participates in losses. The party contribution may include certain information delivery (like marketing offers), access to client groups (via client database) or technical means to execute an application or to establish a communication session with a customer.

In general revenue sharing processes are not simple, but they are getting even more difficult if one or more companies involved in this process obey the telecommunication law.

Also personal data protection law as well as the law regulating the process of service provisioning via electronic media add additional constrains on the revenue sharing process and mechanism.

Finally the brand reputation, clients' data confidentiality and transparent corporate policy have to be taken into account while planning the revenue sharing processes.

In the result, although the current legal / regulatory regulations well protect the client privacy and their data all the same implementation of complex, multi-stakeholder revenues sharing scenarios (especially those involving H(e)NBs) are difficult and not often met in real business environments.

To change this situation (and to speed up deployment of new advanced services for clients) a few measures can be taken. The most important of them relate to:

- Legal changes which would follow the technology advancement and new business cases / service ideas being currently created (and address more directly situations which haven't been foreseen before)
- Further regulatory effort aimed at more wide telco infrastructure sharing (including concept of H(e)NBs sharing)
- Working out (business and clients) fair practices / trade of regarding using customer's generated data and service personalisation.

7. References

[1] BeFEMTO D5.1, “Femtocells Access Control, Networking, Mobility and Management Concepts”, ICT 248523 FP7 BeFEMTO project, December 2010.

[2] BeFEMTO D5.2, “Femtocells Access Control, Networking, Mobility and Management Mechanisms (Final)”, ICT 248523 FP7 BeFEMTO project, December 2011.

[3] BeFEMTO D2.3, “The BeFEMTO System Concept and its Performance”, ICT 248523 FP7 BeFEMTO project, June 2012.

[4] J. Fitzpatrick “Voice call capacity analysis of long range WiFi as a femto backhaul solution” Computer Networks, Vol 56, Issue 5, March 2012, pp 1538-1553.

[5] Cisco Press “Cisco Enterprise QoS Solution Reference Network Design Guide”, Cisco Press, November, 2005.

[6] Rui Zhang-Shen and Nick McKeown “Designing a Predictable Internet Backbone with Valiant Load-Balancing”, in Proceedings of Quality of Service—IWQoS, Spinger Publications, 2005, pp-178-192.

[7] M.J. Neely, “Stochastic Network Optimization with Application to Communication and Queueing Systems”, Morgan&Claypool Publishers, 2010.

[8] “The ns-3 network simulator.” [Online]. Available: http://www.nsnam.org/

[9] L. Georgiadis, M. Neely, and L. Tassiulas. Resource allocation and cross layer control in wireless networks. Now Publishers. 2006.

[10] Cisco Visual Networking Index: Global Mobile Data Traffic Forecast Update, 2010-2015, Whitepaper, February 2011

[11] K. Lee, Y. Yi, J. Lee, I. Rhee, S. Chong, "Mobile Data Offloading: How Much Can WiFi Deliver?", in proc. of ACM CoNEXT 2010, USA, December, 2010.

[12] Stoev, G. Michailidis, and J. Vaughan, "On Global Modeling of Network Traffic", INFOCOM 2010, The 29th Conference on Computer Communications, San Diego, California, March 2010.

[13] M. Taqqu, W. Willinger, and R. Sherman, "Proof of a fundamental result in self-similar traffic modeling", Computer Communications Review 26:5-23, 1997.

[14] D. Heath, S. Resnick, G. Samorodnitsky, ”Heavy-tails and long-range dependence in ON/OFF processes and associated fluid models”, Mathematics of operations research, February 1998.

[15] B. M. Hill, ”A simple general approach to inference about the tail of a distribution”, Annals Statis. 3, pp. 1163-1174, 1975.

[16] J.A. Hernandez, I.W. Phillips, J. Aracil, ”Discrete-Time Heavy-Tailed Chains, and Their Properties in Modeling Network Traffic”, ACM Transactions on Modeling and Computer Simulation, Vol. 17, No. 4, Article 17, September, 2007.

[17] E. Casilary et al, ”Modeling of Individual and Aggregate Web Traffic”, HSNMC 2004, LNCS 3079, pp. 84-95, 2004.

[18] I. Norros, ”On the use of fractional Brownian motion in the theory of connectionless networks”. IEEE J. Select. Areas Commun. 13, 6, 953-962, 1995.

[19] I. Norros, ”A storage model with self-similar input”, Queueing Systems Volume 16, Numbers 3-4, pp. 387-396, 1994.

[20] A. Krendzel, J. Mangues, M. Requena, J. Núñez, “VIMLOC: Virtual Home Region Multi-Hash Location Service in Wireless Mesh Networks”, in Proceedings of the IFIP Wireless Days Conference. 24-27 November 2008, Dubai (United Arab Emirates).

[21] J. Ferragut, J. Mangues, A Self-Organized Tracking Area List Mechanism for Large-Scale Networks of Femtocells, in Proceedings of IEEE International Conference on Communications (ICC 2012), 10-15 June, 2012, Ottawa (Canada).

[22] A. Chandra, K. Mal, Genetic Algorithm-Based Optimization for Location Update and Paging in Mobile Networks, in Proceedings of 2004 Asian Applied Computing Conference (AACC), pp. 222-231.

[23] D. Kim, M. Sawhney, H. Lee, H. Yoon, and N. Kim, "A velocity-based bicasting handover scheme for 4G mobile systems," in Proc. Intl. Wireless Commun. and Mobile Comput. Conf. (IWCMC), Crete Island, Greece, 2008.

[24] A. Rath and S. Panwar, "Fast handover in cellular networks with femtocells," in Proc. IEEE Intl. Conf. Commun.(ICC), Ottawa, Canada, 2012.

[25] Evolved Universal Terrestrial Radio Access (E-UTRA) and Evolved Universal Terrestrial Radio Access Network (EUTRAN); Overall description; Stage 2 (Release 11), 3GPP Std. TS 36.300 v11.1.0, Mar. 2012.

[26] Qualcomm, Latency in HSPA Data Networks. [Online]. Available: http://www.qualcomm.com/media/documents/latency-hspa-datanetworks

[27] A.-C. Pang, Y.-B. Lin, H.-M. Tsai, and P. Agrawal, "Serving radio network controller relocation for UMTS all-IP network," IEEE J. Sel. Areas Commun., vol. 22, no. 4, pp. 617–629, 2004.

[28] Y. Fang and I. Chlamtac, "Teletraffic analysis and mobility modeling of PCS networks," IEEE Trans. Commun. vol. 47, no. 7, pp. 1062–1072, 1999.

[29] Feasibility study for evolved Universal Terrestrial Radio Access (UTRA) and Universal Terrestrial Radio Access Network (UTRAN) (Release 10), 3GPP Std. TR 25.912 v10.0.0, Mar. 2011.

[30] R3-110030, "Dynamic H(e)NB Switching by Means of a Low Power Radio Interface for Energy Savings and Interference Reduction"

[31] 3GPP technical specification TS22.220. "Service requirements for Home Node B (HNB) and Home eNode B (HeNB), version 11.4.0, December 2011.

[32] 3GPP document SP-100706, "WID for VPLMN Autonomous CSG Roaming (VCSG)", TSG SA meeting #50, December 2010.

[33] 3GPP technical report TR 23.830. "Architecture aspects of Home NodeB and Home eNodeB (Release 9)," version 9.0.0, September 2009.

[34] 3GPP technical specification TS23.401. "General Packet Radio Service (GPRS) enhancements for Evolved Universal Terrestrial Radio Access Network (E-UTRAN) access (Release 11), version 11.1.0, March 2012.

[35] 3GPP technical specification TS 23.002, "Network architecture (Release 11)," version 11.2.0, March 2012.

[36] 3GPP technical specification TS 23.008, "Organization of subscriber data (Release 11)," version 11.3.0, March 2012.

[37] Gavin Horn "3GPP Femtocells:Architecture and Protocols," QUALCOMM Incorporated White paper, Sept. 2010.

[38] 3GPP technical specification TS 29.061, "Interworking between the Public Land Mobile Network (PLMN) supporting packet based services and Packet Data Networks (PDN) (Release 11)," version 11.0.0, March 2012.

[39] B. Carroll, "Cisco Access Control Security: AAA Administrative Services", Cisco Press, May, 2004.